



Calhoun: The NPS Institutional Archive
DSpace Repository

Theses and Dissertations

1. Thesis and Dissertation Collection, all items

1970

A numerical investigation of finite-amplitude disturbances in a plane Poiseuille flow.

O'Brien, George Donoghue

Monterey, California ; Naval Postgraduate School

<http://hdl.handle.net/10945/15113>

Downloaded from NPS Archive: Calhoun



<http://www.nps.edu/library>

Calhoun is the Naval Postgraduate School's public access digital repository for research materials and institutional publications created by the NPS community. Calhoun is named for Professor of Mathematics Guy K. Calhoun, NPS's first appointed -- and published -- scholarly author.

Dudley Knox Library / Naval Postgraduate School
411 Dyer Road / 1 University Circle
Monterey, California USA 93943

A NUMERICAL INVESTIGATION OF FINITE-
AMPLITUDE DISTURBANCES IN A PLANE
POISEUILLE FLOW

by

George Donoghue O'Brien

United States Naval Postgraduate School



THESIS

A NUMERICAL INVESTIGATION OF FINITE-AMPLITUDE
DISTURBANCES IN A PLANE POISEUILLE FLOW

by

George Donoghue O'Brien

June 1970

*This document has been approved for public re-
lease and sale; its distribution is unlimited.*

T137243

A Numerical Investigation of Finite-Amplitude Disturbances
in a Plane Poiseuille Flow

by

George Donoghue O'Brien
Lieutenant Commander, United States Navy
B.S., United States Naval Academy, 1960

Submitted in partial fulfillment of the
requirements for the degree of

DOCTOR OF PHILOSOPHY

from the
NAVAL POSTGRADUATE SCHOOL
June 1970

ABSTRACT

A consistent and stable finite-difference approximation of the vorticity transport equations has been applied to a plane Poiseuille flow with spatially periodic disturbances of finite amplitude.

By application of the discrete Fourier transform to the solution of a Poisson equation significant improvements in the speed and accuracy of the calculations have been obtained. Numerical tests indicate that the usual iterative schemes are inadequate if a large number of mesh points are employed.

The effect of mesh size has been determined by extensive calculations based on a consistent second-order representation of the linear eigenvalue problem. The results indicate that a fine mesh is required to accurately represent the behavior of even the large-scale unstable motions. The stability and accuracy of the present formulation was demonstrated, in the linear range, by comparison with the established results of the linear theory.

Calculations in the non-linear range, at a moderate value of the Reynolds number, indicate the existence of an equilibrium state. The calculated values of the mean spectral density of kinetic energy are consistent with the exponential law predicted by Kraichnan for two-dimensional turbulence. The program, developed in this investigation, provides a means, of demonstrated accuracy, for the extensive investigation of two-dimensional turbulence in a shear flow.

TABLE OF CONTENTS

| | | |
|------|--|----|
| I. | INTRODUCTION | 11 |
| A. | BACKGROUND AND OBJECTIVES | 11 |
| B. | DIFFERENCES BETWEEN TWO AND THREE-DIMENSIONAL UNSTEADY MOTION | 14 |
| C. | PREVIOUS NUMERICAL WORK | 15 |
| 1. | Preliminary Remarks | 15 |
| 2. | Summary of Selected Numerical Investigations | 17 |
| II. | STATEMENT OF THE PROBLEM AND BASIC EQUATIONS | 21 |
| III. | ANALYSIS OF THE TRANSFORMED EQUATIONS | 28 |
| A. | BASIC EQUATIONS IN TERMS OF FOURIER COMPONENTS | 28 |
| B. | LINEAR THEORY | 30 |
| C. | NON-LINEAR ANALYSIS | 36 |
| IV. | THE FINITE-DIFFERENCE EQUATIONS AND SOLUTION | 40 |
| A. | CHOICE OF THE METHOD | 40 |
| B. | THE FINITE-DIFFERENCE EQUATIONS | 45 |
| C. | CONVERGENCE OF THE NUMERICAL SOLUTION | 53 |
| 1. | Consistency | 54 |
| 2. | Stability Analysis of an Analogous Linear Equation | 56 |
| 3. | Stability and Accuracy of the Complete Non-Linear Equations | 62 |
| D. | SOLUTION OF POISSONS' EQUATION FOR THE STREAM FUNCTION | 67 |
| E. | DESCRIPTION OF THE PROGRAM AND COMPUTATIONAL PROCEDURE | 77 |
| F. | FINITE-DIFFERENCE REPRESENTATION OF THE LINEAR EIGENVALUE PROBLEM | 80 |

| | | |
|---------------------------|--|-----|
| V. | RESULTS AND DISCUSSION | 87 |
| A. | LINEAR CALCULATIONS | 87 |
| B. | NUMERICAL INTEGRATIONS | 98 |
| 1. | Preliminary | 98 |
| 2. | Results | 100 |
| VI. | CONCLUSIONS | 126 |
| VII. | RECOMMENDATIONS FOR FUTURE WORK | 128 |
| APPENDIX A | Derivation of Discrete Relations for the Spectral Densities of Squared Vorticity and Kinetic Energy . | 129 |
| APPENDIX B | Listing of the FORTRAN Code for the Numerical Integration | 132 |
| APPENDIX C | Listing of the FORTRAN Code for the Solution of the Algebraic Eigenvalue Problem | 179 |
| BIBLIOGRAPHY | | 200 |
| INITIAL DISTRIBUTION LIST | | 204 |
| FORM DD 1473 | | 205 |

LIST OF TABLES

| Table | | Page |
|-------|---|------|
| I | Computer Storage Requirements | 42 |
| II | Results of Test Solutions of a Poisson Equation | 75 |
| III | Coefficients for Vorticity Boundary Conditions | 82 |
| IV | Summary of Numerical Integrations | 100 |

LIST OF FIGURES

| Figure | | Page |
|--------|--|------|
| 1 | Curve of Neutral Stability for Plane Poiseuille Flow | 34 |
| 2 | Coordinates and Domain | 46 |
| 3 | Finite Difference Mesh | 46 |
| 4 | Effect of Mesh Size on Curve of Neutral Stability | 90 |
| 5 | Effect of N on Calculated Growth Rates | 91 |
| 6 | Calculated Eigenvalues, $R = 6666.7$, $\alpha = 1.0$ | 92 |
| 7 | Calculated Eigenvalues, $R = 11333.3$, $\alpha = 1.0$ | 93 |
| 8 | Calculated Eigenvalues, $R = 25000$, $\alpha = 1.0$ | 94 |
| 9 | Comparison of Calculated Growth Rates, $R = 11333.3$ | 95 |
| 10 | Comparison of Calculated Growth Rates, $R = 7333.3$ | 96 |
| 11 | Comparison of Calculated Eigenvectors, $R = 6666.7$, $\alpha = 1.0$ | 97 |
| 12 | Test for Linear Solution, Run 1 | 107 |
| 13 | Test for Linear Solution, Run 2 | 108 |
| 14 | Distortion of Eigenvector after 1000 time steps, Run 1 | 109 |
| 15 | Effect of Amplitude on Initial Growth Rate | 110 |
| 16 | Energies vs. Time, Run 7 | 111 |
| 17a | Energies vs. Time, Run 8 | 112 |
| 17b | Energies vs. Time, Run 8 | 113 |
| 17c | Energies vs. Time, Run 8 | 114 |
| 18a | Energies vs. Time, Run 9 | 115 |
| 18b | Energies vs. Time, Run 9 | 116 |

| | | |
|----|--|-----|
| 19 | Mean Velocity Profiles, Run 8 | 117 |
| 20 | Mean Velocity, Vorticity, Turbulent Energy, Run 8 | 118 |
| 21 | Spectral Energy Density, $y = \pm .85$, Run 8 | 119 |
| 22 | Spectral Energy Density, Mean Values, Run 8 | 120 |
| 23 | Initial Amplitude and Phase, Mode 1, Run 8 | 121 |
| 24 | Final Amplitude and Phase, Mode 1, Run 8 | 122 |
| 25 | Final Amplitude and Phase, Mode 2, Run 8 | 123 |
| 26 | Final Amplitude and Phase, Mode 3, Run 8 | 124 |
| 27 | Final Amplitude and Phase, Mode 4, Run 8 | 125 |

ACKNOWLEDGEMENTS

The author expresses his gratitude and appreciation to the following:

Dr. Theodore H. Gawain for his supervision and aid, and for giving so generously of his knowledge and time during the entire course of this work.

Drs. Daniel J. Collins, Frank D. Faulkner, James A. Miller and James V. Saunders for their service on the examination committee and for their useful criticisms.

Dr. Roger T. Williams for his encouragement, and a number of valuable suggestions.

The staff of the Computer Facility of the Naval Postgraduate School, and, in particular, the Operations Manager, Mr. David F. Norman, for their aid and cooperation in making available large amounts of computer time.

Finally to his wife, Elise, and his children for their encouragement and patient acceptance of the demands this undertaking put upon him.

I. INTRODUCTION

A. BACKGROUND AND OBJECTIVES

The phenomenon of turbulent flow has been the subject of numerous theoretical and experimental investigations since the publication of the results of the definitive experiments of Reynolds (1883). Yet, despite these efforts, our knowledge and ability to predict quantities of technical importance in a turbulent shear flow remain severely limited.

The fundamental difficulty encountered in theoretical investigations of turbulence arises from the non-linear character of the equations of motion. The operation of statistical averaging introduces an additional dependent variable, the Reynolds stress, to the equations for the mean flow. The dynamic equation for the Reynolds stress involves higher order correlations, and so on. Although the basic equations are determinate, the statistically averaged equations are not. This is the so-called closure problem of the statistical theory. Hypotheses for the closure of the averaged equations range from the mixing length approach of Prandtl (1925) to the rather formidable Direct-Interaction approximation of Kraichnan (1964).

The advent of the high-speed digital computer has excited interest in a new approach to the problem of turbulence, the numerical integration of the basic equations by means of a suitable finite-difference representation. The potential value of such an approach lies not in the determination of the mean quantities in a particular flow, but rather in the possibility of determining, subject to the uncertainties which beset any numerical experiment, detailed and comprehensive

information about the structure of the turbulent motion. This information would be useful for the development of suitable models for the effects of the turbulence, and for the testing of existing closure hypotheses.

The numerical approach is not without serious difficulties. The representation of the wide range of scales of motion involved in a turbulent flow produces staggering demands on the capacity and speed of the computer. In fact, the requirements are far beyond what is presently available (Orsag 1969). However, such calculations, at moderate values of the Reynolds number, may be possible within a decade.

A second difficulty concerns the development and testing of a finite-difference model which is stable, accurate and, in terms of computational requirements, efficient. A rigorous proof of the stability and convergence of finite-difference approximations to non-linear partial differential equations does not seem possible. Certain necessary conditions can be obtained by analysis of the linearized equations, but sufficient conditions are generally not available. The usual recourse is to demonstrate that the numerical solution does give a known result in some special case. A number of distinct finite-difference representations have been developed and employed for fluid dynamics problems, each with different strong points and weaknesses. There does not seem to be any general agreement as to which approach might be the best for a given application.

The present capabilities of digital computers do permit numerical integrations for three-dimensional shear flows if a fairly coarse mesh is employed. In a number of recent investigations attempts have been

made to determine the behavior of the mean flow by means of a finite-difference representation which includes a model for the subgrid-scale motion (Deardorff 1970), (Galloway 1968). These are considered in somewhat greater detail in Section C.2. There are three fundamental difficulties associated with such undertakings. The first is the present lack of a sufficiently accurate model for the subgrid-scale motion. Secondly, the effect of the mesh size on the model for the subgrid-scale motion, and on the mean flow is largely undetermined. Finally the requirements for the accurate representation of even large-scale motions in the high shear layers near the boundaries may be greater than the coarse mesh permits. Despite these difficulties, qualitatively satisfying results have been obtained.

Another approach, which is within the capabilities of current digital computers, is the numerical integration of the two-dimensional equations. There are fundamental and significant differences between two- and three-dimensional unsteady motions, which are considered briefly in Section B. However, the equally fundamental non-linearity of the equations remains. Two-dimensional disturbances in a parallel shear flow will, to a limited degree, excite motions of different scale and create apparent stresses which deform the mean flow. The results of a numerical simulation of a two-dimensional turbulent motion might be useful, to some degree, for the development of a suitable model for the effects of the small scales of motion, and the testing of various hypotheses concerning the structure of the turbulence.

Considerations affecting the finite-difference formulation and solution are qualitatively the same for the two-dimensional problem as for the ultimate three-dimensional one. Whatever difficulties beset

the former will be increased in the latter, due to the greatly increased number of mesh points. Schemes, which are unsuitable in the two-dimensional case, will almost certainly be unsuitable in the three-dimensional one. Schemes which are stable and accurate in two dimensions are likely to be stable and accurate in three, although the fairly well-known stability constraints will be more severe in the three-dimensional case.

For the case of a channel flow with periodic boundary conditions upstream and downstream, the two-dimensional problem offers the possibility of testing the stability and accuracy of the linear features of the formulation by comparison with the established results of the Orr-Sommerfeld theory.

The present investigation involves just such a numerical integration for a two-dimensional plane Poiseuille flow with periodic disturbances. The objectives are:

1. To develop a stable, accurate and efficient finite-difference formulation for the plane Poiseuille flow, and to test its accuracy in a long-term integration by comparison with established results from the linear theory.
2. To apply the method for the determination of finite-amplitude effects on the stability of small disturbances.
3. To determine, if possible, an equilibrium condition for the two-dimensional flow by long-term integration with a growing disturbance.

B. DIFFERENCES BETWEEN TWO- AND THREE-DIMENSIONAL UNSTEADY MOTION

There are fundamental differences between the kinds of non-linear interactions that can take place in two- and three-dimensional unsteady

flows. The effects of these differences are often described by noting the absence of "vortex stretching" in a two-dimensional flow. For zero viscosity, the circulation about all closed curves which move with a fluid particle remains constant. In a two-dimensional flow, all such curves remain in the plane, and the well-known result is the invariance of the vorticity of a particle. A three-dimensional flow is capable of bending or twisting a closed curve which moves with a particle. The curl of the velocity vector can change its direction: the component of vorticity in a specified plane can change.

Kraichnan (1967) has shown that as a result of the existence of local inviscid constants, a two-dimensional flow admits of two formal inertial ranges, the usual $-5/3$ range and an additional -3 range. The -3 range, in this case, involves a cascade of vorticity to higher wave numbers, and the $-5/3$ range a cascade of energy to lower wave numbers, larger scales of motion.

C. PREVIOUS NUMERICAL WORK

1. Preliminary Remarks

The equations of motion for an incompressible flow can be written in the familiar way, in terms of the velocity vector and the pressure.

$$\frac{\partial \bar{V}}{\partial t} + (\bar{V} \cdot \nabla) \bar{V} = -\nabla P + \nu \nabla^2 \bar{V} \quad (1.1)$$

with the additional requirement that

$$\nabla \cdot \bar{V} = 0 \quad (1.2)$$

to satisfy the conservation of mass. The equation for the pressure is found by taking the divergence of equation (1.1).

$$\nabla \cdot [(\bar{V} \cdot \nabla) \bar{V}] = -\nabla^2 P \quad (1.3)$$

Another formulation, which implicitly satisfies the conservation of mass, is in terms of the curl of the velocity vector, $\bar{\Gamma}$, and a vector velocity potential, $\bar{\psi}$, which may be regarded as a generalized stream function.

$$\frac{\partial \bar{\Gamma}}{\partial t} = - [(\nabla \times \bar{\psi}) \cdot \nabla] \bar{\Gamma} + (\bar{\Gamma} \cdot \nabla) (\nabla \times \bar{\psi}) + \nabla^2 \bar{\Gamma} \quad (1.4)$$

where

$$\bar{\Gamma} = \nabla(\nabla \cdot \bar{\psi}) - \nabla^2 \bar{\psi} \quad (1.5)$$

and

$$\bar{V} = \nabla \times \bar{\psi} \quad (1.6)$$

Without restricting the solution, $\bar{\psi}$ can be specified to be non-divergent (Aziz 1967). Then (1.5) becomes

$$\bar{\Gamma} = - \nabla^2 \bar{\psi} \quad (1.7)$$

In the case of a two-dimensional motion, this formulation becomes the ordinary stream function-vorticity expression.

Finite-difference approximations to the equations of motion in terms of \bar{V} and P generally involve a staggered mesh arrangement in which pressures are defined at one family of mesh points and velocities at the other. The treatment of the boundary conditions for the pressure at the walls requires the establishment of virtual mesh points outside the domain and somewhat arbitrary specifications for the values of velocity at those points. Conservation of mass is not satisfied exactly, but the solution of a Poisson equation (1.3) for the pressure is designed so that at each point the divergence of the velocity is given a rate of change that will tend to correct for the accumulated divergence at that point.

Finite-difference representations based on equations (1.4) and (1.7) conserve mass implicitly. It is generally possible to derive a consistent explicit treatment of the boundary values for the vorticity without defining virtual points outside of no-slip boundaries. For three-dimensional integrations based on these equations a corrective procedure, similar to the one employed for the pressure calculation above, is required to maintain the zero divergence of $\bar{\psi}$.

The essential mathematical features of both approaches are the same. At each time step a forecast for new values of \bar{V} or \bar{T} is obtained from the finite-difference representation of (1.1) or (1.4). The solution of a Poisson equation for the pressure in the first case, or three such equations for the components of $\bar{\psi}$ in the second, completes a time step. It is the Poisson solution which generally takes up most of the computing time.

2. Summary of Selected Numerical Investigations

In a very well-known work, Fromm (1963) has employed a finite-difference representation based on the vorticity transport equations to follow the development of the vortex street behind a rectangular obstacle in a two-dimensional flow. The agreement between his computed streak lines and photographs of similar real flows is striking. The finite-difference representation involved an energy-conserving representation of the non-linear terms, an explicit formulation of boundary values of the vorticity at the moving walls, and periodic boundary conditions upstream and downstream. The time differencing was by the Du Fort-Frankel method. The domain of numerical stability was determined by analysis of the linearized equations and extensive numerical experiment. The finite-difference mesh contained 25×57 points. The

Poisson equation for the stream function was solved by Gauss-Seidel iteration.

Perhaps the best-known finite-difference representation based on the momentum equations is the Marker and Cell method of Harlow and Welsh (1965). The scheme, which was designed to be suitable for the representation of a flow with a free surface, employs a staggered mesh in which the components of velocity and the pressure are defined at distinct families of points. The treatment of solid boundaries requires the establishment of virtual points outside the domain, and somewhat arbitrary relations between values at the virtual and interior points. The failure of the representation of the non-linear terms to conserve kinetic energy is an important defect for reasons which will be considered in Chapter IV. Reported calculations employed first-order forward time differencing. The Poisson equation for the pressure was solved by Gauss-Seidel iteration.

An investigation which is closely related to the present work is due to Dixon (1966). It is an application of finite-difference methods to the problem of spatially-growing disturbances in Poiseuille and plane Poiseuille flow. The finite-difference equations are based on a version of the vorticity transport equations with an explicit separation of the laminar components. The representation of the non-linear terms failed to conserve kinetic energy. In addition the particular first-order explicit formulation of the boundary values of vorticity was inconsistent with the otherwise second-order finite-difference representation. Alternating direction methods were employed for the time differencing and the Poisson equation was solved by Successive Over-relaxation. For the plane Poiseuille flow Dixon assumed symmetry about the midstream, and employed a mesh with external

streamwise dimension 37 times the radius. The mesh contained 10 points between the centerline and the wall, and 296 in the direction of the stream. Conditions at the entrance region were specified, and the evolution of the disturbance was followed downstream. The results were somewhat uncertain. No evidence of growing disturbances was found. At very low values of the Reynolds number the disturbance decayed. In all other cases the behavior of the disturbance was characterized by periodic amplification and decay.

Pearson (1964) has considered several finite difference approaches to the solution of a test problem. He asserted that if the representation is based on the vorticity transport equations, an iterative method for the time step, which includes a method of forecasting new values of the vorticity at the boundaries, is required. This was based on the observation that the basic equations do not include a specification of boundary values of the vorticity. It turned out, however, that the calculations were unstable unless the forecast was "smoothed" by weighting it with a fraction of the old value, and that the required weighting factor was in excess of 80 per cent. The procedure did produce a more rapid convergence of the iterative solution to the implicit equations for the time step. However, the results do not seem to constitute a convincing argument for the necessity of an iterative treatment of vorticity at no-slip boundaries.

Galloway (1968) has employed a second-order finite-difference representation of the momentum equations in an application to the three-dimensional flow in a channel of square cross section. The approach employs Du Fort-Frankel time differencing and an energy-conserving

representation of the non-linear terms. The Poisson equation for the pressure was solved by an interesting iterative procedure which takes advantage of the weak coupling between various groups of the algebraic equations. Calculations were performed in meshes containing 9^3 , 11^3 and 17^3 points. It was noted that the resolution was inadequate to accurately represent the unsteady motion, however refinements of the mesh produced marked improvements in the results. An integral representation of the sub-grid-scale motion was proposed for subsequent calculations.

Very recently Deardorff (1970) has performed calculations for a similar channel flow, at a high Reynolds number, which employed such an integral representation of the sub-grid-scale motion. The results are qualitatively satisfying, although it was noted that a number of improvements in the sub-grid model are needed.

II. STATEMENT OF THE PROBLEM AND BASIC EQUATIONS

The equations of motion for a two-dimensional incompressible flow are

$$\frac{\partial u}{\partial t} + u \frac{\partial u}{\partial x} + v \frac{\partial u}{\partial y} = - \frac{\partial P}{\partial x} + \frac{1}{R} \left(\frac{\partial^2 u}{\partial x^2} + \frac{\partial^2 u}{\partial y^2} \right) \quad (2.1)$$

$$\frac{\partial v}{\partial t} + u \frac{\partial v}{\partial x} + v \frac{\partial v}{\partial y} = - \frac{\partial P}{\partial y} + \frac{1}{R} \left(\frac{\partial^2 v}{\partial x^2} + \frac{\partial^2 v}{\partial y^2} \right) \quad (2.2)$$

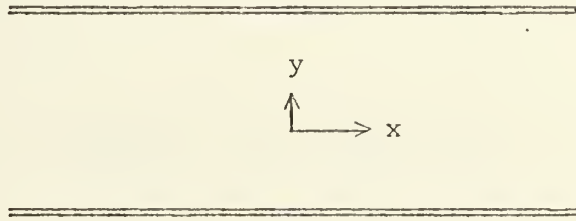
where u and v are the dimensionless components of velocity, P is the pressure and R is the Reynolds number which is defined by

$$R = \frac{VL}{\nu} \quad (2.3)$$

where V is the unit of velocity, L is the unit of length and ν is the kinematic viscosity. The equation of continuity is

$$\frac{\partial u}{\partial x} + \frac{\partial v}{\partial y} = 0 \quad (2.4)$$

We consider the two-dimensional flow between fixed parallel planes. The origin of coordinates is midway between the planes with the x -axis parallel and the y -axis normal to them.



Let the reference unit of length be one-half the distance between the parallel planes, and the reference unit of velocity be the mean value of the steady laminar flow velocity distribution.

Then the laminar flow velocity distribution and pressure gradient are given by

$$U(y) = -\frac{3}{2} (y^2 - 1) \quad (2.5)$$

$$\frac{dP}{dx} = \frac{3}{R} \quad (2.6)$$

If for the general case we let

$$u(x,y,t) = U(y) + u'(x,y,t) \quad (2.7)$$

$$v(x,y,t) = v'(x,y,t) \quad (2.8)$$

$$p(x,y,t) = P(x) + p'(x,y,t) \quad (2.9)$$

Then equations (2.1), (2.2) and (2.3) become

$$\frac{\partial u'}{\partial t} + U \frac{\partial u'}{\partial x} + v' \frac{dU}{dy} + u' \frac{\partial u'}{\partial x} + v' \frac{\partial u'}{\partial y} = -\frac{\partial P}{\partial x} - \frac{\partial p'}{\partial x} + \frac{1}{R} \left(\frac{\partial^2 u'}{\partial x^2} + \frac{\partial^2 u'}{\partial y^2} \right) \quad (2.10)$$

$$\frac{\partial v'}{\partial t} + U \frac{\partial v'}{\partial x} + u' \frac{\partial v'}{\partial x} + v' \frac{\partial v'}{\partial y} = -\frac{\partial P}{\partial y} - \frac{\partial p'}{\partial y} + \frac{1}{R} \left(\frac{\partial^2 v'}{\partial x^2} + \frac{\partial^2 v'}{\partial y^2} \right) \quad (2.11)$$

$$\frac{\partial u'}{\partial x} + \frac{\partial v'}{\partial y} = 0 \quad (2.12)$$

The no-slip boundary conditions require that at $y = \pm 1$

$$u' = v' = 0$$

An equation for the disturbance pressure can be obtained by differentiating equation (2.10) with respect to x , equation (2.11) with respect to y , and summing. Thus

$$\frac{\partial^2 p'}{\partial x^2} + \frac{\partial^2 p'}{\partial y^2} = 2 \left[\frac{\partial u'}{\partial x} \frac{\partial v'}{\partial y} - \left(\frac{dU}{dy} + \frac{\partial u'}{\partial y} \right) \frac{\partial v'}{\partial x} \right] \quad (2.13)$$

We can, without confusion, delete the primes in the subsequent notation for the disturbance quantities.

If we specify in addition that the disturbance makes no contribution to the total mass flow;

i.e. that
$$\int_{-1}^1 u(x,y,t) dy = 0 \quad (2.14)$$

then the reference unit of velocity, as previously defined, is as well the mean transport velocity. This conforms to the usual choice of reference velocity for turbulent channel flows.

A more compact, and for purposes of computing, more efficient formulation of the basic equations is obtained by introducing the stream function and the vorticity.

Let
$$u = - \frac{\partial \psi}{\partial y}, \quad v = \frac{\partial \psi}{\partial x} \quad (2.15)$$

$$\Gamma = \frac{\partial v}{\partial x} - \frac{\partial u}{\partial y} \quad (2.16)$$

Then equation (2.12) is implicitly satisfied. Equations (2.10) and (2.11) become

$$\frac{\partial \Gamma}{\partial t} + U \frac{\partial \Gamma}{\partial x} - U'' \frac{\partial \psi}{\partial x} - \frac{\partial \psi}{\partial y} \frac{\partial \Gamma}{\partial x} + \frac{\partial \psi}{\partial x} \frac{\partial \Gamma}{\partial y} = \frac{1}{R} \left(\frac{\partial^2 \Gamma}{\partial x^2} + \frac{\partial^2 \Gamma}{\partial y^2} \right) \quad (2.17)$$

where

$$\Gamma = \frac{\partial^2 \psi}{\partial x^2} + \frac{\partial^2 \psi}{\partial y^2} \quad (2.18)$$

and

$$U'' = \frac{d^2 U}{dy^2} = -3$$

The no-slip boundary conditions require that at $y = \pm 1$

$$\frac{\partial \psi}{\partial x} = \frac{\partial \psi}{\partial y} = 0 \quad (2.19)$$

Equation (2.14) becomes

$$\int_{-1}^1 \frac{\partial \psi}{\partial y} dy = \psi(x, +1, t) - \psi(x, -1, t) = 0 \quad (2.20)$$

Thus the no-slip boundary conditions become

$$\psi(x, \pm 1, t) = \psi(x, -1, t) = \text{const} \quad (2.21)$$

$$\frac{\partial \psi}{\partial y}(x, \pm 1, t) = 0. \quad (2.22)$$

If we consider a finite region of the space between the parallel planes, and specify the initial state of the disturbance and the conditions at the upstream and downstream boundaries of the region, then, in principle, the evolution of the disturbance can be determined by means of a suitable numerical method. Unfortunately the question of the proper boundary conditions upstream and downstream is somewhat moot. A reasonable recourse is to assume that the motion is periodic in the direction of the mean flow. Thus we consider a disturbance such that

$$\psi(x \pm 2nh, y, t) = \psi(x, y, t) \quad (2.23)$$

$$\Gamma(x \pm 2nh, y, t) = \Gamma(x, y, t) \quad (2.24)$$

$$n = 0, 1, 2, \dots$$

where the basic period is $2h$.

It should be emphasized that, in the present formulation, the disturbance quantities do not describe a two-dimensional turbulent motion, but rather the total departure of the motion from the steady laminar flow. The turbulent motion is described by the difference between the disturbance and an appropriately defined mean value of the disturbance.

In the present case, as a consequence of the assumed periodicity of the motion, the disturbance is homogeneous in the streamwise direction. That is, all statistical correlations are independent of the origin of the x coordinate. Then an appropriate definition of the statistical mean value of a disturbance quantity is the average value over a period in the x direction.

Some remarks about notation are in order. It has become necessary to distinguish between quantities associated with the laminar flow, the disturbance, the mean flow and the turbulence. Some indulgence on the part of the reader will be required.

With the exception of certain quadratic quantities such as turbulent energy or Reynolds stress, mean values, obtained by means of the linear operator

$$\frac{1}{2h} \int_{-h}^h dx$$

are denoted by an overbar. All quantities associated with the two-dimensional turbulence are denoted by a circumflex.

The distinction between local and mean values of quadratic quantities associated with the turbulence is indicated in the arguments of the various functions, or in the case of finite-difference expressions, the subscripts. Thus, since the averaging operator is linear,

$$\begin{aligned}\hat{u}(x,y,t) &= u(x,y,t) - \bar{u}(y,t) \\ \hat{v}(x,y,t) &= v(x,y,t) - \bar{v}(y,t) \\ \hat{\psi}(x,y,t) &= \psi(x,y,t) - \bar{\psi}(y,t) \\ \hat{\Gamma}(x,y,t) &= \Gamma(x,y,t) - \bar{\Gamma}(y,t)\end{aligned}\tag{2.25}$$

where

$$\begin{aligned}\hat{u}(x,y,t) &= -\frac{\partial}{\partial y} \hat{\psi}(x,y,t) \\ \bar{u}(y,t) &= -\frac{\partial}{\partial y} \bar{\psi}(y,t) \\ \hat{v}(x,y,t) &= \frac{\partial}{\partial x} \hat{\psi}(x,y,t) \\ \bar{v}(y,t) &= \frac{\partial}{\partial x} \bar{\psi}(y,t) \equiv 0\end{aligned}\tag{2.26}$$

The mean flow velocity and vorticity are given by

$$w(y,t) = U(y) - \frac{\partial}{\partial y} \bar{\psi}(y,t) \quad (2.27)$$

$$\Omega(y,t) = -U'' + \bar{\Gamma}(y,t) \quad (2.28)$$

It is convenient at this point to define a number of quantities which are calculated in the numerical scheme, and to derive expressions for them in terms of the stream function. The kinetic energy in the mean flow is

$$\begin{aligned} E(y,t) &= 1/2 w^2(y,t) \\ &= 1/2 \left[U(y) - \frac{\partial}{\partial y} \bar{\psi}(y,t) \right]^2 \end{aligned} \quad (2.29)$$

The normalized sum of mean flow kinetic energy over a domain which includes one period of the disturbance is

$$\begin{aligned} E(t) &= \frac{1}{2h} \int_{-h}^h dx \frac{1}{2} \int_{-1}^1 E(y,t) dy \\ &= \frac{1}{2} \int_{-1}^1 E(y,t) dy \end{aligned} \quad (2.30)$$

The kinetic energy in the turbulent motion is

$$\hat{E}(x,y,t) = \frac{1}{2} \left[\left(-\frac{\partial \hat{\psi}}{\partial y} \right)^2 + \left(\frac{\partial \hat{\psi}}{\partial x} \right)^2 \right] \quad (2.31)$$

The mean value is

$$\hat{E}(y,t) = \frac{1}{2h} \int_{-h}^h \hat{E}(x,y,t) dx \quad (2.32)$$

And the normalized sum of turbulent kinetic energy over the domain is

$$\begin{aligned}
\hat{E}(t) &= \frac{1}{2h} \int_{-h}^h dx \frac{1}{2} \int_{-1}^1 \hat{E}(x,y,t) dy \\
&= \frac{1}{2} \int_{-1}^1 \hat{E}(y,t) dy
\end{aligned} \tag{2.33}$$

Finally the Reynolds stress produced by the two-dimensional turbulent motion is

$$S(y,t) = \frac{1}{2h} \int_{-h}^h \frac{\partial \hat{\psi}}{\partial x} \frac{\partial \hat{\psi}}{\partial y}(x,y,t) dx$$

III. ANALYSIS OF THE TRANSFORMED EQUATIONS

A. BASIC EQUATIONS IN TERMS OF FOURIER COMPONENTS

The equations of motion for the plane Poiseuille flow with periodic disturbances can also be expressed in terms of the wave number in the x direction by means of the finite Fourier Transform.

$$\begin{aligned} \text{Let} \quad f_n(y,t) &= \frac{1}{2h} \int_{-h}^h \psi(x,y,t) e^{i\alpha n x} dx \\ g_n(y,t) &= \frac{1}{2h} \int_{-h}^h \Gamma(x,y,t) e^{i\alpha n x} dx \end{aligned} \quad (3.1)$$

Then

$$\begin{aligned} \psi(x,y,t) &= \sum_{n=-\infty}^{\infty} f_n(y,t) e^{-i\alpha n x} \\ \Gamma(x,y,t) &= \sum_{n=-\infty}^{\infty} g_n(y,t) e^{-i\alpha n x} \end{aligned} \quad (3.2)$$

where $\alpha = \pi/h$. Since both ψ and Γ are real,

$$\begin{aligned} f_{-n}(y,t) &= f_n^*(y,t) \\ g_{-n}(y,t) &= g_n^*(y,t) \end{aligned} \quad (3.3)$$

where the asterisk indicates a complex conjugate.

By means of the transform operator

$$\frac{1}{2h} \int_{-h}^h e^{i\alpha n x} dx$$

and the associated orthogonality relation

$$\frac{1}{2h} \int_{-h}^h e^{-i\alpha(n-s)x} dx = 1 \quad \text{if } s = n$$

$$= 0 \quad \text{otherwise}$$

it can be shown that equations (2.17) and (2.18) are satisfied if

$$(g_n'' - \alpha^2 n^2 g_n) - R \frac{\partial}{\partial t} g_n + i\alpha n R \left[(U-f'_0) g_n - (U''-f'''_0) f_n \right]$$

$$- i\alpha R H_n = 0 \quad (3.4)$$

$$n = 0, 1, 2, \dots$$

where

$$g_n = f_n'' - \alpha^2 n^2 f_n \quad (3.5)$$

$$H_n = \sum_{s=1}^{\infty} \left\{ (n-s) (f'_s g_{n-s} - g'_s f_{n-s}) + (n+s) (f_{s+s}^* g_{n+s} - g_{s+s}^* f_{n+s}) \right\} \quad (3.6)$$

and primes denote derivatives with respect y . The no-slip boundary conditions require that at $y = \pm 1$

$$f_n = f'_n = 0 \quad (3.7)$$

$$n = 0, 1, \dots$$

The functions $f_0(y,t)$ and $g_0(y,t)$ represent the mean values of the disturbance stream function and vorticity respectively. In terms of these variables, the mean velocity, equation (2.27), is given by

$$w(y,t) = U(y) - f'_0(y,t) \quad (3.8)$$

The non-linear interaction between the n^{th} mode of the disturbance with the distorted mean flow is represented by the term

$$(U-f'_0) g_n - (U''-f'''_0) f_n$$

in equation (3.4). The non-linear interaction between the n^{th} mode and the other disturbance modes is given by H_n . The equation for the

mean flow is, from equations (3.4), (3.5) and (3.6),

$$f_o''' - R \frac{\partial}{\partial t} f_o'' - i\alpha R \sum_{s=1}^{\infty} \left\{ s \left[(g_s f_s^*) - (g_s f_s^*)^* \right] \right\} = 0 \quad (3.9)$$

Equations (3.4) and (3.7) govern the behavior of periodic disturbances of finite amplitude in a plane Roiseuille flow. They are an infinite set of coupled non-linear partial differential equations.

Previous analysis of the finite-amplitude disturbances has generally involved the truncation of this set of equations, the deletion of certain non-linear terms to uncouple the remaining equations and various assumptions about the time dependence of the remaining modes. A brief description of the most prominent investigations is given in Section C.

B. LINEAR THEORY

If the amplitude of the disturbance is sufficiently small so that the terms quadratic in the amplitude, the non-linear terms, may be ignored in comparison with the linear terms, then equations (3.4) and (3.5) become

$$(g_n'' - \alpha^2 n^2 g_n) - R \frac{\partial}{\partial t} g_n + i\alpha n R \left[U g_n - U'' f_n \right] = 0 \quad (3.10)$$

$$g_n = f_n'' - \alpha^2 n^2 f_n \quad (3.11)$$

In this case the solutions for the various modes are uncoupled. By absorbing the index n into the definition of α , and assuming the separation of variables

$$\begin{aligned} f(y,t) &= \Phi(y) e^{i\beta t} \\ g(y,t) &= \theta(y) e^{i\beta t} \end{aligned} \quad (3.12)$$

where β is, in general, complex.

Equations (3.10) and (3.11) become

$$(\theta'' - \alpha^2 \theta) + i\alpha R \left[(U - \beta/\alpha) \theta - U''\Phi \right] = 0 \quad (3.13)$$

$$\theta = \Phi'' - \alpha^2 \Phi \quad (3.14)$$

Or in terms of Φ alone,

$$(\Phi^{IV} - 2\alpha^2 \Phi'' + \alpha^4 \Phi) + i\alpha R \left[(U - \beta/\alpha) (\Phi'' - \alpha^2 \Phi) - U''\Phi \right] = 0 \quad (3.15)$$

The boundary conditions, equation (3.7), require that at $y = \pm 1$

$$\Phi = \Phi' = 0 \quad (3.16)$$

If the spatial wave number, α , and the Reynolds number, R , are specified, then equation (3.15) has solutions which satisfy the homogeneous boundary conditions only for discrete values of the complex number β . Equation (3.15) is the well-known Orr-Sommerfeld equation.

From equation (3.15) it is evident that, if the imaginary part of β is negative, the amplitude of the disturbance increases with time. The disturbance is said to be unstable. If the imaginary part is positive the disturbance is stable. Of particular interest are conditions of neutral stability. The largest value of the Reynolds number at which, for all α , all the eigenvalues of equation (3.15) are stable is termed the critical Reynolds number. Schensted (1960) has shown that for a plane Poiseuille flow the eigenfunctions of equation (3.15) form a complete set. Any continuous function which satisfies the boundary conditions, equations (3.16), can be represented as a linear combination of them. Thus if, at given values of α and R , all of the eigensolutions of equation (3.15) are stable, the flow is stable with respect to all infinitesimal disturbances.

The solutions of equation (3.15) for the case of plane Poiseuille flow have been extensively investigated. The zone of linear instability in the Reynolds number-wave number domain, and the associated curve of neutral stability, have been established in a number of investigations, the most prominent of which is due to Lin (1945). Following a procedure based on asymptotic expansions, which was outlined by Heisenberg (1924), Lin calculated values of α and R on the neutral curve and determined a critical Reynolds number (in terms of the reference length and velocity of the present investigation) of 3540 at a wave number of 1.04.

Thomas (1953) employed a basically fourth-order finite-difference representation of equation (3.15) for the determination of the primary eigenvalues associated with the symmetric modes at eighteen points in the vicinity of the critical point. The discrete representation of the eigenfunction involved 101 points between the centerline and the wall. The resulting algebraic equations were solved by direct Gauss elimination. The calculations, which were performed on an early electronic calculator, required two weeks of machine time. He determined by interpolation a critical value of the Reynolds number equal to 3850 at a wave number of 1.04. For the calculation at $R = 6666.7$ and $\alpha = 1.0$ the values of the primary eigenfunction at the 101 grid points are tabulated.

Potter (1966) has used methods generally similar to those of Lin, but with a different expansion for the inviscid solution, to investigate the linear modes of a combined plane Couette-Poiseuille flow. His results for the Poiseuille flow indicate that there are slight errors in Lin's neutral curve for $\alpha > .8$. Potter suggested that this was due to the slow convergence of Lin's expansion in that region.

More recently Grosch (1968) has employed an expansion of the solutions of equation (3.15) in terms of the known eigenfunctions of

$$\begin{aligned}\Phi''' - \alpha^2 \Phi'' + \alpha^4 \Phi &= \lambda^4 \Phi \\ \Phi(\pm 1) &= \Phi'(\pm 1) = 0\end{aligned}$$

The expansion was truncated generally after thirty terms, and the resulting algebraic eigenvalue problem was solved by means of the Q R algorithm (Wilkinson 1965). His results showed excellent agreement with those of Thomas for both the various eigenvalues and the tabulated eigenvector at $R = 6666.7$, $\alpha = 1$. The results for the neutral curve confirm Potter's observations. Solutions are obtained for both symmetric and antisymmetric modes. Instabilities are found only for the symmetric modes, and in no case is more than one of the calculated modes, at a given α and R , unstable.

A portion of the neutral curve for the Plane Poiseuille flow based on the data of Lin and Grosch is shown in Fig. 1.

All reference to Reynolds numbers and dimensionless wave numbers has been in terms of the reference length and velocity employed in this investigation, one half the channel width and the mean laminar velocity. In the investigations of Lin and Thomas the reference unit of velocity is the maximum laminar velocity. Based on that value, the Reynolds number is exactly 1.5 times values given here. In the works of Grosch and Potter (for the case of zero Couette component) the reference unit of length is the channel width, and the reference velocity is the maximum laminar velocity. Wave numbers are twice those given here, and Reynolds numbers three times those given here.

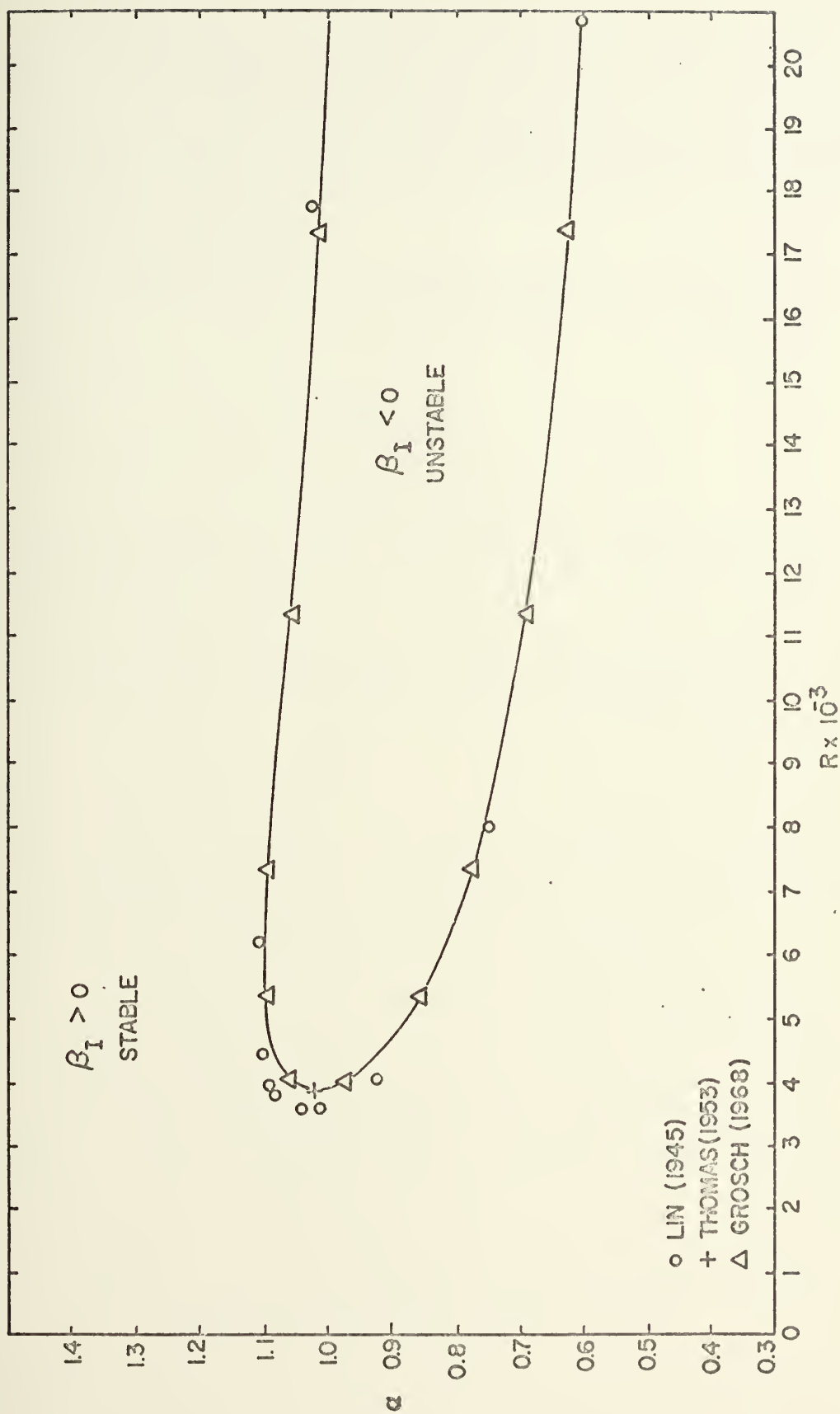


FIGURE 1 CURVE OF NEUTRAL STABILITY FOR PLANE POISEUILLE FLOW.

It is convenient, and useful for the interpretation of some of the results of the numerical integrations of the linearized equations, to indicate at this point certain relations for the total kinetic energy in the linear solutions. Equations (3.2) and (3.12) for the linear solutions are equivalent to

$$\psi(x,y,t) = 2e^{-\beta_I t} \bar{\phi}_R(y) \cos(\alpha x - \beta_R t) + \bar{\phi}_I(y) \sin(\alpha x - \beta_R t) \quad (3.17)$$

where

$$\dot{\beta} = \beta_R + i\beta_I$$

$$\dot{\phi} = \bar{\phi}_R \text{ \& } i\bar{\phi}_I$$

It is easy to show that, if $h = \pi/\alpha$, the total disturbance energy, equation (2.33) is given by

$$\begin{aligned} \hat{E}(t) &= \alpha/2 e^{-2\beta_I t} \int_{-1}^1 \left[(\bar{\phi}_R'^2 + \bar{\phi}_I'^2) + \alpha^2 (\bar{\phi}_R^2 + \bar{\phi}_I^2) \right] dy \\ &= \text{const} \times e^{-2\beta_I t} \end{aligned} \quad (3.18)$$

The disturbance energy grows, or decays exponentially at twice the rate of the disturbance amplitude. The disturbance itself grows or decays exponentially and changes its phase at the rate β_R/α .

If, in the linear problem, the disturbance is composed of a number of the linear eigenfunctions with the same wave number, α , then the total disturbance energy will contain terms like equation (3.18) peculiar to each eigenfunction $\bar{\phi}$ and eigenvalue β , plus cross-coupling terms which involve pairs of the modes.

For example, if the disturbance is composed of two eigenfunctions

$$\psi(x,y,t) = \psi_1(x,y,t) + \psi_2(x,y,t)$$

where

$\Phi(y)$ and β describe ψ_1

$\eta(y)$ and γ describe ψ_2

Then it can be shown that the total disturbance energy is given by

$$\begin{aligned} \hat{E}(t) = & \hat{E}_1(t) + \hat{E}_2(t) \\ & + \alpha e^{-(\beta_I + \gamma_I)t} \left\{ A \cos [(\beta_R - \gamma_R)t] - B \sin [(\beta_R - \gamma_R)t] \right\}. \end{aligned} \quad (3.19)$$

where $E_1(t)$ and $E_2(t)$ are from equation (3.18), and A and B are given by

$$\begin{aligned} A = & \int_{-1}^1 \left[(\Phi'_R \eta'_R + \Phi'_I \eta'_I) + \alpha^2 (\Phi_R \eta_R + \Phi_I \eta_I) \right] dy \\ B = & \int_{-1}^1 \left[\Phi'_R \eta'_I - \Phi'_I \eta'_R - \alpha^2 (\eta_R \Phi_I - \Phi_R \eta_I) \right] dy. \end{aligned}$$

Thus, in this case, the total disturbance energy contains terms with exponential growth rates $-2\beta_I$, $-2\gamma_I$ and $-(\beta_I + \gamma_I)$, and the last term oscillates with frequency $(\beta_R - \gamma_R)$.

If

$$-2\beta_I > -2\gamma_I$$

then eventually $\hat{E}_1(t)$ will overshadow the other terms.

C. NON-LINEAR ANALYSIS

A fundamental consequence of the non-linearity of the equations of motion is the production of the Reynolds stress and the resulting deformation of the mean flow. The distortion of the mean flow, which is dependent on the amplitude of the disturbance, can alter the rate of transfer of energy from the mean flow to the disturbance and, as a result, change its rate of growth or decay.

A second non-linear effect is the excitation of disturbance motions of other wave lengths. Dynamical constraints on the non-linear interactions in a two-dimensional motion limit the systematic transfer of kinetic energy to smaller scales of motion (Lilly 1965, Kraichnan 1967). As a result, it is expected that, in terms of the kinetic energy in the various disturbance modes, the primary mode will remain dominant. Thus the question of non-linear stability centers on the behavior of the amplitude of the primary mode. If, with increasing time, the amplitude approaches zero, it is stable; if not, it is unstable. Stuart (1958) has employed the terms subcritical and supercritical to describe the stable and unstable regions in the wave number-Reynolds number domain for infinitesimal (linear) disturbances. Subcritical instability refers to the growth of a disturbance of finite amplitude at a wave number and Reynolds number for which it is stable in the linear analysis.

A question separate from that of stability concerns the existence of an equilibrium state. It seems reasonable to expect that at some sufficiently large amplitude the non-linear interactions will limit the growth of the disturbance motion.

In an early investigation, Meksyn and Stuart (1958) employed a variation of the asymptotic methods of the linear problem which included the distortion of the mean velocity. Their results suggest the existence of subcritical instabilities at values of the Reynolds number as low as 1933.3.

Subsequently Stuart (1958) derived an approximate expression for the time dependence of the amplitude of the primary mode of the disturbance. The analysis is based on an energy balance and, as Stuart

indicates, may have questionable applicability to flows, such as the plane Poiseuille flow, for which the precise details of the mean motion are of crucial importance to the question of stability. In the development only the interaction between the primary mode and the mean flow is considered; the generation of higher harmonics in the disturbance motion is ignored. In addition it is assumed that the time derivative of the mean velocity is always negligible and that the phase velocity and the shape of the primary mode are as given by the linear theory.

With reference to equations (3.4) this is equivalent to

$$f_n(y,t) = 0 \quad n = 2, 3, \dots$$

$$f_1(y,t) = A(t) \Phi_1(y) e^{i\beta_R t}$$

$$\beta_R \ll 1$$

where $A(t)$ is an amplitude factor and $\Phi(y)$ and β_R are from the linear analysis. From the energy balance it is deduced that $A(t)$ satisfies an equation of the form

$$\frac{d(A^2)}{dt} = (K_1 - K_2) A^2 - K_3 A^4$$

where K_1 is associated with the energy production terms, K_2 with the viscous dissipation, and K_3 is determined by the non-linear interactions. At sufficiently small amplitudes the latter term is negligible and the sign of $(K_1 - K_2)$ determines the stability. If $K_3 < 0$, then regardless of the sign of $(K_1 - K_2)$ there is the possibility of finite amplitude instability.

In subsequent undertaking, Stuart (1960) and Watson (1960) derived a formal expansion for the solutions to the non-linear equations (3.4). Based on certain order-of-magnitude arguments, the Fourier expansion

(3.2) for the solution is truncated after $n=2$, and enough of the non-linear terms are deleted so that the remaining equations are uncoupled. A separation of variables is assumed for the functions $f_1(y,t)$ and $f_2(y,t)$, in which they are expressed in terms of perturbations of the corresponding linear solutions, and a complex amplitude function, $A(t)$, which includes the changes in the phase speed due to the non-linear interactions. This function is assumed to satisfy

$$\frac{d|A|^2}{dt} = -\beta_1 |A|^2 + a_1 |A|^4 + \dots \quad (3.20)$$

The result $a_1 < 0$ is taken to indicate either the existence of supercritical equilibrium condition or finite-amplitude stability in the subcritical domain. If $a_1 > 0$ then, in the subcritical case an unstable equilibrium is implied, and in the supercritical case this result is taken to indicate the absence of an equilibrium condition (at least at small amplitudes). The last conclusion must be qualified since if the disturbance continues to grow then eventually higher order terms in (3.20) will become significant: the assumptions upon which the formal expansion is based will no longer apply.

Reynolds and Potter (1967) have developed a somewhat more straightforward formulation of the Stuart-Watson expansion and performed the indicated calculations for the case of a combined plane Couette-Poiseuille flow. The results for Poiseuille flow indicate values of $a_1 < 0$ only near the lower branch of the neutral curve.

In similar but more extensive calculations, Pekeris and Shkoller (1967) found the zone of negative a_1 in the wave number-Reynolds number domain. It includes the lower branch, but excludes the vicinity of the upper branch of the curve of neutral stability for the linear problem.

IV. THE FINITE DIFFERENCE EQUATIONS AND SOLUTION

A. CHOICE OF THE METHOD

The formulation of the finite-difference model for the equations of motion is determined by considerations of accuracy, numerical stability and computational efficiency. The latter consideration refers to some weighted measure of computing time and storage requirement.

The fundamental equations of motion contain three dependent variables: pressure and two components of velocity. The vorticity transport equations contain two: stream function and vorticity. The essential mathematical features of each are the same: non-linear parabolic equations for the time derivatives; a linear elliptic equation for the pressure in the first case, and the stream function in the second. Thus, although there are important differences in the treatment of the boundary conditions, similar finite difference methods can be applied to each set of equations. The same kinds of stability and accuracy constraints on the finite-difference parameters, δx and δt , will occur in each case.

The stability and efficiency of the finite-difference representation of such equations is principally determined by the method of time differencing. A number of direct and implicit methods are available.

Consider equations of the form

$$\frac{\partial f}{\partial t} = D(f,g); \quad A(f) = B(g)$$

where

$$f = f(x,y,t) \quad g = g(x,y,t)$$

and A, B and D are differential operators in x and y. For the discrete representation in t let

$$f(x,y,t_K) = f^K(x,y)$$

$$g(x,y,t_K) = g^K(x,y)$$

where

$$t_K = K\delta t$$

Both Forward, and Modified Euler implicit time differencing require the simultaneous storage of two levels of the variables involved in the time differencing.

$$\frac{f^{N+1} - f^N}{\delta t} = D(f^N g^N) + O(\delta t)$$

$$\frac{f^{N+1} - f^N}{\delta t} = \frac{1}{2} D(f^{N+1} g^{N+1}) + \frac{1}{2} D(f^N g^N) + O(\delta t^2)$$

If, in the case of Modified Euler differencing, the implicit equations for f^{N+1} are solved by Gauss-Seidel iteration then it can be shown that the total storage requirement is the same as for forward differencing.

Central time differencing requires the simultaneous storage of three levels of the variables involved in the time differencing.

$$\frac{f^{N+1} - f^{N-1}}{2\delta t} = D(f^N g^N) + O(\delta t^2)$$

Thus, for an M x N finite-difference grid, the basic storage requirements may be summarized as follows.

TABLE I

Computer Storage Requirements

| | Momentum Equations | Vorticity Transport Equations |
|---|-----------------------|-------------------------------------|
| Forward, or Modified Euler Time Differencing | 5 (M x N) | 3 (M x N) |
| Central Time Differencing | 7 (M x N) | 4 (M x N) |

Clearly, in terms of the storage requirement, a formulation based on the vorticity transport equations is superior. In addition there are advantages in computing time. The velocity components, when they are required, can be obtained from the stream function with fewer operations than are required to perform the additional evaluation of a time derivative. A determination of the pressure field requires the additional solution of a Poisson equation. If this is required then some of these advantages disappear.

Of the three methods of time differencing considered, the Modified Euler method is, in principle, the most accurate and, in particular for non-linear problems such as this one, the least susceptible to numerical instability. However it is implicit: the solution of a set of simultaneous equations is required at each time step. The

most practical means of solving the equations is by Gauss Seidel Iteration or Successive Over-relaxation. Each step in the iteration will require a solution of the Poisson equation for the stream function; this demands all the operations that are involved in the course of a complete time step by an explicit method. Thus if an explicit method, of similar truncation error, can be made stable by reducing the time step by a factor less than the average number of iterations for the implicit case, it is to be preferred.

Forward time differencing is subject to linear stability constraints on the ratios $\delta t / \delta y$ and $\delta t / \delta y^2$, which are associated respectively with the diffusion and linear advection terms. Early experiments with this method indicated that even if these constraints were observed numerical instability occurred when the non-linear terms became sufficiently large.

If the ordinary second order finite difference representation of the diffusion term is employed, then the central time differencing is unstable at all values of δt . This instability is removed by the Du Fort-Frankel (1953) approximation to the diffusion term. There still remains a constraint on the ratio $\delta t / \delta y$, which is associated with the advection terms. Experiments were conducted with both the Central and the Modified Euler methods. At values of δt small enough so that the Central differencing is stable, the Modified Euler method required from six to eight iterations: that is between six and eight times the computational effort to produce essentially the same results. Increasing the magnitude of the time step produced a predictable instability with the Central differencing and an increased number of iterations for convergence with the Modified Euler method. At the

stability boundary for the Central differencing the ratio $\delta t/\delta y$ is of the order unity. Thus the Modified Euler method offers advantages only in a domain where the truncation errors associated with δt may be sufficiently large so as to obscure some transients in the solution. Accordingly, a formulation based on the vorticity transport equations, which employs the Du Fort-Frankel Central time differencing was used in this undertaking.

It should be noted that an important group of methods of time differencing has not been considered in the preceeding remarks. These are the Alternating Direction Implicit methods of Peaceman and Rachford (1955) and Douglas and Rachford (1956) and their variants. In each case the time increment is performed in two steps. In the first step, an intermediate value of the dependent variable is obtained by expressing certain of the spatial derivatives implicitly as in the Modified Euler method, and the others explicitly. In the second step the arrangement is reversed. Each step requires the solution of a set of simultaneous equations. The essential feature of the method is that these equations, in matrix form, are tri-diagonal: they may be solved directly and without storage penalty by a particularly simple case of Gauss Elimination (Richtmyer 1967). In applications to the equations for incompressible flow, the variations of the methods are due primarily to the particular treatment of the advection terms.

In the present investigation, the formulation of the upstream and downstream boundary conditions as well as the conservative finite difference representation of the advection terms introduce additional non-zero diagonals to the matrices which define the equations for each step. The matrices are no longer tri-diagonal: the essential advantages of the alternating direction methods do not obtain.

B. THE FINITE DIFFERENCE EQUATIONS

The computational domain, coordinates and the arrangement of the finite difference mesh are shown schematically in Figures (2) and (3). The mesh spacings are denoted by δx and δy , the value of the time step by δt . The mesh contains $M \times N$ points: M points in the x direction and N points in the y direction. The external dimensions are $2h$ and 2 respectively.

The particular treatment of the periodic boundary conditions requires the definition of virtual points just beyond the upstream and downstream boundaries. The boundaries lie midway between these points and the adjacent interior columns of points. The mesh is arranged so that points lie on the no-slip boundaries. Thus there are M intervals in the x direction and $N-1$ in the y direction.

Let

$$\Gamma_{K,J}^l = \Gamma(x_K, y_J, t_l)$$

$$\psi_{K,J}^l = \psi(x_K, y_J, t_l)$$

$$U_J = U(y_J)$$

where

$$\begin{aligned} x_K &= (K-1) \delta x - h + \delta x/2 & K &= 1, 2, \dots, M \\ y_J &= (J-1) \delta y - 1 & J &= 1, 2, \dots, N \end{aligned} \tag{4.1}$$

$$t_l = \sum_{n=1}^l \delta t_n$$

and

$$\begin{aligned} \delta x &= 2h/M \\ \delta y &= 2/(N-1) \end{aligned} \tag{4.2}$$

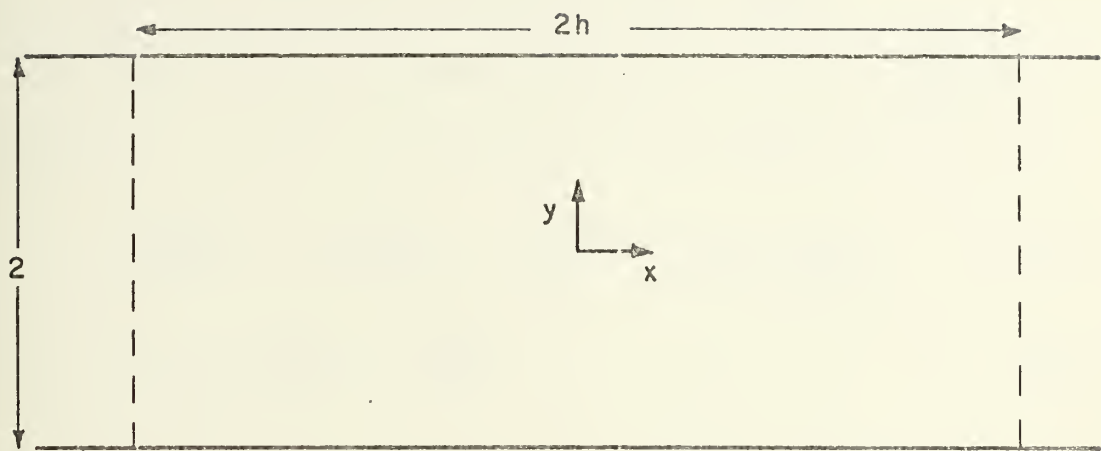
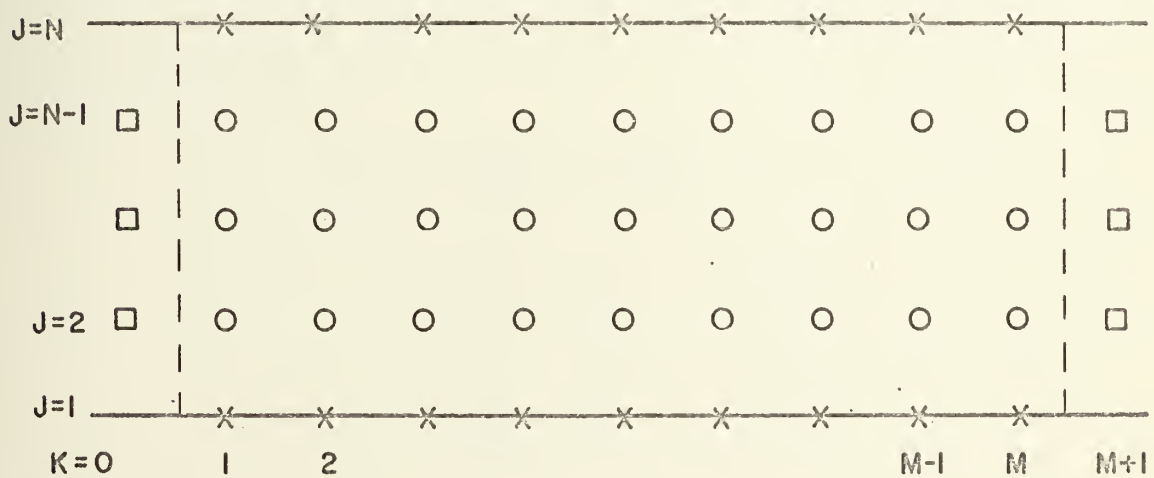


FIGURE 2 COORDINATES AND DOMAIN



- — INTERIOR POINTS
- — VIRTUAL POINTS FOR PERIODIC BOUNDARY CONDITIONS
- × — NO-SLIP BOUNDARY POINTS

FIGURE 3 FINITE DIFFERENCE MESH

In the calculations M is always even, and N odd. Thus the origin of the coordinates is at the mesh point $K = M/2$; $J = \frac{N+1}{2}$.

The finite difference approximation to the vorticity transport equation is

$$\frac{\delta \Gamma^1}{\delta t}_{K,J} = - U_J \frac{\delta \Gamma^1}{\delta x}_{K,J} + U'' \frac{\delta \psi^1}{\delta x}_{K,J} + J^1_{K,J} + \frac{1}{R} D^1_{K,J} \quad (4.3)$$

$$\Gamma^1_{K,J} = \frac{\delta^2 \psi^1}{\delta x^2}_{K,J} + \frac{\delta^2 \psi^1}{\delta y^2}_{K,J} \quad (4.4)$$

where $\frac{\delta}{\delta x}$, $\frac{\delta^2}{\delta x^2}$, etc., are the usual second-order central difference representations, $D^1_{K,J}$ is the Du Fort-Frankel approximation for the diffusion term and $J^1_{K,J}$ is the conservative representation due to Arakawa (1966). It may be regarded as a central difference approximation to the mean of three distinct, but equivalent, expressions for the non-linear terms.

$$\begin{aligned} J(\psi, \Gamma) &= \frac{\partial \psi}{\partial y} \frac{\partial \Gamma}{\partial x} - \frac{\partial \psi}{\partial x} \frac{\partial \Gamma}{\partial y} \\ &= \frac{\partial}{\partial y} \left(\psi \frac{\partial \Gamma}{\partial x} \right) - \frac{\partial}{\partial x} \left(\psi \frac{\partial \Gamma}{\partial y} \right) \\ &= \frac{\partial}{\partial x} \left(\Gamma \frac{\partial \psi}{\partial y} \right) - \frac{\partial}{\partial y} \left(\Gamma \frac{\partial \psi}{\partial x} \right) \end{aligned} \quad (4.5)$$

In terms of the central difference operators

$$J^1_{K,J} = \frac{1}{3} (JA^1_{K,J} + JB^1_{K,J} + JC^1_{K,J})$$

where

$$JA_{K,J}^1 = \frac{\delta \psi_{K,J}^1}{\delta y} \frac{\delta \Gamma_{K,J}^1}{\delta x} - \frac{\delta \psi_{K,J}^1}{\delta x} \frac{\delta \Gamma_{K,J}^1}{\delta y}$$

$$JB_{K,J}^1 = \frac{\delta}{\delta y} \left(\psi \frac{\delta \Gamma}{\delta x} \right)_{K,J}^1 - \frac{\delta}{\delta x} \left(\psi \frac{\delta \Gamma}{\delta y} \right)_{K,J}^1 \quad (4.6)$$

$$JC_{K,J}^1 = \frac{\delta}{\delta x} \left(\Gamma \frac{\delta \psi}{\delta y} \right)_{K,J}^1 - \frac{\delta}{\delta y} \left(\Gamma \frac{\delta \psi}{\delta x} \right)_{K,J}^1$$

Each of the finite-difference forms, JA, JB and JC is a second order representation of the non-linear terms. The mean value has a number of important and desirable characteristics which are discussed in Section C.3.

In detail equations (4.3), (4.4) and (4.6).

$$\begin{aligned} \frac{\Gamma_{K,J}^{l+1} - \Gamma_{K,J}^{l-1}}{2\delta t} = & -U_J \frac{\Gamma_{K+1,J}^l - \Gamma_{K-1,J}^l}{2\delta x} + U'' \frac{\psi_{K+1,J}^l - \psi_{K-1,J}^l}{2\delta x} + J_{K,J}^l \\ & + \frac{1}{R} \left[\frac{\Gamma_{K+1,J}^l - (\Gamma_{K,J}^{l+1} + \Gamma_{K,J}^{l-1}) + \Gamma_{K-1,J}^l}{\delta x^2} \right. \\ & \left. + \frac{\Gamma_{K,J+1}^l - (\Gamma_{K,J}^{l+1} + \Gamma_{K,J}^{l-1}) + \Gamma_{K,J-1}^l}{\delta y^2} \right] \end{aligned} \quad (4.7)$$

$$\Gamma_{K,J}^l = \frac{\psi_{K+1,J}^l - 2\psi_{K,J}^l + \psi_{K-1,J}^l}{\delta x^2} + \frac{\psi_{K,J+1}^l - 2\psi_{K,J}^l + \psi_{K,J-1}^l}{\delta y^2} \quad (4.8)$$

$$\begin{aligned}
J_{K,J}^t = \frac{1}{3} \Bigg\{ & \left[\frac{\psi_{K,J+1}^t - \psi_{K+1,J-1}^t}{2\delta x} \frac{\Gamma_{K+1,J}^t - \Gamma_{K-1,J}^t}{2\delta y} - \frac{\psi_{K+1,J}^t - \psi_{K-1,J}^t}{2\delta x} \frac{\Gamma_{K,J+1}^t - \Gamma_{K,J-1}^t}{2\delta y} \right] \\
& + \left[\left(\frac{\psi_{K,J+1}^t}{2\delta y} \frac{\Gamma_{K+1,J+1}^t - \Gamma_{K-1,J+1}^t}{2\delta x} - \frac{\psi_{K,J-1}^t}{2\delta y} \frac{\Gamma_{K+1,J-1}^t - \Gamma_{K-1,J-1}^t}{2\delta x} \right) \right. \\
& - \left. \left(\frac{\psi_{K+1,J}^t}{2\delta x} \frac{\Gamma_{K+1,J+1}^t - \Gamma_{K+1,J-1}^t}{2\delta y} - \frac{\psi_{K-1,J}^t}{2\delta x} \frac{\Gamma_{K-1,J+1}^t - \Gamma_{K-1,J-1}^t}{2\delta y} \right) \right] \\
& + \left[\left(\frac{\Gamma_{K+1,J}^t}{2\delta x} \frac{\psi_{K+1,J+1}^t - \psi_{K+1,J-1}^t}{2\delta y} - \frac{\Gamma_{K-1,J}^t}{2\delta x} \frac{\psi_{K-1,J+1}^t - \psi_{K-1,J-1}^t}{2\delta y} \right) \right. \\
& - \left. \left(\frac{\Gamma_{K,J+1}^t}{2\delta y} \frac{\psi_{K+1,J+1}^t - \psi_{K-1,J+1}^t}{2\delta x} - \frac{\Gamma_{K,J-1}^t}{2\delta y} \frac{\psi_{K+1,J-1}^t - \psi_{K-1,J-1}^t}{2\delta x} \right) \right] \Bigg\}. \tag{4.9}
\end{aligned}$$

The periodic boundary conditions are approximated for equation (4.7) by assigning values of Γ and ψ at the virtual points as follows.

$$\begin{aligned}
\psi_{0,J}^t &= \psi_{M,J}^t & \psi_{M+1,J}^t &= \psi_{1,J}^t & J &= 1, 2, \dots, N \\
\Gamma_{0,J}^t &= \Gamma_{M,J}^t & \Gamma_{M+1,J}^t &= \Gamma_{1,J}^t & J &= 1, 2, \dots, N
\end{aligned} \tag{4.10}$$

Equation (3.8) is solved for $\psi_{K,J}^t$ by means of a discrete Fourier transform. The periodicity of Γ and ψ in the direction of the mean flow is implicit in the solution of that equation.

The no slip boundary conditions, equations (2.21) and (2.22), require that

$$\psi_{K,1}^t = \psi_{K,N}^t = \text{const} \quad K = 1, 2, \dots, M$$

and that, at the walls, the normal derivative of the stream function be zero. The first condition is satisfied most conveniently by assigning a zero value to the stream function at the wall. The second is employed

to derive a boundary condition for the vorticity in equation (4.7). Since, at the wall, all derivatives of the stream function with respect to x are zero, the vorticity there is given by

$$\Gamma_w = \frac{\partial^2 \psi}{\partial y^2} w.$$

By means of Taylor series expansions, the interior values of the stream function can be expressed in terms of the stream function and its derivatives at the wall. Based on these expansions, finite-difference expressions for Γ_w which satisfy

$$\frac{\partial \psi}{\partial y} w = 0 \quad (4.11)$$

can be derived. For example, at the lower wall ($J=1$), we have

$$\begin{aligned} \psi_2 &= \psi_1 + \delta y \frac{\partial \psi}{\partial y} w + \frac{\delta y^2}{2} \frac{\partial^2 \psi}{\partial y^2} w + \frac{\delta y^3}{6} \frac{\partial^3 \psi}{\partial y^3} w + \frac{\delta y^4}{24} \frac{\partial^4 \psi}{\partial y^4} + \dots \\ \psi_3 &= \psi_1 + 2\delta y \frac{\partial \psi}{\partial y} w + 4 \frac{\delta y^2}{2} \frac{\partial^2 \psi}{\partial y^2} w + 8 \frac{\delta y^3}{6} \frac{\partial^3 \psi}{\partial y^3} w + 16 \frac{\delta y^4}{24} \frac{\partial^4 \psi}{\partial y^4} + \dots \end{aligned}$$

where, for simplicity, only the index J has been retained in the notation. Applying (4.11), we have, from the first expansion

$$\Gamma_w = \frac{\partial^2 \psi}{\partial y^2} w = \frac{2(\psi_2 - \psi_1)}{\delta y^2} + \frac{\delta y}{3} \left(\frac{\partial^3 \psi}{\partial y^3} w + \dots \right) \quad (4.12)$$

Equation (4.12) is the first-order expression for the boundary values of the vorticity. It can also be obtained by applying equation (4.8) at the wall with the assumption of a virtual point outside the domain to satisfy (4.11). Although equation (4.8) is, in the interior region, of second order, the application at the boundary is not. A second order formula can be obtained by combining the two expansions.

$$\Gamma_w = \frac{8 \psi_2 - \psi_3 - 7 \psi_1}{2 \delta y^2} + \frac{\delta y^2}{6} \left(\frac{\partial^4 \psi}{\partial y^4} w + \dots \right) \quad (4.13)$$

By including additional interior points third and fourth order formulas may be derived. They are

$$\Gamma_w = \frac{108 \psi_2 - 27 \psi_3 + 4 \psi_4 - 85 \psi_1}{18 \delta y^2} + \frac{\delta y^3}{10} \left(\frac{\partial^5 \psi}{\partial y^5} w + \dots \right) \quad (4.14)$$

$$\Gamma_w = \frac{576 \psi_2 - 216 \psi_3 + 64 \psi_4 - 9 \psi_5 - 415 \psi_1}{72 \delta y^2} + \frac{\delta y^4}{15} \left(\frac{\partial^6 \psi}{\partial y^6} + \dots \right) \quad (4.15)$$

An integration based on equation (4.7) is not self-starting: another method is required for the first step. In addition the suppression of a certain weak instability associated with the central differencing requires the periodic averaging over two consecutive time steps and the performance of a step by another method. These points are considered in greater detail in Section C.3. The Modified Euler scheme is employed for these purposes. The associated finite difference equation is

$$\begin{aligned} \frac{\Gamma_{K,J}^{t+1} - \Gamma_{K,J}^t}{\delta t} = & \frac{1}{2} \left\{ - U_J \frac{\Gamma_{K+1,J}^{t+1} - \Gamma_{K-1,J}^{t+1}}{2 \delta x} + U'' \frac{\psi_{K+1,J}^{t+1} - \psi_{K-1,J}^{t+1}}{2 \delta x} + J_{K,J}^{t+1} \right. \\ & \left. + \frac{1}{R} \left[\frac{\Gamma_{K+1,J}^{t+1} - 2 \Gamma_{K,J}^{t+1} + \Gamma_{K-1,J}^{t+1}}{\delta x^2} + \frac{\Gamma_{K,J+1}^{t+1} - \Gamma_{K,J}^{t+1} + \Gamma_{K,J-1}^{t+1}}{\delta y^2} \right] \right\} \\ & + \frac{1}{2} \left\{ - U_J \frac{\Gamma_{K+1,J}^t - \Gamma_{K-1,J}^t}{2 \delta x} + U'' \frac{\psi_{K+1,J}^t - \psi_{K-1,J}^t}{2 \delta x} + J_{K,J}^t \right. \\ & \left. + \frac{1}{R} \left[\frac{\Gamma_{K+1,J}^t - 2 \Gamma_{K,J}^t + \Gamma_{K-1,J}^t}{\delta x^2} + \frac{\Gamma_{K,J+1}^t - 2 \Gamma_{K,J}^t + \Gamma_{K,J-1}^t}{\delta y^2} \right] \right\} \end{aligned} \quad (4.16)$$

where $J_{K,J}$ is as given by equation (4.9).

Finite-difference expressions for the various quantities which describe the mean flow and the two-dimensional turbulent motion follow in a straightforward way from equations (2.25) through (2.34).

In terms of the discrete representation the relation for the mean value of the disturbance stream function

$$\bar{\psi}(y,t) = \frac{1}{2h} \int_{-h}^h \psi(x,y,t) dx$$

becomes

$$\begin{aligned} \bar{\psi}_J^t &= \frac{1}{2h} \sum_{K=1}^M \psi_{K,J}^t \delta x \\ &= \frac{1}{M} \sum_{K=1}^M \psi_{K,J}^t \end{aligned} \quad (4.17)$$

Thus, in the discrete representation, the averaging operator simply implies the arithmetic mean value over the index K , or the zero mode in a discrete Fourier representation with respect to x (See Section D). The stream function which describes the turbulent motion is

$$\hat{\psi}_{K,J}^t = \psi_{K,J}^t - \bar{\psi}_J^t \quad (4.18)$$

The velocity and vorticity of the mean flow are given by

$$w_J^t = U_J - \frac{\bar{\psi}_{J+1}^t - \bar{\psi}_{J-1}^t}{2\delta y} \quad (4.19)$$

$$\Omega_J^t = -U'' + \bar{\Gamma}_J^t \quad (4.20)$$

Equation (2.29), for the mean flow kinetic energy, becomes

$$E_J^t = \frac{1}{2} \left[U_J - \frac{\bar{\psi}_{J+1}^t - \bar{\psi}_{J-1}^t}{2\delta y} \right]^2 \quad (4.21)$$

The normalized sum is, by the trapezoidal rule

$$\begin{aligned} E^t &= \frac{1}{2} \left\{ E_1^t \frac{\delta y}{2} + \sum_{J=2}^{N-1} E_J^t \delta y + E_N^t \frac{\delta y}{2} \right\} \\ &= \frac{\delta y}{2} \sum_{H=2}^{N-1} E_J^t = \frac{1}{N-1} \sum_{J=2}^{N-1} E_J^t \end{aligned} \quad (4.22)$$

Similarly, equation (2.31) for the kinetic energy in the turbulent motion becomes,

$$\hat{E}_{K,J}^t = \frac{1}{2} \left\{ \left[\frac{\hat{\psi}_{K,J+1}^t - \hat{\psi}_{K,J-1}^t}{2\delta y} \right]^2 + \left[\frac{\hat{\psi}_{K+1,J}^t - \hat{\psi}_{K-1,J}^t}{2\delta x} \right]^2 \right\} \quad (4.23)$$

The associated mean value is

$$\hat{E}_J^t = \frac{1}{M} \sum_{K=1}^M \hat{E}_{K,J}^t \quad (4.24)$$

And the normalized sum over the domain is

$$\hat{E}^t = \frac{1}{N-2} \sum_{J=2}^{N-1} \hat{E}_J^t \quad (4.25)$$

Equation (2.34) for the Reynolds stress becomes

$$S_J^t = \frac{1}{M} \sum_{K=1}^M \left\{ \frac{\hat{\psi}_{K+1,J}^t - \hat{\psi}_{K-1,J}^t}{2\delta x} \frac{\hat{\psi}_{K,J+1}^t - \hat{\psi}_{K,J-1}^t}{2\delta y} \right\} \quad (4.26)$$

C. CONVERGENCE OF THE NUMERICAL SOLUTION

A rigorous proof of the convergence of the numerical solution to the solution of the non-linear partial differential equation is not possible. Even if the non-linear terms are ignored in the analysis, certain difficulties remain. However, reasonable assurance of convergence can be obtained by analysis of the linear equations, and by numerical experiments. Finally, the convergence and stability of the

scheme, in the linear range, can be demonstrated by calculations which employ as initial conditions the eigenfunctions of the Orr-Sommerfeld equation.

Richtmyer (1967) has shown that, for certain properly posed, linear initial value problems, a finite difference approximation of the partial differential equation which is both consistent and stable, is necessarily convergent. A finite difference approximation is consistent with the differential equation if the associated truncation error tends to zero, as the magnitudes of the time and space increments tend to zero. It is stable if the growth of errors in the numerical solution is bounded.

The consistency of the finite-difference equations is considered in Section C.1. An analysis of the stability of an analogous linear difference equation is given in Section C.2. Finally, in Section C.3., the stability of the complete non-linear system is considered.

1. Consistency

The truncation error in a finite difference approximation is obtained by means of Taylor Series expansions. The results for typical terms in equations (4.3) and (4.4) are

$$\frac{\delta \psi}{\delta x} = \frac{\partial \psi}{\partial x} + \frac{\delta x^2}{6} \left(\frac{\partial^3 \psi}{\partial x^3} + \frac{\delta x^2}{20} \frac{\partial^5 \psi}{\partial x^5} + \dots \right)$$

$$\frac{\delta^2 \psi}{\delta x^2} = \frac{\partial^2 \psi}{\partial x^2} + \frac{\delta x^2}{12} \left(\frac{\partial^4 \psi}{\partial x^4} + \frac{\delta x^2}{30} \frac{\partial^6 \psi}{\partial x^6} + \dots \right)$$

$$\begin{aligned} J_{K,J} = J(\psi, \Gamma) &+ \frac{\delta x^2}{6} \left[\frac{\partial \psi}{\partial y} \frac{\partial^3 \Gamma}{\partial x^3} + 3 \frac{\partial}{\partial x} \left(\frac{\partial \Gamma}{\partial x} \frac{\partial^2 \psi}{\partial x \partial y} - \frac{\partial \psi}{\partial x} \frac{\partial^2 \Gamma}{\partial x \partial y} \right) - \frac{\partial \Gamma}{\partial y} \frac{\partial^3 \psi}{\partial x^3} \right] \\ &+ \frac{\delta y^2}{6} \left[\frac{\partial \Gamma}{\partial x} \frac{\partial^3 \psi}{\partial y^3} + 3 \frac{\partial}{\partial y} \left(\frac{\partial \psi}{\partial y} \frac{\partial^2 \Gamma}{\partial x \partial y} - \frac{\partial \Gamma}{\partial y} \frac{\partial^2 \psi}{\partial x \partial y} \right) - \frac{\partial \psi}{\partial x} \frac{\partial^3 \Gamma}{\partial y^3} \right] \\ &+ \dots \end{aligned}$$

$$\begin{aligned}
D_{K,J}^1 &= \frac{\partial^2 \Gamma}{\partial x^2} + \frac{\partial^2 \Gamma}{\partial y^2} - \delta t^2 \left(\frac{\delta x^2 + \delta y^2}{\delta x^2 \delta t^2} \right) \left[\frac{\partial^2 \Gamma}{\partial t^2} + \frac{\delta t^2}{12} \left(\frac{\partial^4 \Gamma}{\partial t^4} + \frac{\delta t^2}{30} \frac{\partial^6 \Gamma}{\partial t^6} + \dots \right. \right. \\
&\quad \left. \left. + \frac{\delta x^2}{12} \left(\frac{\partial^4 \Gamma}{\partial x^4} + \frac{\delta x^2}{30} \frac{\partial^6 \Gamma}{\partial x^6} + \dots \right. \right. \right. \\
&\quad \left. \left. + \frac{\delta y^2}{12} \left(\frac{\partial^4 \Gamma}{\partial y^4} + \frac{\delta y^2}{30} \frac{\partial^6 \Gamma}{\partial y^6} + \dots \right. \right. \right.
\end{aligned}$$

Gathering terms we find that, to the second order, the total truncation error in equation (4.3) is

$$\begin{aligned}
& - \frac{\delta t^2}{R} \left(\frac{\delta x^2 + \delta y^2}{\delta x^2 \delta y^2} \right) \frac{\partial^2 \Gamma}{\partial t^2} - \frac{\delta t^2}{6} \left[\frac{\partial^3 \Gamma}{\partial t^3} + \frac{\delta t^2}{2R} \left(\frac{\delta x^2 + \delta y^2}{\delta x^2 \delta y^2} \right) \frac{\partial^4 \Gamma}{\partial t^4} \right] \\
& + \frac{\delta x^2}{6} \left[- U_J \frac{\partial^3 \Gamma}{\partial x^3} + U'' \frac{\partial^3 \psi}{\partial x^3} + \frac{\partial \psi}{\partial y} \frac{\partial^3 \Gamma}{\partial x^3} + 3 \frac{\partial}{\partial x} \left(\frac{\partial \Gamma}{\partial x} \frac{\partial^2 \psi}{\partial x \partial y} - \frac{\partial \psi}{\partial x} \frac{\partial^2 \Gamma}{\partial x \partial y} \right) \right. \\
& \quad \left. - \frac{\partial \Gamma}{\partial y} \frac{\partial^3 \psi}{\partial x^3} + \frac{1}{2R} \frac{\partial^4 \Gamma}{\partial x^4} \right] \\
& + \frac{\delta y^2}{6} \left[\frac{\partial \Gamma}{\partial x} \frac{\partial^3 \psi}{\partial y^3} + 3 \frac{\partial}{\partial y} \left(\frac{\partial \psi}{\partial y} \frac{\partial^2 \Gamma}{\partial x \partial y} - \frac{\partial \Gamma}{\partial y} \frac{\partial^2 \psi}{\partial x \partial y} \right) - \frac{\partial \psi}{\partial x} \frac{\partial^3 \Gamma}{\partial y^3} + \frac{1}{2R} \frac{\partial^4 \Gamma}{\partial x^4} \right]
\end{aligned} \tag{4.27}$$

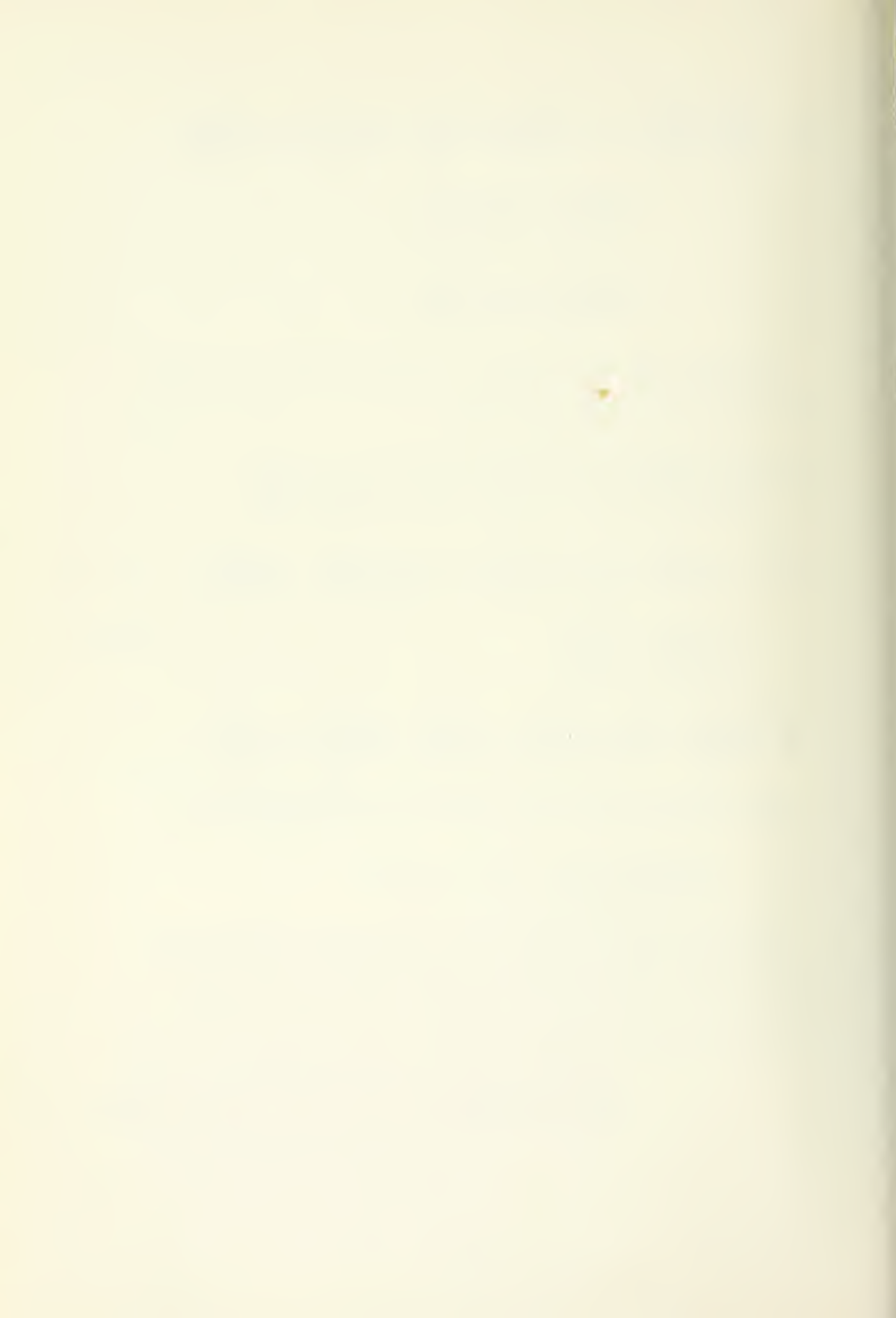
Thus the truncation error contains terms proportional to

$$\frac{\delta t^2}{R} \left(\frac{\delta x^2 + \delta y^2}{\delta x^2 \delta y^2} \right), \delta t^2, \delta x^2 \text{ and } \delta y^2$$

The first terms arises from the Du Fort-Frankel approximation.

Compatibility requires that $\delta t \rightarrow 0$ faster than δx or δy . The truncation error in equation (4.4) is

$$\frac{\delta x^2}{12} \frac{\partial^4 \psi}{\partial x^4} + \frac{\delta y^2}{12} \frac{\partial^4 \psi}{\partial y^4} \tag{4.28}$$



Similarly the truncation error associated with the second-order formulation of the vorticity boundary condition is

$$\frac{\delta y^2}{6} \frac{\partial^4 \psi}{\partial y^4} \quad (4.29)$$

It should be noted that the approximation for the boundary values of the vorticity involves values of the stream function at time level i . This approximation is correctly centered with respect to the time differencing which involves values at $i+1$ and $i-1$.

The over-all order of the approximation is

$$O \left[\frac{\delta t^2}{R} \left(\frac{\delta x^2 + \delta y^2}{\delta x^2 \delta y^2} \right) + \delta t^2 + \delta x^2 + \delta y^2 \right]$$

and the scheme is consistent if

$$\lim_{\substack{\delta x \rightarrow 0 \\ \delta y \rightarrow 0 \\ \delta t \rightarrow 0}} \left[\frac{\delta t^2}{R} \left(\frac{\delta x^2 + \delta y^2}{\delta x^2 \delta y^2} \right) + \delta t^2 + \delta x^2 + \delta y^2 \right] = 0 \quad (4.30)$$

2. Stability Analysis of an Analogous Linear Equation

The numerical solution of the finite difference equations is stable if the round-off errors due to the finite decimal representation of real numbers are bounded in their growth. In the case of linear equations, the errors introduced at a given step are propagated by the same system of finite difference equations. In addition, the linearity permits, in the analysis, the superposition of random errors introduced at each step. For the purpose of determining what constraints, if any, must obtain for stability, it is only necessary to consider the amplification, by the equations, of errors introduced at the initial or an arbitrary step.

Two approaches are in wide use. The first involves the determination of the spectral radius of the matrix which defines the time step (Smith 1965). The finite-difference equations are expressed in the form

$$\bar{E}_t = A\bar{E}_{t-1} \quad (4.31)$$

Where \bar{E}_t is a vector whose components are spatial values of the dependent variable, (or in this analysis, the errors), at time step t . If the matrix A , of dimension σ , has σ linearly independent eigenvectors, $\bar{\eta}_s$, then an arbitrary initial error can be expressed in terms of them.

$$\bar{E}_0 = \sum_{s=1}^{\sigma} c_s \bar{\eta}_s$$

It follows from equation (3.39) that

$$\bar{E}_t = A^t \bar{E}_0$$

Thus if v_s are the eigenvalues of A then

$$\bar{E}_t = \sum_{s=1}^{\sigma} c_s v_s^t \bar{\eta}_s \quad (4.32)$$

Thus \bar{E}_t is bounded if the largest of the moduli of v_s is less than unity. In some fairly simple cases, which generally involve two-level finite-difference formulas such as Forward or Modified Euler differencing, the bounds can be determined in a straightforward way by application of theorems due to Gerschgorin and Brauer (Smith 1965).

If multi-level formulas, such as central time differencing are employed then the expression of the finite difference equations in the form of equation (4.31) is not so easy. In addition the determination of the eigenvalues or the spectral radius of the resulting matrix can be a formidable task.

A second approach which generally offers fewer difficulties, but which, unlike the matrix approach, does not take into account the effect of the boundary conditions is due to von Neumann. It was introduced in a paper by O'Brien, Hyman and Kaplan (1951), and is employed here. The initial errors are expressed in terms of their Fourier components. If none of the modes grow with increasing time the scheme is stable. Because the equations considered in the analysis are linear the various modes do not interact, and we need only to consider the behavior of an arbitrary mode.

We consider a finite difference equation for the initial errors which is linear, but analogous to equation (4.7).

$$\begin{aligned}
 \frac{E_{K,J}^{t+1} - E_{K,J}^{t-1}}{2\delta t} = u_0 \frac{E_{K+1,J}^t - E_{K-1,J}^t}{2\delta x} + v_0 \frac{E_{K,J+1}^t - E_{K,J-1}^t}{2\delta y} \\
 + \frac{1}{R} \left[\frac{E_{K+1,J}^t - (E_{K,J}^{t+1} + E_{K,J}^{t-1}) + E_{K-1,J}^t}{\delta x^2} \right. \\
 \left. + \frac{E_{K,J+1}^t - (E_{K,J}^{t+1} + E_{K,J}^{t-1}) + E_{K,J-1}^t}{\delta y^2} \right]
 \end{aligned} \tag{4.33}$$

Let

$$\begin{aligned}
 r_x &= u_0 \frac{\delta t}{\delta x} & r_y &= v_0 \frac{\delta t}{\delta y} \\
 \lambda_x &= \frac{2\delta t}{R\delta x^2} & \lambda_y &= \frac{2\delta t}{R\delta y^2} & \lambda &= \lambda_x + \lambda_y
 \end{aligned} \tag{4.34}$$

Then equation (4.33) becomes (4.35)

$$\begin{aligned}
 (1+\lambda) E_{K,J}^{t+1} = (1-\lambda) E_{K,J}^{t-1} + r_x (E_{K+1,J}^t - E_{K-1,J}^t) + r_y (E_{K,J+1}^t - E_{K,J-1}^t) \\
 + \lambda_x (E_{K+1,J}^t + E_{K-1,J}^t) + \lambda_y (E_{K,J+1}^t + E_{K,J-1}^t)
 \end{aligned}$$

Let

$$\begin{aligned}
 E_{K,J}^I &= \sum_{n=0}^N \sum_{m=0}^M A_{nm} e^{\alpha_{nm} t} e^{i \frac{n\pi x}{h} K} e^{i m\pi y J} \\
 &= \sum_{n=0}^N \sum_{m=0}^M A_{nm} \xi_{nm}^I e^{i \gamma_x n K} e^{i \gamma_y m J}
 \end{aligned} \tag{4.36}$$

Where A_{nm} are determined from the specified initial errors and

$$\xi_{nm} = e^{\alpha_{nm} \delta t}.$$

For stability it is required that

$$|\xi_{nm}| \leq 1$$

Since for the linear equation we need only to consider an arbitrary combination of spatial modes, the substitution

$$E_{K,J}^I = \xi^I e^{i \gamma_x K} e^{i \gamma_y J}$$

in equation (4.35) will reveal the necessary constraints. After cancelling the common factor $\xi^{I-1} e^{i \gamma_x K} e^{i \gamma_y J}$ and rearranging, equation (4.35) becomes

$$\begin{aligned}
 \xi^2 - \frac{2}{1+\lambda} \left[(\lambda_x \cos \gamma_x + \lambda_y \cos \gamma_y) + i (r_x \sin \gamma_x + r_y \sin \gamma_y) \right] \xi \\
 - \frac{1-\lambda}{1+\lambda} = 0
 \end{aligned} \tag{4.37}$$

Which has roots

$$\begin{aligned}
 \xi = \frac{1}{1+\lambda} \left\{ (\lambda_x \cos \gamma_x + \lambda_y \cos \gamma_y) + i (r_x \sin \gamma_x + r_y \sin \gamma_y) \right. \\
 \left. \pm \sqrt{\left[(\lambda_x \cos \gamma_x + \lambda_y \cos \gamma_y) + i (r_x \sin \gamma_x + r_y \sin \gamma_y) \right]^2 + (1-\lambda^2)} \right\}
 \end{aligned} \tag{4.38}$$

Fromm (1963) has performed the analysis for the case $\delta x = \delta y$, which in the present notation means

$$r_x = r_y$$

$$\lambda_x = \lambda_y \quad \lambda = 2\lambda_x$$

Because of the obvious difficulty in determining bounds on the modulus of ξ in equation (4.38), Fromm performed the analysis in two steps. In the first step only the diffusion terms are treated: the transport terms are assumed to be zero. In the second step the procedure is reversed. The following is an extension of Fromm's analysis for the case $\delta x \neq \delta y$.

Let

$$\omega = \lambda_x \cos \gamma_x + \lambda_y \cos \gamma_y$$

$$\Omega = r_x \sin \gamma_x + r_y \sin \gamma_y$$

Equation (4.38) becomes

$$\xi = \frac{1}{1+\lambda} \left\{ \omega + i\Omega \pm \sqrt{(\omega+i\Omega)^2 + 1-\lambda^2} \right\} \quad (4.39)$$

For diffusion with no transport $\Omega = 0$.

Equation (4.39) becomes

$$\xi = \frac{1}{1+\lambda} \left\{ \omega \pm \sqrt{\omega^2 + 1-\lambda^2} \right\} \quad (4.40)$$

Note that

$$-\lambda \leq \omega \leq \lambda$$

If the radical in (4.40) is real then $|\xi|$ reaches a maximum for

$$\omega^2 = \lambda^2 \text{ where}$$

$$\xi = \pm \frac{(\lambda+1)}{(\lambda+1)} = \pm 1$$

If the radical is imaginary then

$$\xi = \frac{1}{1+\lambda} \left\{ \omega \pm i \sqrt{\lambda^2 - \omega^2 - 1} \right\}$$

$$|\xi| = \frac{\sqrt{\lambda^2 - 1}}{1+\lambda} = \sqrt{\frac{\lambda-1}{\lambda+1}}$$

In each case $|\xi| \leq 1$ for all values of λ_x and λ_y . Thus, in relation to the diffusion terms, the Du Fort-Frankel Central differencing is stable at all values of δt . This result is given by Richtmyer (1967) for the one-dimensional case.

For transport with no diffusion, $\omega = 0$, and $\lambda = 0$.

Equation (4.39) becomes

$$\xi = i\Omega \pm \sqrt{-\Omega^2 + 1} \quad (4.41)$$

If $\Omega^2 \leq 1$ the radical is real and

$$|\xi| = 1$$

If, however, $\Omega^2 > 1$, the radical is imaginary and

$$\xi = i \left(-\Omega \pm \sqrt{\Omega^2 - 1} \right)$$

$$|\xi| = 2\Omega^2 - 1 \mp 2\Omega \sqrt{\Omega^2 - 1}$$

For the second root

$$|\xi| > 1$$

Thus, in relation to the transport terms the Central differencing is stable if

$$\Omega^2 = (r_x \sin \gamma_x + r_y \sin \gamma_y)^2 \leq 1$$

Then from equations (4.34)

$$\delta t \left| \frac{u_0}{\delta x} + \frac{v_0}{\delta y} \right| \leq 1$$

A more conservative form is

$$\delta t \left(\frac{|u_0|}{\delta x} + \frac{|v_0|}{\delta y} \right) \leq 1$$

which is equivalent to

$$\delta t \leq \frac{\delta x \delta y}{|u_0| \delta y + |v_0| \delta x} \quad (4.42)$$

Although a complete analysis of even the linear equations is not carried out it is reasonable to expect that a constraint of the form of equation (4.42) will be required.

3. Stability and Accuracy of the Complete Non-linear Equations

From the stability analysis of the linear equations it was expected that a constraint of the form of equation (4.42) would be required for the general case where both diffusion and advection terms are present, the latter including the non-linear terms. Accordingly, the value of the time increment was determined by

$$\delta t = \frac{f \delta x \delta y}{u_0 \delta y + v_0 \delta x} \quad (4.43)$$

where u_0 and v_0 are the maximum absolute values of the x and y components of total velocity over a large sample of the mesh points, and f is a parameter which was determined by numerical experiment. The values of u_0 and v_0 were recomputed at regular intervals, and δt was adjusted accordingly. Experiments with a variety of mesh sizes and disturbance amplitudes indicated critical values of the parameter f in the range $.95 < f_c < 1.02$. When the critical value of f was exceeded,

the instabilities developed quite rapidly, always within 100 time steps and in most cases within 50 steps. At low disturbance amplitudes the instability developed first in the midstream region, where the laminar transport velocity is the greatest. At higher amplitudes of the disturbance, the instability occurred first in the wall region where, owing to the character of the disturbance, the advection was the greatest. The instabilities were, in most cases, unmistakable: an explosive growth in the numerical values of the disturbance quantities immediately preceded an abnormal termination of the calculation due to numerical overflow. At values of f very close to the critical, a more insidious situation occurred in which the initial amplification of errors in the disturbance stream function and vorticity, and hence in the computed quantities u_0 and v_0 , was inhibited by the ensuing automatic reduction of δt . The calculations were characterized by periodic amplification and decay of large errors. The results were in poor agreement with recalculations with a reduced value of δt . If the automatic recalculation of the time step was bypassed then the explosive instability described above would occur. Accordingly f was limited to values less than .6, where no such difficulties were encountered.

In similar numerical experiments with the Du Fort-Frankel Central differencing applied to the non-linear vorticity transport equations, Fromm determined a critical value of f equal to .8. An important difference between the finite-difference equations employed by Fromm and those in the present work is associated with the treatment of the non-linear terms. Fromm employed a representation of those terms equivalent to $JB_{K,J}$ of equations (3.6). As has been

noted, in the present case the mean of $JA_{K,J}$, $JB_{K,J}$, and $JC_{K,J}$, is employed. The significance of the various finite difference representations of the non-linear terms is considered below.

Phillips (1959) has shown the existence of numerical instabilities, associated with the non-linear terms, which result from the discrete representation of continuous functions, but which, in principle, cannot always be eliminated by reducing the time step or the mesh spacing. This kind of instability is the result of uncontrolled "aliasing" or confusion of frequencies (Hamming 1962). To illustrate, note that at a given value of the index J the M values

$$\psi_{K,J} \quad K = 1, 2, \dots, M$$

can be expressed in terms of $\frac{M}{2} + 1$ distinct Fourier modes.

$$\psi_{K,J} = \frac{1}{M} \left\{ a_{0,J} + 2 \sum_{n=1}^{M/2-1} \left(a_{n,J} \cos \frac{2n\pi K}{M} + b_{n,J} \sin \frac{2n\pi K}{M} \right) + a_{M/2,J} \right\}$$

where the period associated with the highest mode number is $2\delta x$.

Since,

$$\cos \frac{2n\pi K}{M} \cos \frac{2m\pi K}{M} = \frac{1}{2} \left(\cos \frac{2(n+m)\pi K}{M} + \cos \frac{2(n-m)\pi K}{M} \right) \quad \text{etc.,}$$

the non-linear interaction between modes n and m will produce excitation in modes $n+m$ and $n-m$. If $n+m$ is greater than $M/2$ that interaction will be misrepresented by the discrete system.

$$\text{Let } m + n = \frac{M}{2} + r, \quad r < \frac{M}{2}$$

$$\cos \frac{2(M/2 + r)\pi K}{M} = \cos \frac{2r\pi K}{M}$$

$$\sin \frac{2(M/2 + r)\pi K}{M} = -\sin \frac{2r\pi K}{M}$$

Thus the aliasing involves a spurious interaction with mode $r = n+m - M/2$. If both m and n are less than $M/4$, that is if each wave has a period greater than $4\delta x$, no misrepresentation will occur. The instability that results from aliasing occurs after a large number of time steps and is characterized by explosive growth of the energy in the system. Phillips was able to suppress this instability by, "periodically eliminating all Fourier components with wave lengths smaller than $4\delta x$ ", that is, by zeroing the upper half of the representable spectrum. In effect, in each spatial or spectral coordinate, twice as many degrees of freedom are carried in the calculations as are retained in the solution. For calculations explicitly in terms of the spectral form of the equations this seems to be the only recourse.

Arakawa (1966) has devised a number of finite difference forms for the non-linear advection terms which eliminate this instability by controlling or limiting the aliasing. They are various linear combinations of the forms JA, JB and JC as given, in terms of the central difference operators, by equations (4.6). For a confined flow or one with identical conditions at inflow and outflow boundaries it is easy to show that, in the absence of viscosity, the spatial integrals of kinetic energy and any function of vorticity are fixed quantities. In a viscous flow the advection terms make no contribution to the rates of change of these quantities. Lilly (1965) has shown that the feature essential to the control of the aliasing is the conservation of mean kinetic energy or mean squared vorticity implicit in the finite-difference representation of the advection terms. A number of stable conservative schemes are given by both Arakawa and Lilly. The only scheme which conserves both mean kinetic energy and squared vorticity is

$$J(\psi, l') = \frac{1}{3} (JA + JB + JC)$$

which is the form used in the present undertaking.

There is, in addition, a third type of instability which is associated with the central time differencing. This weak instability is a computational mode associated with the three-time level central difference representation of $\frac{\partial \Gamma}{\partial t} = f(\Gamma)$. In effect, the central difference representation replaces a first order (in time) continuous equation with a second order discrete one, which has an additional, non-physical, solution (Lilly 1965). It takes the form of a slowly growing oscillation, of period $2\delta t$, about the true solution. If it remains unchecked then eventually the solutions at even and odd time steps diverge. This computational mode can be suppressed quite simply by periodically averaging the solutions over successive time steps and restarting the calculations with the averaged values (Williams 1969).

This periodic interruption of the sequence of the calculation provides a convenient opportunity for the readjustment of the value of δt . In the midst of the continued central time differencing δt must remain fixed. However when the averaging takes place it can be adjusted in accordance with equation (4.43), a single time step performed by the Modified Euler method (which does not require values at the previous time level), and the normal sequence can be continued. This procedure proved to be quite effective for both purposes. No evidence of the growth of the computational mode was observed.

Fischer (1965) tested the accuracy of four methods of time differencing on a one-dimensional linearized version of the equations of motion, and found that the central differencing was decidedly

superior. In similar tests on the wave equation Kurihara (1965) found that, provided the computational mode is suppressed, it was superior in terms of measured errors in amplitude and phase velocity to the other methods tested.

D. SOLUTION OF POISSON'S EQUATION FOR THE STREAM FUNCTION

The finite-difference relation between the stream function and the vorticity is given by equation (4.8). In the course of each time step new values of the vorticity are obtained from equation (4.7). Equation (4.8) must then be solved for the matching values of the stream function.

$$\Gamma_{K,J} = \frac{\psi_{K+1,J} - 2\psi_{K,J} + \psi_{K,J-1}}{\delta x^2} + \frac{\psi_{K,J+1} - 2\psi_{K,J} + \psi_{K,J-1}}{\delta y^2} \quad (4.8)$$

$$K = 1, 2, \dots, M$$

$$J = 2, 3, \dots, N-1$$

In matrix form equations (4.8) are

$$\bar{\Gamma} = B\bar{\psi} \quad (4.44)$$

where $\bar{\Gamma}$ and $\bar{\psi}$ are vectors of dimension $d = (N-2)M$ and B is a banded symmetric matrix of dimension $d \times d$. The solution to equation (4.44),

$$\bar{\psi} = B^{-1} \bar{\Gamma}$$

is obtained in three steps by means of the discrete Fourier transform. In the transformed domain the finite-difference relation between the stream function and the vorticity has the form

$$\bar{\Gamma}_n = A_n \bar{\psi}_n \quad n = 1, 2, \dots, \frac{M}{2} + 1 \quad (4.45)$$

where $\bar{\Gamma}_n$ and $\bar{\psi}_n$ are vectors of dimension $N-2$ and the A_n are symmetric tridiagonal matrices of dimension $(N-2) \times (N-2)$. Because the matrices

A_n are tridiagonal, the solutions to equations (4.45) can be obtained by a particularly simple case of Gauss elimination (Richtmyer 1967).

The discrete Fourier transform pair is given by

$$\begin{aligned} T_n &= \sum_{K=1}^M F_K e^{i \theta_{n,K}} & n &= 1, 2, \dots, M \\ F_K &= \frac{1}{M} \sum_{n=1}^M T_n e^{-i \theta_{n,K}} & K &= 1, 2, \dots, M \end{aligned} \quad (4.46)$$

Where T_n and F_K are, in general, complex and,

$$\theta_{n,K} = \frac{2\pi(n-1)(K-1)}{M} \quad (4.47)$$

The associated orthogonality relation is

$$\begin{aligned} \frac{1}{M} \sum_{n=1}^M e^{i \theta_{n,s-K+1}} &= 1 & \text{if } s=k \\ &= 0 & \text{otherwise} \end{aligned} \quad (4.48)$$

For the solution of equation (4.8) let

$$\begin{aligned} G_{n,J} &= \sum_{K=1}^M \Gamma_{K,J} e^{i \theta_{n,K}} & K &= 1, 2, \dots, M \\ F_{n,J} &= \sum_{K=1}^M \psi_{K,J} e^{i \theta_{n,K}} & J &= 1, 2, \dots, N \end{aligned} \quad (4.49a)$$

Then from equations (3.65) $\Gamma_{K,J}$ and $\psi_{K,J}$, are given by

$$\begin{aligned} \Gamma_{K,J} &= \frac{1}{M} \sum_{n=1}^M G_{n,J} e^{-i \theta_{n,K}} & K &= 1, 2, \dots, M \\ \psi_{K,J} &= \frac{1}{M} \sum_{n=1}^M F_{n,J} e^{-i \theta_{n,K}} & J &= 1, 2, \dots, N \end{aligned} \quad (4.49b)$$

From equations (3.1) and (3.2) it is evident that

$$\theta_{n,K} = \frac{(x_K - c) 2\pi (n-1)}{2h}$$

where

$$c = \frac{\delta x}{2} - h$$

Therefore equations (4.48) and (4.49) implicitly satisfy the periodic boundary conditions on Γ and ψ . The no-slip boundary conditions require that

$$F_{n,1} = F_{n,N} = 0 \quad n = 1, 2, \dots, M$$

Substitution of equations (4.49) in equation (4.8) yields,

$$\sum_{n=1}^M \left\{ \delta y^2 G_{n,J} - \left[F_{n,J+1} - \alpha_n F_{n,J} + F_{n,J+1} \right] \right\} e^{-i \theta_{n,K}} = 0 \quad (4.50)$$

$$K = 1, 2, \dots, M$$

$$J = 2, 3, \dots, N-1$$

where

$$\alpha_n = 2 \left[1 - \frac{\delta y^2}{\delta x^2} (\cos \theta_{n,2} - 1) \right] \quad (4.51)$$

Equation (4.50) can be satisfied at all values of K only if

$$\delta y^2 G_{n,J} = F_{n,J+1} - \alpha_n F_{n,J} + F_{n,J+1} \quad (4.52)$$

$$n = 1, 2, \dots, M$$

$$J = 2, 3, \dots, N-1$$

Although $F_{n,J}$ and $G_{n,j}$ are complex, the coefficients in equation (4.52) are all real. The solutions for the real and imaginary parts may be obtained separately. Because $\Gamma_{K,J}$ and $\psi_{K,J}$ are real, the real and imaginary parts of $G_{n,J}$ and $F_{n,J}$ are symmetric and anti-symmetric respectively about $n = \frac{M}{2} + 1$. (Recall that M , as defined, is always even.) Thus $M \times (N-2)$ quantities in the x domain beget exactly $M \times (N-2)$ distinct quantities in the wave number domain. There are

exactly M distinct sets of equations of the form equation (4.52) in terms of real variables.

Equations (4.8) can be solved in this manner without the heavy storage penalties that are usually associated with direct methods. In this case the additional storage requirements are trivial: an M dimensional complex vector for the row by row transformation of $\Gamma_{K,J}$ and the inverse transformation of $\psi_{K,J}$, and three $N-2$ dimensional vectors to accommodate the solution of the tridiagonal systems. The vorticity array is transformed row by row, and the transformed quantities are stored in the array reserved for the stream function. The tridiagonal equations (4.52) are solved column by column. In each step, the solution for the transform of the stream function replaces the stored values of the transform of the vorticity which are no longer required. Finally the transform of the stream function is inverted row by row. In order to minimize the accumulation of roundoff errors in the direct solution, the calculations associated with both the discrete transform and the Gauss elimination are performed in double precision. The equivalent of sixteen decimal digits are carried in the calculations.

The transforms and inverse transforms are obtained by means of the remarkably efficient Fast Fourier Transform algorithm of Cooley and Tukey (1965). The computational effort required to perform the transform on an M dimensional vector is proportional to $M \log (M)$. There are roughly $2 N$ such transforms required in the solution of equation (4.8). The effort required to solve each of the M tridiagonal systems is proportional to $3 N$. Hence the total computational effort is proportional to $NM (2 \log (M) + 3)$.

In an early version of the program equation (4.8) was solved by Successive Over-relaxation. It is an iterative method which is easy to program, involves no storage penalties and which, at least for small arrays, is rapidly convergent.

Equation (4.8) can be written

$$\psi_{K,J} = \frac{\delta y^2}{2(\delta x^2 + \delta y^2)} \left[\psi_{K+1,J} + \psi_{K-1,J} + \frac{\delta x^2}{\delta y^2} (\psi_{K,J+1} + \psi_{K,J-1}) - \delta x^2 \Gamma_{K,J} \right] \quad (4.53)$$

Equation (4.53) can be used as the basis for various iterative formulations. If the superscript denotes the iteration number then

$$\psi_{K,J}^{t+1} = \frac{\delta y^2}{2(\delta x^2 + \delta y^2)} \left[\psi_{K+1,J}^t + \psi_{K-1,J}^t + \frac{\delta x^2}{\delta y^2} (\psi_{K,J+1}^t + \psi_{K,J-1}^t) - \delta x^2 \Gamma_{K,J} \right] \quad (4.54)$$

defines a Jacobi iteration. With this method separate computer storage must be reserved for the t and $t+1$ iterates. If the current values are employed in the formula as soon as they are available then the extra storage requirement is eliminated. In addition the convergence rate is, for the Poisson equation, approximately doubled (Varga 1962).

Equation (4.54) becomes

$$\psi_{K,J}^{t+1} = \frac{\delta y^2}{2(\delta x^2 + \delta y^2)} \left[\psi_{K+1,J}^t + \psi_{K-1,J}^{t+1} + \frac{\delta x^2}{\delta y^2} (\psi_{K,J+1}^t + \psi_{K,J-1}^{t+1}) - \delta x^2 \Gamma_{K,J} \right] \quad (4.55)$$

Equation (4.55) defines a Gauss-Seidel iteration.

By the addition of an acceleration or over-relaxation parameter to equation (4.55) the convergence rate can be considerably increased

$$\psi_{K,J}^{t+1} = (1-\omega) \psi_{K,J}^t + \frac{\omega \delta y^2}{2(\delta x^2 + \delta y^2)} \left[\psi_{K+1,J}^t + \psi_{K-1,J}^{t+1} + \frac{\delta x^2}{\delta y^2} (\psi_{K,J+1}^t + \psi_{K,J-1}^{t+1}) - \delta x^2 \Gamma_{K,J} \right] \quad (4.56)$$

Equation (4.56) defines the Successive Over-relaxation. In this case the convergence rate is strongly dependent on the choice of ω . The optimum value of ω , which for the Poisson equation falls between one and two, is determined by the modulus of the largest eigenvalue of the matrix which defines the system of equations (Varga 1962), however it is generally easier to determine it by experiment.

With each of the various iterative methods an approximate solution to the system of equations is obtained by systematically applying the iteration formula at each point in the field until some measure of the changes in the various values falls below a specified tolerance. In order to equalize the influence of the boundary conditions it is necessary to start successive sweeps at opposite boundaries.

Early experiments with certain contrived test problems indicated that with the optimum value of ω , convergence was generally obtained with one fifth the number of iterations required for the Gauss-Seidel Iteration, and that the errors in the solution were reduced by as much as a factor of ten. Unfortunately in application to the present problem the performance of even the Over-relaxation is inadequate. The computational effort required to perform one iteration in an M by N array is proportional to $M N$. The number of iterations required for convergence to a fixed tolerance was roughly proportional to $(M N)^{1/4}$. Finally the tolerance required for a fixed error in the solution varied nearly inversely as $(M N)^{1/2}$. The over-all computational effort was roughly proportional to $(M N)^{7/4}$. In the integration of the vorticity transport equations the relaxation solution to the Poisson equation required more than 80 per cent of the total computing time. More sophisticated relaxation techniques, such as line or block over-relaxation,

might double the convergence rate (Varga 1962), but the essential difficulties remain for sufficiently large dimensions.

A number of numerical tests were conducted in order to compare the efficiency and accuracy of the various schemes. In these tests values of $\psi_{K,J}$ were established from

$$\psi_{K,J} = \left(1 - Y_J^2\right)^2 \left\{ Y_J^2 + \sum_{m=1}^6 1/m^2 \left[\sin (mx_K) + Y_J^2 \cos (mx_K) \right] \right\}$$

Values of $\Gamma_{K,J}$, were obtained from the prescribed values of $\psi_{K,J}$ by application of equation (4.8). Thus the stored values of $\psi_{K,J}$, are an exact solution of the finite-difference equations (4.8) corresponding to the values of $\Gamma_{K,J}$. Solutions of equations (4.8) denoted by $s_{K,J}$, were obtained by Gauss-Seidel iteration, Successive Over-relaxation and by the direct method.

The mean and maximum relative errors defined by,

$$E_{\text{mean}} = \frac{1}{M(N-2)} \sum_{J=2}^{N-1} \sum_{K=1}^M \left| \frac{s_{K,J} - \psi_{K,J}}{\psi_{K,J}} \right|$$

$$E_{\text{max}} = \max \left\{ \left| \frac{s_{K,J} - \psi_{K,J}}{\psi_{K,J}} \right|, \begin{array}{l} K = 1, 2, \dots, M \\ J = 2, 3, \dots, N-1 \end{array} \right\}$$

were calculated for each test.

The iterative processes were assumed to have converged when at every point in the field

$$\frac{|s_{K,J}^{t+1} - s_{K,J}^t|}{\bar{s}} < \epsilon$$

where \bar{s} is the mean absolute value of $s_{K,J}$, at the start of the iteration procedure and ϵ is an assigned tolerance. In order to minimize the computer time expended in testing for convergence, the

test was applied only at even-numbered sweeps. In addition the test was bypassed at all points following the first point at which it was not met. Initial values of $s_{K,J}$, were established reasonably close to the exact solution in order to approximate the situation in the numerical integration, where values of $\psi_{K,J}$ at time t are used as a first guess for values at $t + \delta t$ in the iterative procedure. These initial values were

$$s_{K,J}^0 = \psi_{K,J} + \frac{1}{10} \left[1 - |Y_J| \right] \left[\sin (2x_K) + \cos (5x_K) \right]$$

In every case the experimentally determined optimum value of the relaxation parameter, ω , was employed for the Successive Over-relaxation.

Internal timers were started and stopped at the beginning and at the end of each solution and the elapsed times, in seconds, were printed along with errors. The results are given in Table II. They indicate rather dramatically the superiority of the direct solution in terms of both accuracy and speed.

Tests with the iterative methods were performed at two and three values of the convergence tolerance in order to verify that the procedures were still converging systematically at the specified tolerances. Generally a reduction of the convergence tolerance by a factor of two produced a solution with the errors reduced by about the same factor. The effects of the rapid reduction of the convergence rates of the iterative methods due to increased array dimensions are quite evident.

The Gauss-Seidel iteration is, in particular, quite useless in application to large arrays. For the 64 by 201 point mesh, a comparison of the tests at $\epsilon = 10^{-4}$ and 5×10^{-5} shows that the expenditure of

| E | Gauss Seidel Iteration | | | | Successive Over-Relaxation | | | Fourier Trans-form Solution | M N ω |
|---------------|------------------------|--------|--------|--------|----------------------------|-------|--------|-----------------------------|----------------|
| | .0002 | .0001 | .00005 | .00005 | .0002 | .0001 | .00005 | | |
| Iterations | | 214 | | 260 | | 58 | 66 | | 32x41 |
| Time | | 20.4 | | 24.05 | | 5.8 | 6.6 | .9 | |
| Mean Error | | .017 | | .0086 | | .0025 | .0010 | .00006 | |
| Maximum Error | | 2.262 | | 1.159 | | .4747 | .1980 | .00094 | $\omega=1.785$ |
| Iterations | | 484 | | 666 | | 104 | 120 | | 64x81 |
| Time | | 179.1 | | 245.8 | | 41.0 | 48.0 | 3.8 | |
| Mean Error | | .1646 | | .0820 | | .0065 | .0040 | .0004 | |
| Maximum Error | | 238.4 | | 117.3 | | 3.393 | 1.772 | .2104 | $\omega=1.875$ |
| Iterations | | 586 | | 894 | | 130 | 156 | | 128x101 |
| Time | | 564.0 | | 856.9 | | 135.3 | 154.8 | 10.8 | |
| Mean Error | | .1755 | | .0821 | | .0078 | .0066 | .0005 | |
| Maximum Error | | 159.1 | | 65.47 | | 5.065 | 5.830 | .2455 | $\omega=1.910$ |
| Iterations | 82 | 478 | | 1000 | 168 | 206 | 252 | | 64x201 |
| Time | 83.1 | 451.3 | | 929.9 | 168.9 | 211.6 | 255.0 | 9.4 | |
| Mean Error | .7928 | .5290 | | .3923 | .0334 | .0168 | .0075 | .0006 | |
| Maximum Error | 1542.9 | 1124.9 | | 814.6 | 47.81 | 19.46 | 8.189 | .4928 | $\omega=1.948$ |

TABLE II
Test Solutions of Poisson Equation

eight minutes of computer time, in the performance of 522 iterations, reduced the mean error by only twenty-five percent, and that the errors in the resulting solution are such that it contains no significant figures!

The performance of the Successive Over-relaxation is considerably better, though still inadequate for the long-term integration. The results for the 128 by 101 and the 64 by 201 point arrays indicate that solutions with two significant figures can be obtained in from two to four minutes of computer time.

The rate of convergence which occurs at any point in an iterative solution is proportional to the difference between the current estimate and the solution. As the gap is reduced the rate of approach decreases to some limiting value. It is this asymptotic convergence rate which is the significant factor in the determination of the computational effort required to obtain a solution of specified accuracy (Varga 1962). The three tests with the Successive Over-relaxation in the 64 by 201 point array permit the estimation of two successive convergence rates. The second rate is only very slightly less than the first: their ratio is about .97. These are therefore close to the asymptotic rate. Thus, in this application, the asymptotic rate of convergence is achieved when the mean errors are between one and five percent. If the initial guess is within (say) five percent of the solution, the performance of forty or fifty iterations will reduce the error by only one-half. The final values may have no more significant figures than the first guess.

It is sometimes suggested that, in a numerical integration of the equations for fluid motion, if the time step is kept small, and if the

previous values of the stream function are used as a first guess for the new values, only a few iterations are needed for the solution of the Poisson equation. It is evident that this is not true if the number of mesh points is large. Even if only a very small change in the stream function, or pressure, is required, only a very small fraction of that change will be accomplished with a few iterations. Significant errors will be introduced at each time step. These errors, due to incomplete convergence, unlike round-off errors, are systematic in some sense and unacceptable in a long-term numerical integration.

The errors in the direct solution by the Fourier transform arise from round-off and, in every case tested, were less by at least a factor of ten than the best iterative solution. The computing time was far less, and generally equal to that required for about nine iterations by the Over-relaxation. In the case of the 201 by 64 point array the Transform method produced a solution with errors less, by a factor of ten, than the best iterative solution, and reduced the computing time by a factor of twenty-five.

E. DESCRIPTION OF THE PROGRAM AND COMPUTATIONAL PROCEDURE

A listing of the computer program is reproduced as Appendix B. The names and functions of the various subroutines, the definitions of the parameters which control the operation of the program, as well as the dimensions of the various arrays, are given at the beginning of the calling program. The program is written in standard FORTRAN IV. Calculations were performed on an I.B.M. 360/67 computer at the W. R. Church computer center of the Naval Postgraduate School. Object codes were obtained with the I.B.M. H-level compiler, release 18. Data

storage requirements are the equivalent of $4 M N + 26 N + 13 M$ single-precision words, where N is the number of mesh points in the Y direction and M the number in the X direction. The program itself requires the equivalent of about 10^4 single-precision words of main storage. The calculations with a 201 by 64 point mesh required 13 seconds of computer time for the performance of a time step. The program incorporates provisions which enable a long integration to be performed in smaller segments. After a specified number of time steps all quantities involved in the integration are written out on a magnetic tape or disc. The integration can be restarted by reading the data from the tape or disc.

The finite-difference mesh is specified by assigning values to the parameters N , M and $ALPHA$. The last quantity is the basic period of the motion in units of L , one-half the distance between the parallel walls. It fixes the external streamwise dimension of the finite-difference mesh. In all calculations thus far $ALPHA$ was equal to the wave length of the primary unstable mode.

The time step, δt , is controlled by the parameters $FRACEL$ and $XLAMDA$. $FRACEL$ is generally the operating parameter. It is equivalent to f in equation (4.43) and expresses the constraint on δt associated with the advective instability of the central time differencing. $XLAMDA$ is an upper limit on the ratio

$$\frac{4 \delta t}{R \delta x \delta y}.$$

Fixing this ratio insures that the consistency condition, (4.30), is satisfied. All calculations were performed using a value of $1/4$ for $XLAMDA$.

The parameter KINT specifies the number of time steps between the recalculations of δt . At intervals of KINT time steps: the maximum components of horizontal and vertical velocity are determined; the value of δt is adjusted; values of the vorticity are averaged over the last two steps; values of the stream function recalculated; and finally a single time step is performed by the Modified Euler method.

Subroutines SETUP and START begin the operation. Values of the parameters associated with the finite-difference mesh and various other fixed quantities are established in the former. The initial values of the disturbance stream function and vorticity are established in the latter routine.

The subroutines which perform the subsequent integration and their functions are listed below.

ADVANC-----Time step by central differencing.
STEP-----Time step by Modified Euler differencing.
PRESUR-----Solution of Poisson's equation for the
 stream function. Calculation of
 vorticity at the walls.
DHARM-----Calculation of Discrete Fourier transform.
TRISOL-----Solution of tridiagonal system of
 equations.
TIMER-----Calculation of δt .

Subroutines LOAD and RELOAD perform the read and write operations associated with the interruption and restart of the integration. If the data parameter NPROB is less than zero then the main program calls subroutines SETUP and START for the initiation of a new problem. Upon the completion of the specified number of time steps the values of the various quantities are written on a tape or disc by subroutine RELOAD.

The remaining subroutines are associated with the calculation and printing of various derived quantities. The frequency at which the derived quantities are calculated and printed is controlled by the parameters MSCIP and ISCIP. At intervals of MSCIP time steps the main program calls subroutine PRINT. Subroutines EDDYS, ENERGY, and STRESS are called in sequence. The current values of time, δt , the normalized integrals of kinetic energy in the mean flow, the turbulent motion and of total kinetic energy are calculated and printed. At intervals of ISCIP time steps the main program calls subroutine PLOT. Values of the velocity and vorticity of the mean flow as well as the energy and Reynolds stress associated with the turbulent motion, as functions of Y , are printed and plotted. In addition three calling sequences are started in subroutine PRESUR which involve subroutines SPCTRM, MODES and PLOTSP. Values of the spectral densities of squared vorticity and kinetic energy as functions of Y , as well as the normalized sums over Y of those quantities are calculated, printed and plotted. The functions of Y associated with specified disturbance modes are printed.

F. FINITE DIFFERENCE REPRESENTATION OF THE LINEAR EIGENVALUE PROBLEM

The stream function and vorticity are represented by functions which have the form of equation (3.12), but which are discrete in y . Derivatives with respect to y in equation (3.15) are replaced by the same second-order central differences employed for the non-linear case. The result is an algebraic eigenvalue problem. Equation (3.15) is approximated by equations of the form

$$W\bar{\phi} = i\beta\bar{\phi}$$

where, in the general case, W is an $(N-2) \times (N-2)$ complex matrix with eigenvalues β and eigenvectors $\bar{\Phi}$. Of particular interest is the effect of N , the number of mesh points between the walls, on the principle eigenvalues of W .

Let

$$\begin{aligned}\psi &= \Phi_J e^{-i(\alpha x - \beta t)} + \Phi_J^* e^{i(\alpha x - \beta^* t)} \\ \Gamma &= \theta_J e^{-i(\alpha x - \beta t)} + \theta_J^* e^{i(\alpha x - \beta^* t)}\end{aligned}\tag{4.57}$$

Equation (3.13) is satisfied if

$$i\alpha R \left[(\beta/\alpha - U_J) \theta_J + U''\Phi \right] - \frac{\theta_{J+1} - (2 + \alpha^2 \delta y^2) \theta_J + \theta_{J-1}}{\delta y^2} = 0 \tag{4.58}$$

$$J = 2, 3, \dots, N-1$$

where from equation (3.14)

$$\theta_J = \frac{\Phi_{J+1} - (2 + \alpha^2 \delta y^2) \theta_J + \theta_{J-1}}{\delta y^2} \quad J = 2, 3, \dots, N-1 \tag{4.59}$$

The boundary conditions require that

$$\Phi_1 = \Phi_N = 0$$

and that, in accordance with the previous formulation of the vorticity boundary conditions,

$$\begin{aligned}\theta_N &= \frac{p_1 \Phi_{N-1} + p_2 \Phi_{N-2} + p_3 \Phi_{N-3} + p_4 \Phi_{N-4}}{\delta y^2} \\ \theta_1 &= \frac{p_1 \Phi_2 + p_2 \Phi_3 + p_3 \Phi_4 + p_4 \Phi_5}{\delta y^2}\end{aligned}\tag{4.60}$$

where for the various approximation for the boundary conditions, equations (4.12), (4.13), (4.14) and (4.15), p_K , $K = 1, 2, 3, 4$, are given by

COEFFICIENTS FOR VORTICITY BOUNDARY CONDITIONS



$$\bar{\theta} = \begin{pmatrix} \theta_2 \\ \theta_3 \\ \vdots \\ \vdots \\ \theta_{N-2} \\ \theta_{N-1} \end{pmatrix} \quad \bar{\phi} = \begin{pmatrix} \phi_2 \\ \phi_3 \\ \vdots \\ \vdots \\ \phi_{N-2} \\ \phi_{N-1} \end{pmatrix} \quad \bar{\gamma} = \begin{pmatrix} \theta_1 \\ 0 \\ \vdots \\ \vdots \\ 0 \\ \theta_N \end{pmatrix} \quad (4.65)$$

And adopt the notation for a diagonal matrix with diagonal elements

$$\eta_J \quad J = 2, 3, \dots, N-1$$

$$\Lambda(\eta_J) = \begin{bmatrix} \eta_2 & & & & \\ & \eta_3 & & & \\ & & \eta_4 & & \\ & & & \ddots & \\ & & & & \eta_{N-2} \\ & & & & & \eta_{N-1} \end{bmatrix} \quad (4.66)$$

Equations (4.61) and (4.62) become

$$i\beta\bar{\theta} = \Lambda(i\alpha U_J) \bar{\theta} - \Lambda(i\alpha U'') \bar{\phi} + \frac{1}{R\delta y^2} [B \bar{\theta} + \bar{\gamma}] \quad (4.67)$$

$$\bar{\theta} = \frac{1}{\delta y^2} B \bar{\phi} \quad (4.68)$$

The vorticity boundary conditions, equations (4.60), become

$$\bar{\gamma} = \frac{1}{\delta y^2} P \bar{\phi} \quad (4.69)$$

The boundary conditions, $\phi_1 = \phi_N = 0$ are satisfied by equations (4.67) and (4.68). Substituting equations (4.68) and (4.69) in (4.67) we obtain



$$i\beta B\bar{\Phi} = \left\{ i \left[\Lambda (\alpha U_J) B - \Lambda (\alpha U''' \delta y^2) \right] + \frac{1}{R\delta y^2} \left[B^2 + P \right] \right\} \bar{\Phi}$$

Multiplying through by B^{-1} we obtain

$$i\beta\bar{\Phi} = \left\{ \frac{1}{R\delta y^2} \left[B + B^{-1} P \right] + iB^{-1} \left[\Lambda (\alpha U_J) B - \Lambda (\alpha U''' \delta y^2) \right] \right\} \bar{\Phi} \quad (4.70)$$

Thus

$$i\beta\bar{\Phi} = W\bar{\Phi} \quad (4.71)$$

Where

$$W = \frac{1}{R\delta y^2} \left[B + B^{-1} P \right] + iB^{-1} \left[\Lambda (\alpha U_J) B - \Lambda (\alpha U''' \delta y^2) \right] \quad (4.72)$$

For the linear equations the problem is simply the determination of the eigenvalues and eigenvectors of a complex matrix. Because of symmetry of the laminar velocity distribution the symmetric and anti-symmetric solutions of both the differential and algebraic equations are uncoupled. It is useful to take advantage of this fact to reduce the order of the matrix W . The well-known unstable solutions for the Plane Poiseuille flow are all symmetric. It appears that all the anti-symmetric solutions are stable (Grosch 1968). In the present undertaking only symmetric modes are considered.

Thus we consider only the region

$$-1 \leq y \leq 0$$

and add the boundary conditions at the centerline ($y = 0$, $J = \frac{N+1}{2}$)

$$\bar{\Phi}' = \bar{\Phi}''' = \dots = 0$$

In terms of the finite differences this is equivalent to



$$\bar{\Phi} \frac{N-1}{2} = \bar{\Phi} \frac{N+3}{2} \quad \theta \frac{N-1}{2} = \theta \frac{N+3}{2}$$

The matrix formulation remains the same except that the order of the various matrices and vectors is reduced from $N-2$ to $\frac{N-1}{2}$, and equations (4.64) and (4.65) for B , P , $\bar{\Phi}$, $\bar{\theta}$ and $\bar{\gamma}$ become

$$B = \begin{bmatrix} \omega & 1 & & & & \\ & 1 & \omega & 1 & & \\ & & 1 & \omega & 1 & \\ & & & \ddots & \ddots & \\ & & & & \ddots & \\ & & & & & 1 & \omega & 1 \\ & & & & & & 2 & \omega \end{bmatrix} \quad P = \begin{bmatrix} p_1 & p_2 & p_3 & p_4 \end{bmatrix} \quad (4.73)$$

$$\bar{\theta} = \begin{Bmatrix} \theta_2 \\ \theta_3 \\ \vdots \\ \vdots \\ \theta_{\frac{N-1}{2}} \\ \theta_{\frac{N+1}{2}} \end{Bmatrix} \quad \bar{\Phi} = \begin{Bmatrix} \bar{\Phi}_2 \\ \bar{\Phi}_3 \\ \vdots \\ \vdots \\ \bar{\Phi}_{\frac{N-1}{2}} \\ \bar{\Phi}_{\frac{N+1}{2}} \end{Bmatrix} \quad \bar{\gamma} = \begin{Bmatrix} \theta_1 \\ 0 \\ 0 \\ \vdots \\ \vdots \\ 0 \end{Bmatrix} \quad (4.74)$$

The eigenvalues and eigenvectors of equation (4.71) were computed numerically by means of the Q R algorithm (Wilkinson 1965, Parlette 1966). This algorithm, for the solution of an algebraic eigenvalue problem, was developed by Francis (1962). It involves a sequence of unitary transformations which yield an upper canonical form of the eigenvalue problem. The inverse of the matrix B in equation (4.70) is obtained by standard Gauss-Elimination. All calculations were performed in double precision (sixteen decimal digits) on an I.B.M. 360/67 computer. Standard I.B.M. scientific library subroutines, with some



minor modifications, were employed for the calculation of the inverse of B and the eigenvalues and eigenvectors of W . A listing of the FORTRAN program is reproduced as Appendix C.



V. RESULTS AND DISCUSSION

A. LINEAR CALCULATIONS

Symmetric solutions of the algebraic eigenvalue problem, equation (4.71), were obtained at regularly spaced points in a portion of the wave number-Reynolds number domain for various values of N ranging from 41 to 201. The investigation was confined to the vicinity of the unstable region at Reynolds numbers out to 25000. The calculations yield, in each case, $N/2$ symmetric eigenfunctions and the $N/2$ associated eigenvalues. A summary of selected results is depicted in Figs. 4-11.

Preliminary calculations which employed the various order formulations of the vorticity boundary conditions, Table III, indicated substantial differences in the solutions with the first and second order formulations but only slight differences between solutions based on second and higher order formulations. Consequently the consistent second-order formulation was adopted for the subsequent linear calculations, as well as for the numerical integration.

Calculations with $N = 41$ revealed no indication of linear instability, ($\beta_I < 0$), at any point in the region investigated. Calculations were performed for wave numbers from .66 to .94 in increments of .02 for a regular sequence of Reynolds numbers out to 25000. In every case the calculated values of β_I reached a local minimum at a Reynolds number less than 20000. Consequently it is believed that a second-order finite-difference representation of the equations of motion with $N \leq 41$, ($\delta y \geq .05$), completely obscures the phenomenon of linear instability. For $N > 41$, points on the neutral curve were obtained by interpolation.

Neutral curves, determined in this manner, for $N = 61$, 101 and 201 , are shown in Fig. 4, along with the neutral curve established by Grosch. The agreement with established results is poor for $N = 61$, fair for $N = 101$ and for $N = 201$ reasonably good. Although it is not shown, the neutral curve for $N = 161$ differs only slightly from that for $N = 201$ and only on the upper branch. The accuracy of the representation, for a given value of N , is greatest in the vicinity of the lower branch of the neutral curve. This is illustrated in Fig. 5, where the calculated growth rates, β_I , are plotted versus the wave number, α , for a Reynolds number of 15000 . Solutions for the eigenvalues of the least stable mode, in a sequence of calculations with increasing N converge most rapidly for the smaller values of α . The same kind of behavior characterizes the convergence of the asymptotic expansions for the solution to the linear differential equation (Potter 1966).

The sets of calculated eigenvalues for the cases $\alpha = 1.0$, $R = 7333.3$, 11333.3 and 25000 are plotted in Figs. 6, 7, and 8. The orderly arrangements of the eigenvalues in the complex plane are quite striking. None of the eigenvalues has a phase velocity, β_R , greater than 1.5 , the maximum velocity of the laminar flow, and, at the lower Reynolds numbers, the majority have phase speeds equal to the mean laminar velocity. The effect of increased Reynolds number is evidently the greatest on the most stable modes. As the Reynolds number is increased the eigenvalues approach the neutral line ($\beta_I = 0$). As $R \rightarrow \infty$, the matrix W in equation (4.71) becomes Hermitian. In the limit all the solutions are neutrally stable.

A measure of the accuracy of the calculations can be obtained by comparison with selected results of Grosch (1968) and Thomas (1953). Calculated growth rates in the unstable region for $N = 101$, 161 and 201 , as well as values calculated by Grosch are plotted in Figs. 9 and 10, for Reynolds numbers 7333.3 and 11333.3 respectively. The very slow convergence of the second order finite-difference scheme in the vicinity of the upper branch of the neutral curve is evident.

In terms of the reference units employed here, the primary eigenvalues calculated by Thomas were, for $\alpha = 1.0$, $R = 1066.6$ and $R = 6666.7$ respectively

$$\beta = .4847 + i \ .0393$$

$$\beta = .3563 - i \ .0055$$

For these cases the present calculations with $N = 201$ yield

$$\beta = .4891 + i \ .0393$$

$$\beta = .3593 - i \ .0041$$

A comparison of the calculated eigenvectors for the case $R = 6666.7$, $\alpha = 1.0$ is given in Fig. 11. Results for the real part of the eigenvector are identical to four significant digits. There are however small differences in the imaginary parts. Thomas employed a transformation which made his finite-difference approximation basically of fourth order. It is not surprising that a second-order scheme might produce slightly different results for a function with large derivatives and curvature. However test calculations, with a linearized form of the numerical integration, which employed the calculated linear solutions as initial conditions, suggest that most of the differences are attributable to slight numerical errors in the present solutions.

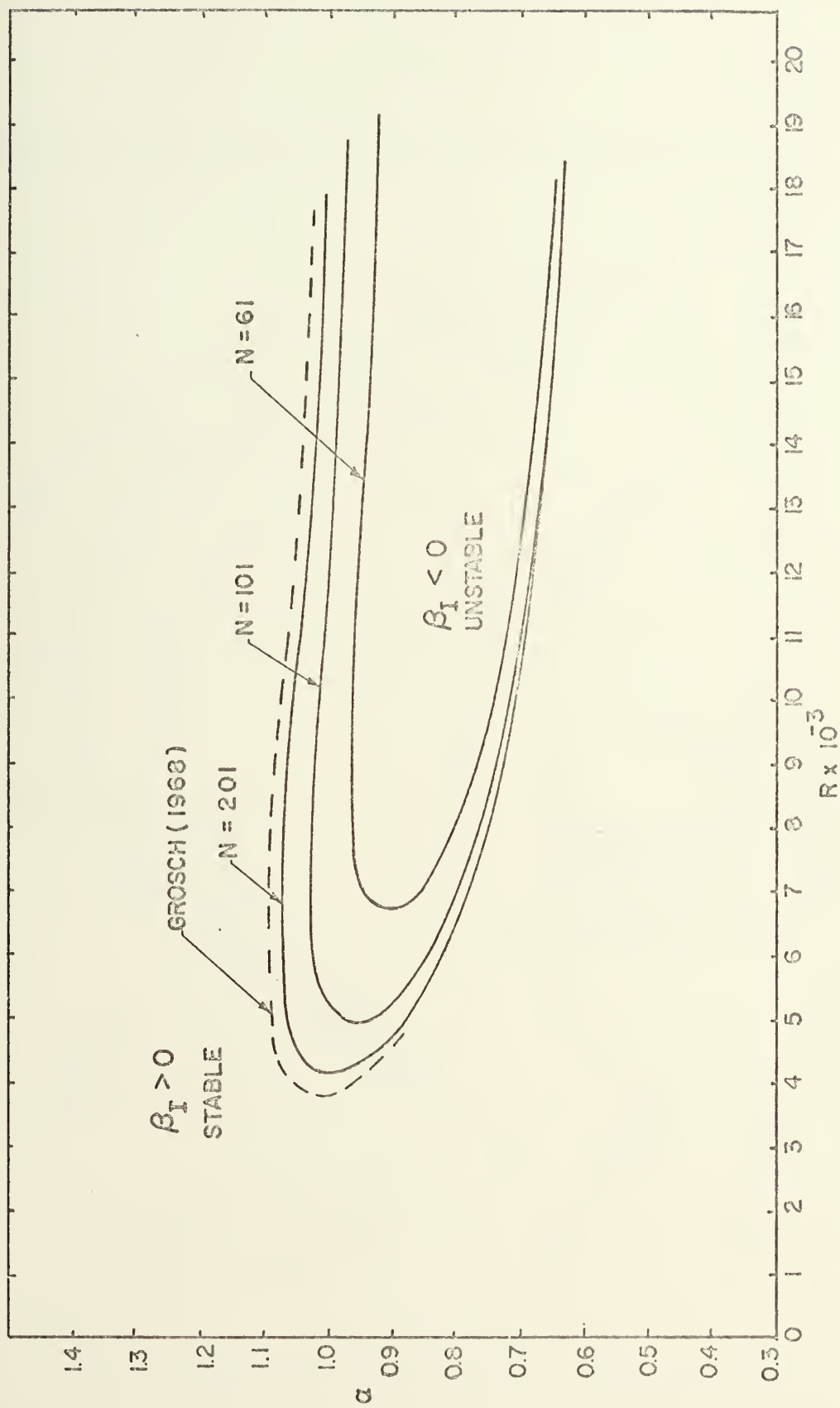


FIGURE 4 EFFECT OF FINITE DIFFERENCE MESH SIZE ON CURVE OF NEUTRAL STABILITY FOR PLANE POISEUILLE FLOW.

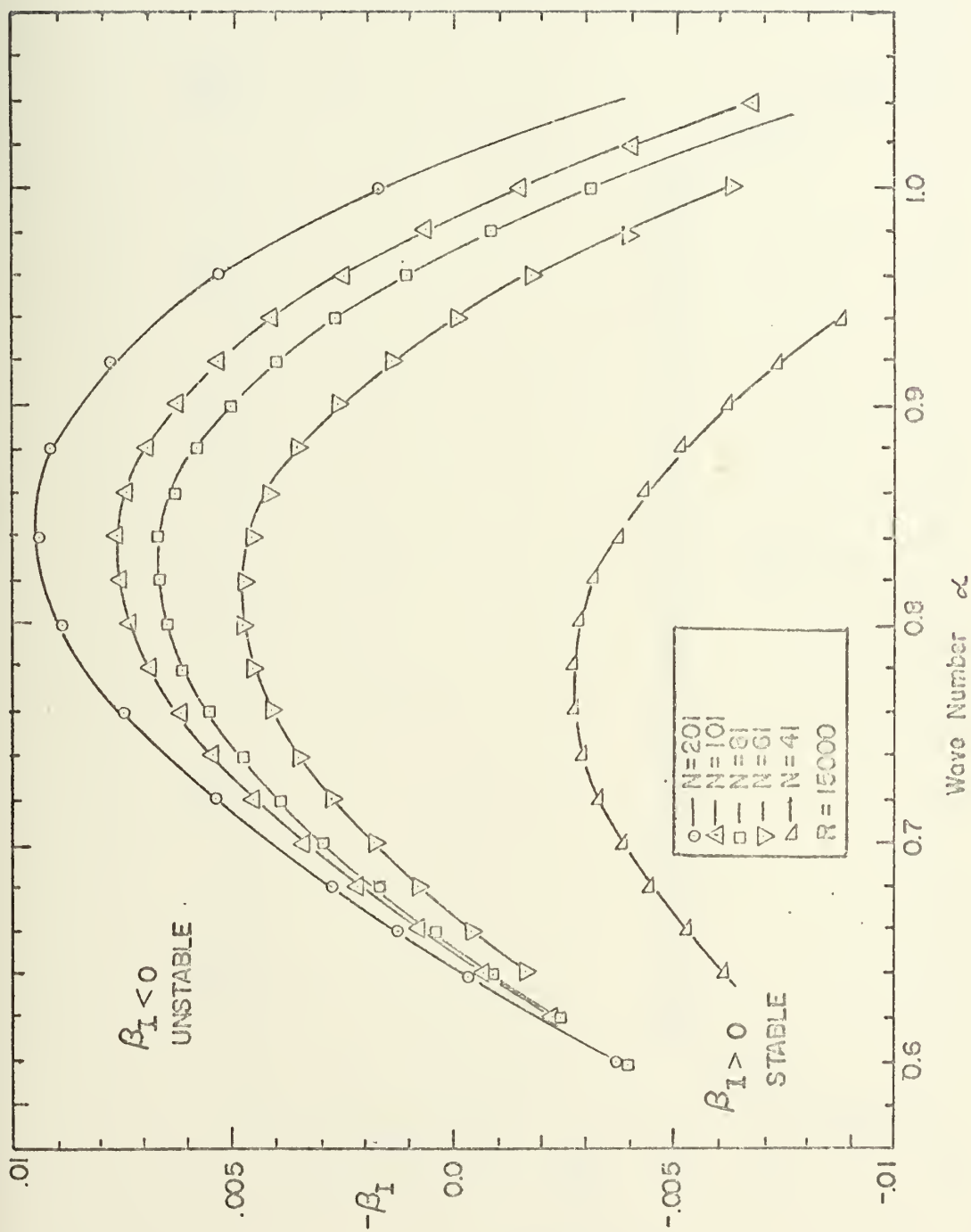


FIGURE 5 EFFECT OF N ON CALCULATED GROWTH RATE

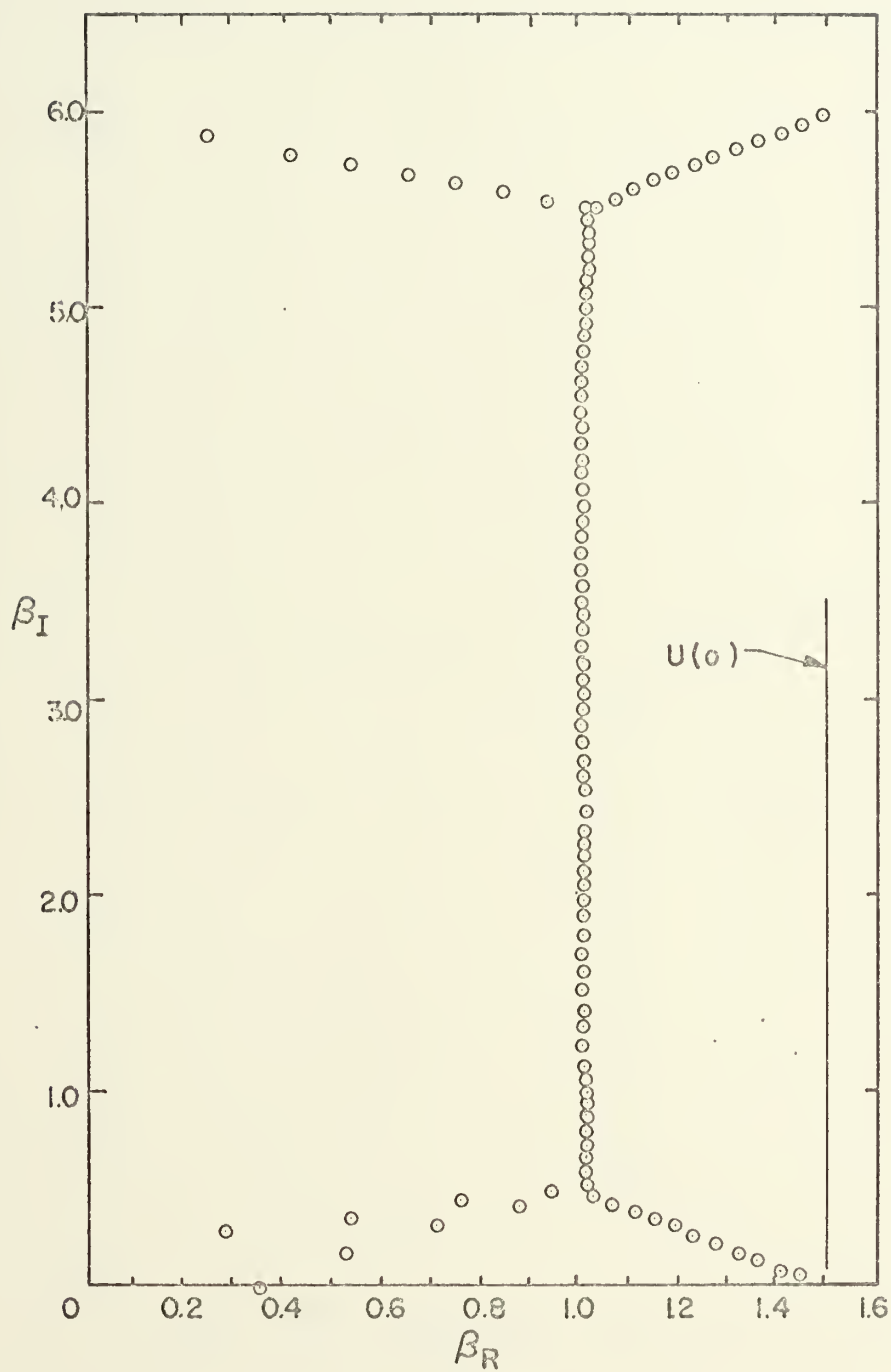


FIGURE 6
 CALCULATED EIGENVALUES - SYMMETRIC MODES
 $R = 6666.7$ $\alpha = 1.0$ $N = 201$

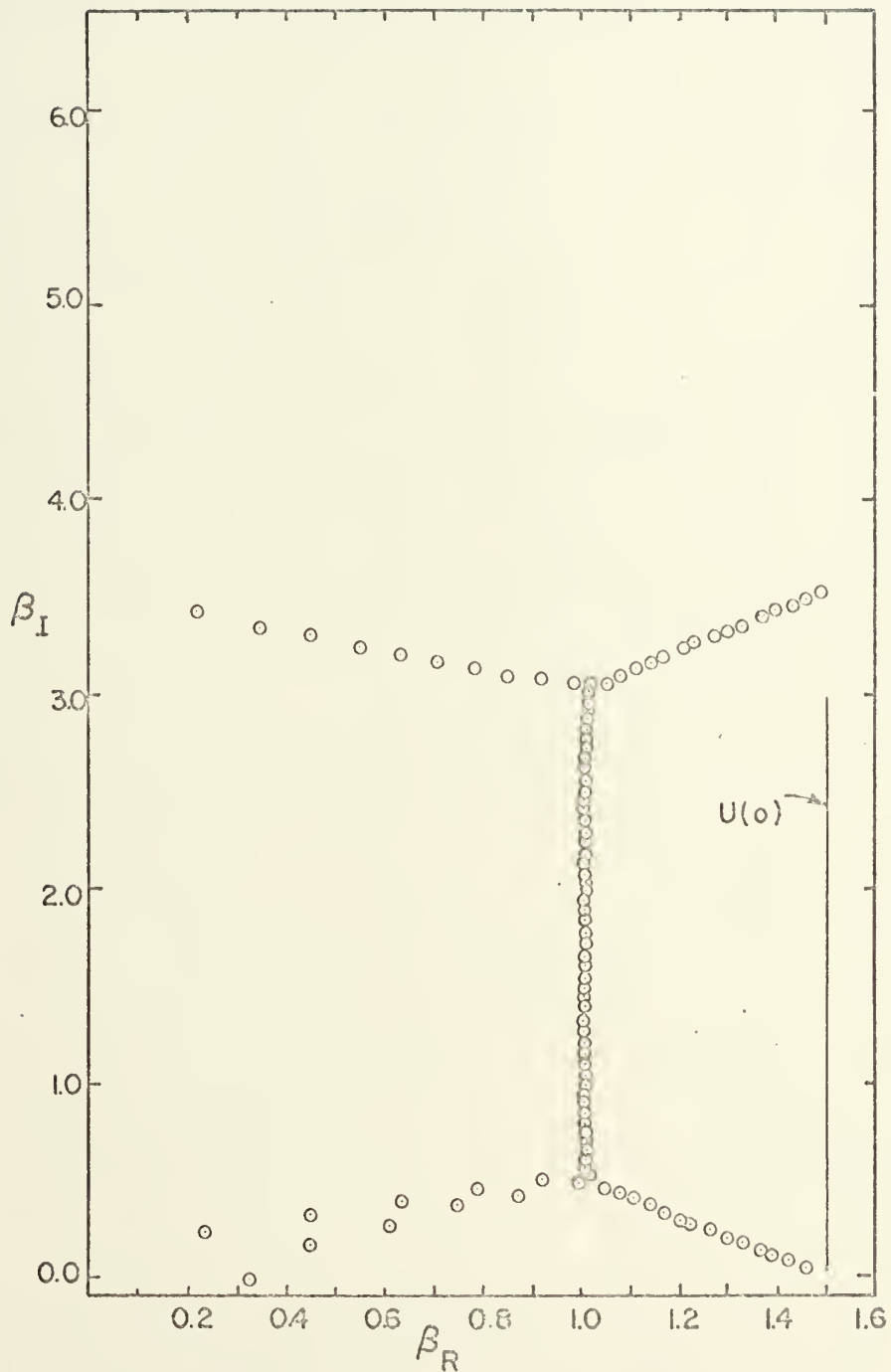


FIGURE 7
 CALCULATED EIGENVALUES - SYMMETRIC MODES
 $R = 11333.4$ $\alpha = 1.0$ $N = 201$

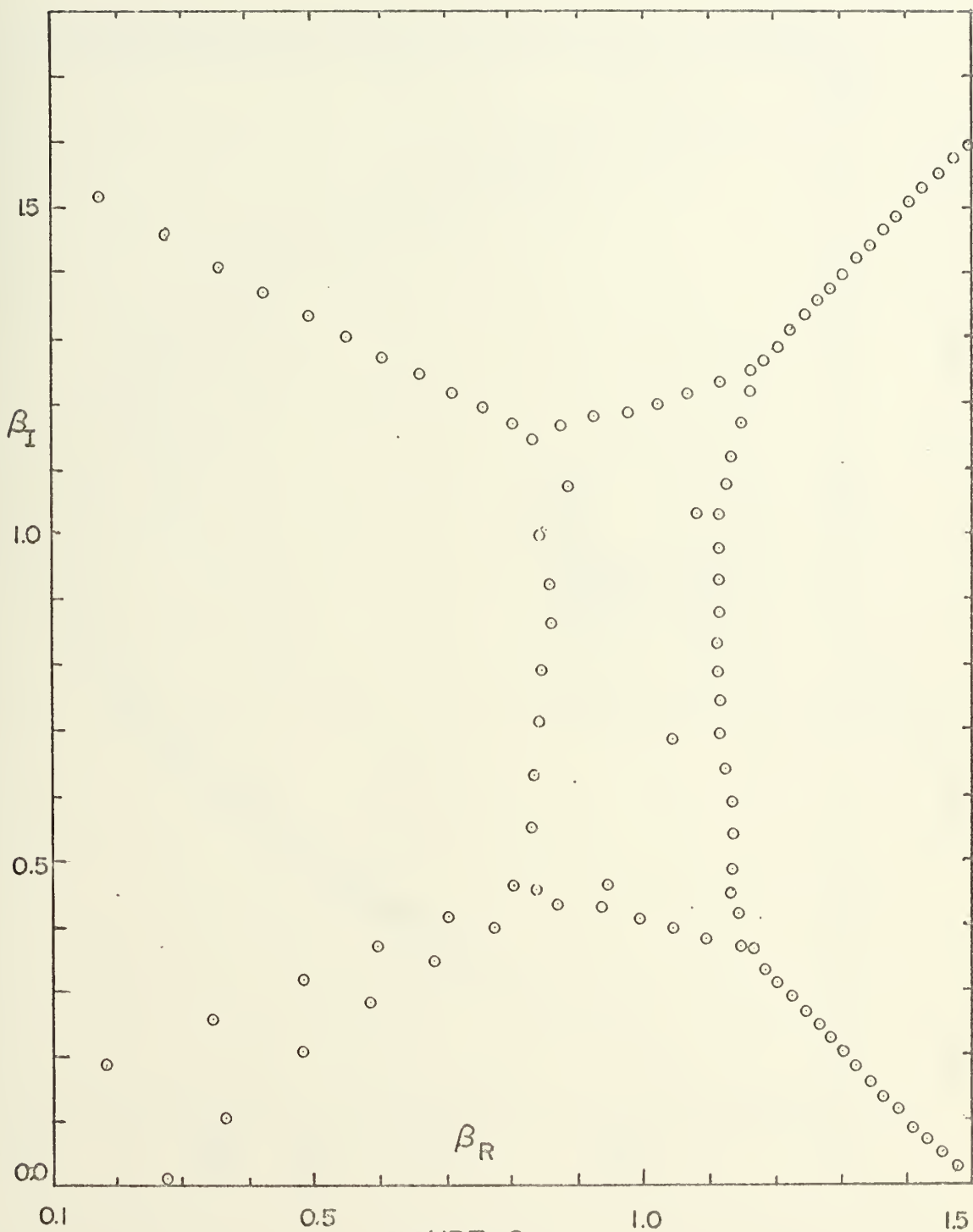


FIGURE 8
 CALCULATED EIGENVALUES — SYMMETRIC MODES
 $R = 25,000$ $\alpha = 1.0$ $N = 201$

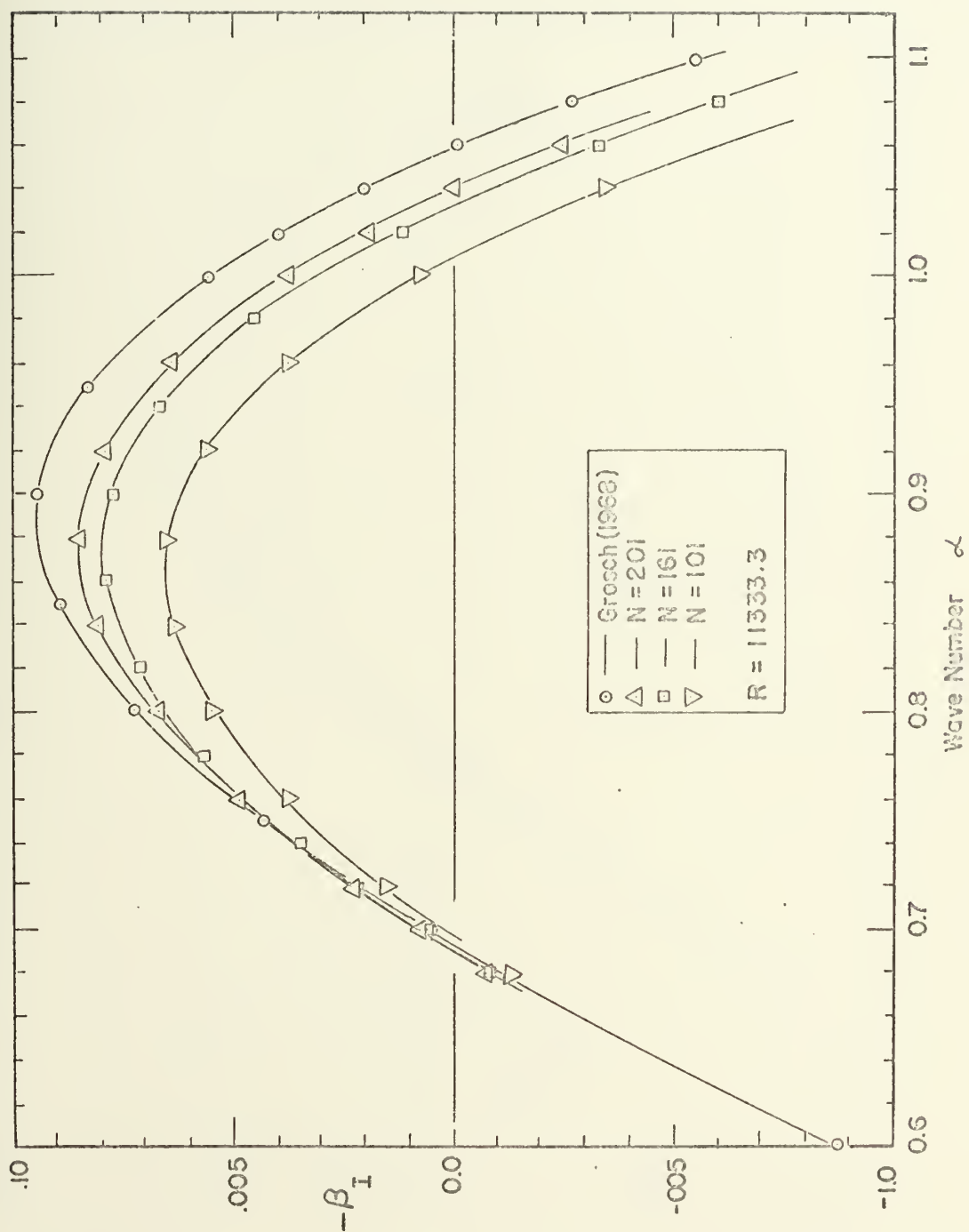


FIGURE 9 COMPARISON OF CALCULATED GROWTH RATES.

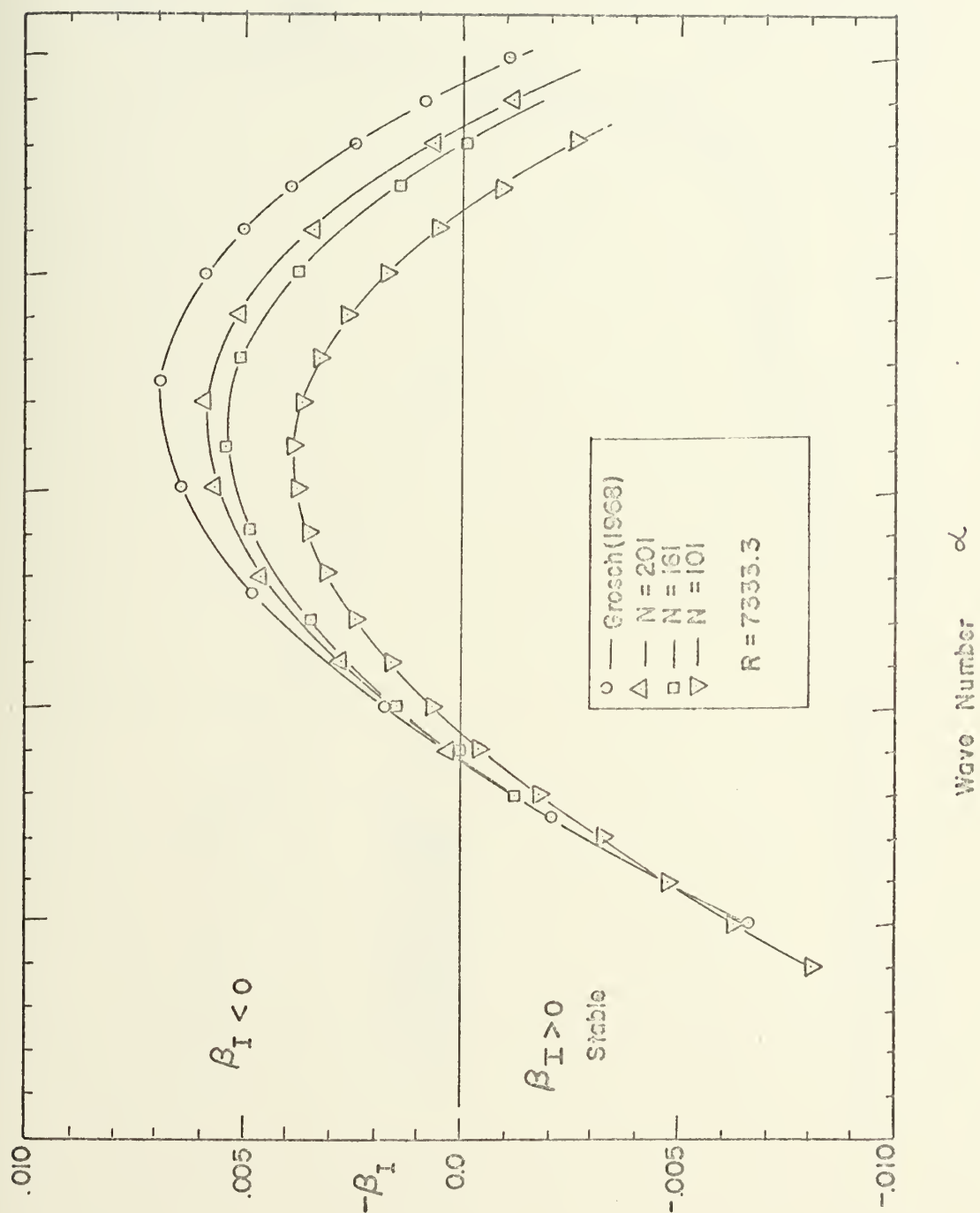


FIGURE 10 COMPARISON OF CALCULATED GROWTH RATES.

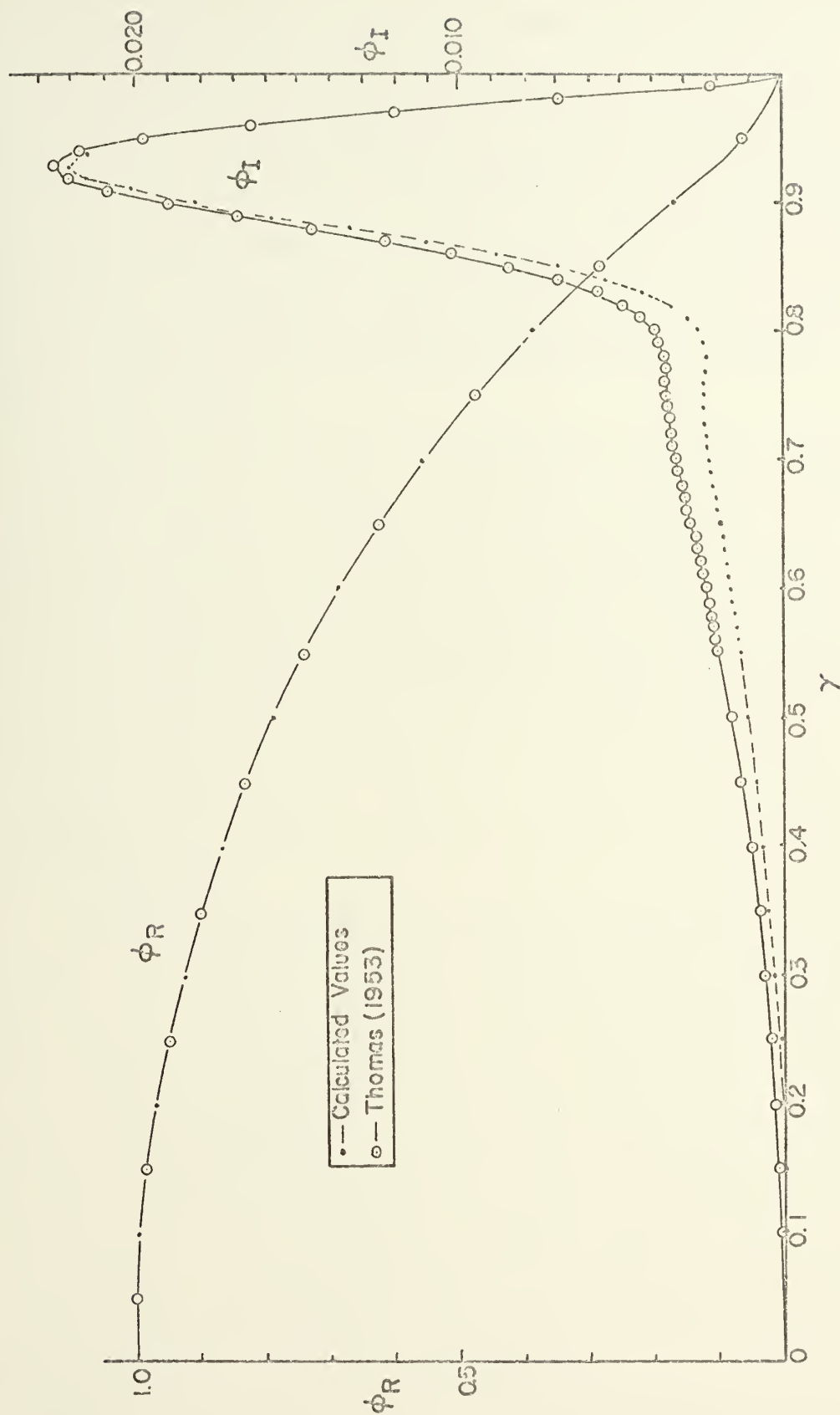


FIGURE II COMPARISON OF CALCULATED EIGENVECTORS $R=6666.7$ $\alpha=1.0$

The errors associated with a particular eigen-solution by the Q. R. algorithm are dependent, among other things, on the ratio of the modulus of the associated eigenvalue to the largest such modulus. Decreased values of that ratio imply increased errors in the solution. In the present application the eigenvalue associated with the least stable mode has the smallest modulus, and it is reasonable to expect that there might be some accumulation of numerical error in the solution for that mode.

In retrospect it seems that, for the linear solutions, an iterative method which focuses on a single mode, such as the approach introduced by Nachtsheim (1964), might have been more appropriate for the limited and definite purposes of the present undertaking. However in any application in which there is interest in the higher modes the matrix approach has definite advantages.

B. NUMERICAL INTEGRATIONS

1. Preliminary

The linear calculations, in addition to providing a measure of the resolution required to represent adequately the two dimensional motions, provide a rational means of establishing initial conditions for the numerical integration. In particular they provide a unique means of testing the stability (in the linear range) and accuracy of the finite-difference formulation and solution. The calculation of the non-linear terms in the finite-difference solution can be bypassed by minor changes in the FORTRAN code. If this is done, the scheme should be capable of reproducing the calculated linear eigensolutions. Specifically, if an unstable mode is employed to establish the initial conditions, the numerical integration should produce the predicted

growth rate and phase speed. The variation of the calculated turbulent kinetic energy with time should be, from equation (3.18), $e^{-2\beta_I t}$. Calculations of the spectral density of turbulent kinetic energy and squared vorticity should reveal no spurious excitation in other represented wave lengths. Finally, perhaps the most stringent requirement is that the performance of a large number of time steps should not produce any significant distortion of the normalized eigenvector.

If the scheme can be demonstrated to be stable and accurate, at least in the linear features, then, since the virtues of the particular non-linear representation have been fairly well established elsewhere, calculations can be performed in the non-linear range with confidence in the accuracy of the results.

The resolution requirements indicated by the linear calculations are very great: about 201 mesh points are required in the Y direction. The requirements for resolution in the X direction are determined by the extent to which higher harmonics, or smaller scales of motion, are excited by the non-linear terms. M points in the X direction represent M/2 Fourier modes. As a result of the well-known constraints on energy cascades in a two-dimensional motion the extent of the excitation of the higher harmonics should not be great. Kraichnan (1967) has predicted a -3 power law for the spectral density of turbulent kinetic energy in the smaller scales. If this is the case, then the energy in wave number 10, for example, should be less by three decades than that in the primary mode of the disturbance. If the basic period of the motion, the external downstream dimension of the finite-difference mesh, is chosen to be equal to the period of the unstable mode, a mesh with $M = 64$, which represents 32 Fourier modes, should be adequate.

2. Results

A tabulation of information which serves to identify the various integrations or runs which will be referred to in this section is given in Table IV.

TABLE IV
SUMMARY OF NUMERICAL INTEGRATIONS

| Run | Initial Con- ditions | 2σ | $E(o)$ | Number of Time Steps | Time | Computer Time (hrs) |
|-----|-------------------------|----------------|----------------------|----------------------------|------|---------------------------|
| 1 | B* | .3 | $.4 \times 10^{-1}$ | 1000 | 11.7 | 4.8 |
| 2 | A* | $.1\sqrt{5}$ | $.25 \times 10^{-1}$ | 1550 | 20.0 | 6.1 |
| 3 | A | .01 | $.5 \times 10^{-4}$ | 800 | 8.3 | 3.8 |
| 4 | A | $.01\sqrt{10}$ | $.5 \times 10^{-3}$ | 800 | 8.3 | 3.8 |
| 5 | A | .1 | $.5 \times 10^{-2}$ | 800 | 8.2 | 3.8 |
| 6 | A | $.1\sqrt{10}$ | $.5 \times 10^{-1}$ | 800 | 7.6 | 3.8 |
| 7 | A | 1.0 | .5 | 3700 | 11.0 | 17.5 |
| 8 | A | $.1\sqrt{5}$ | $.25 \times 10^{-1}$ | 5900 | 61.2 | 28.0 |
| 9 | A | $.1\sqrt{2}$ | $.25 \times 10^{-2}$ | 2700 | 52.5 | 12.0 |

Initial conditions:

$$\psi_{K,J}^o = \sigma \left\{ \Phi_J e^{i\alpha x_K} + \Phi_J^* e^{-i\alpha x_K} \right\}$$

$$A - R = 6666.7, \alpha = 1.0$$

$$\Phi_J \text{ from Thomas (1953)}$$

$$B - R = 15000, \alpha = .86$$

$$\Phi_J \text{ from present calculations}$$

*non-linear terms suppressed.

As indicated in the table, runs one and two were performed with the non-linear terms suppressed. The remaining runs included the non-linear interactions and were at a Reynolds number of 6666.7. The linear solution calculated by Thomas was employed as an initial condition. They differ in the initial amplitude, σ .

Preliminary test calculations, with the non-linear terms suppressed, which employed, as initial conditions, the primary eigenfunctions calculated here indicated not only the accuracy of the integration scheme, but also a slight inaccuracy in the calculated eigenvectors. Run number one is typical of these calculations, most of which were performed in fairly coarse arrays. The logarithm of the ratio of the turbulent energy to its initial value, in that run, is plotted as a function of time, along with predicted rate in Fig. 12. During the course of an initial transient which persists for about six units of time, the growth rate increases and then decreases to about the predicted value. Although the errors in the growth rate, during that period, are large the asymptotic value is very good. Other calculations with $N = 41$ and a decaying disturbance exhibited the same behavior. In both cases the predicted rate was achieved and persisted after the transient. Reference to equation (3.19) suggests the cause of the transient, the presence of small errors in the calculated eigenvectors. In effect, small contributions from higher modes are present in the linear solution for the least stable mode. Figures 6 and 7 illustrate the fact that the stability of the great majority of the higher linear modes far exceeds the instability of the single unstable mode; there are wide variations in the exponential rates of growth or decay. After several units of time the energy associated with the

errors is washed away. The integration routine, if it is accurate, acts as a filter and tends to suppress contributions from all but the least stable mode when the non-linear terms are omitted.

A subsequent run, (run number two), at a Reynolds number of 6666.7 which employed the eigenvector calculated by Thomas as initial conditions tends to confirm this suggestion. For this run, the logarithm of the energy ratio, along with both the growth rates predicted in the present calculations and that of Thomas are plotted in Fig. 13. There is a very slow decrease in the growth rate out to about ten units of time. After that point the variation is linear and very close to the growth rate predicted by the second-order calculations. In effect, the eigenvector calculated by Thomas in a basically fourth-order formulation is a better approximation of the second order solution than those obtained in the present work. After 1000 time steps the vector was renormalized and printed, in order to obtain a measure of the distortion. The variations, where they occur, are plotted in Fig. 14. The maximum distortion in amplitude was .035% and in phase 1.5%.

Calculated spectral densities of kinetic energy and squared vorticity revealed no indication of spurious excitation of other spatial wave lengths in any of the linear runs.

Thus it may be concluded that the integration scheme is stable and highly accurate.

Although the performance of the integration routine in the linear tests was most satisfying, the inaccuracies in the calculated eigenvectors and the resulting transient in the linear integration inhibit a most useful application of the program. That is, to the

determination of critical amplitudes at sub-critical values of the Reynolds number. For this application the representation of the linear behavior in the early stages should be more accurate than that which results from the present calculation. However, more accurate methods, for the determination of the solutions of the algebraic equations in a consistent second-order model of the linear problem, are available. In particular the refinements of the iterative approach of Nachtsheim (1964), which were developed and employed by Reynolds are most promising.

In the subsequent non-linear calculations at $R = 6666.7$ and $\alpha = 1.0$, the linear solution, calculated by Thomas (1953), was employed for the initial condition. The amplitude factor, σ , is based on the normalization of the linear solution given by Thomas. The objectives of the non-linear calculations were, to determine the effect of various amplitudes on the initial development of the disturbance, and, if possible, to achieve an equilibrium state for the two-dimensional turbulence.

In runs three through six the initial amplitudes were such that the initial kinetic energy of the disturbance increased, by decades, from $.5 \times 10^{-4}$ to $.5 \times 10^{-1}$. For reference, the normalized sum of kinetic energy in the laminar motion is .6 in the present units. The growth of turbulent energy for these calculations, as well as for run number nine, are shown in Fig. 15. For run number three, no significant departures from the linear behavior were observed until after five units of time. This provides some measure of the amplitude at which the non-linear interactions become significant. The limit in the growth of the turbulent energy in run number six suggests the existence of an

equilibrium state, in terms of kinetic energy, in the range

$$.005 < \hat{E} < .05.$$

In order to verify the limiting behavior of the turbulence a long calculation was performed at an even higher energy level. This was run number five. In this case the initial kinetic energy of the disturbance was of the same order as the energy in the laminar flow. The subsequent variations in the kinetic energies of the mean flow, the turbulent motion, and of the energy in the primary mode of the disturbance, as well as the total kinetic energy in the domain are shown in Fig. 16. All quantities are normalized with respect to the initial value of the total energy. Points are plotted at intervals of 100 time steps. It is the variation of the total energy which most clearly indicates the trend. It decayed monotonically, and by the end of the run about 13% of the kinetic energy in the system had been dissipated. The early behavior of the turbulence is dominated by large exchanges of energy between it and the mean flow.

Run number eight, in which the initial energy of the disturbance was .025, produced an approximate equilibrium condition. The variation of the various energy terms is shown in Fig. 17. After a slight decrease, the total energy remained virtually constant for the last 25 units of time. Again, there is a periodic exchange of energy between the mean flow and the disturbance. However in this case the period of the oscillation was more than five times as great as in the previous case, and, in the course of the development, the amplitude decreased markedly. A comparison of the variations of the total kinetic energy in the two-dimensional turbulence to the energy in the primary mode suggests that the oscillations are associated with transients in the development of

the higher wave numbers. After 47 units of time the amplitude of the oscillation was much reduced, and the difference between the two kinetic energy terms, which is the total kinetic energy in the higher wave numbers, remained nearly constant. Mean velocity profiles at extreme points in the early variations of the disturbances are given in Fig. 19. Plots of the mean velocity, mean vorticity and turbulent kinetic energy near the final state are given in Fig. 20. The mean velocity profile is only slightly distorted although near the walls there are significant changes in its curvature. Calculated spectral densities of the turbulent kinetic energy are consistent with the -3 power law proposed by Kraichnan. Values of the spectral density of kinetic energy at $y = \pm .85$ are given in Fig. 21, mean values over y , in Fig. 22.

The function of y which describes the primary mode remains symmetric. In addition, it turns out that modes three and five are also symmetric while modes two and four are anti-symmetric. Although the remaining mode shapes were not determined in the calculations, it appears likely that the odd-numbered modes are symmetric and the even-numbered modes anti-symmetric. Mode shapes, in terms of amplitude and phase, for modes one through four are given in Figs. 24 through 27. The initial shape for mode one is given in Fig. 23. It is interesting to note that, although the symmetry and anti-symmetry of the odd and even-numbered modes does not necessarily follow from equations (3.4), it does follow from the equations treated by Watson (1960) and Reynolds (1967), in which certain of the non-linear terms are ignored.

The last calculation, run number nine, was started with a disturbance energy, less by a factor of ten, than that of run eight.

In this case the variations of the various energy terms were nearly monotonic. After 50 units of time the disturbance energy had increased by more than a factor of three. It appears likely that if this calculation were continued the equilibrium energy level would have been attained without the large oscillations which characterized the initial behavior of the previous run.

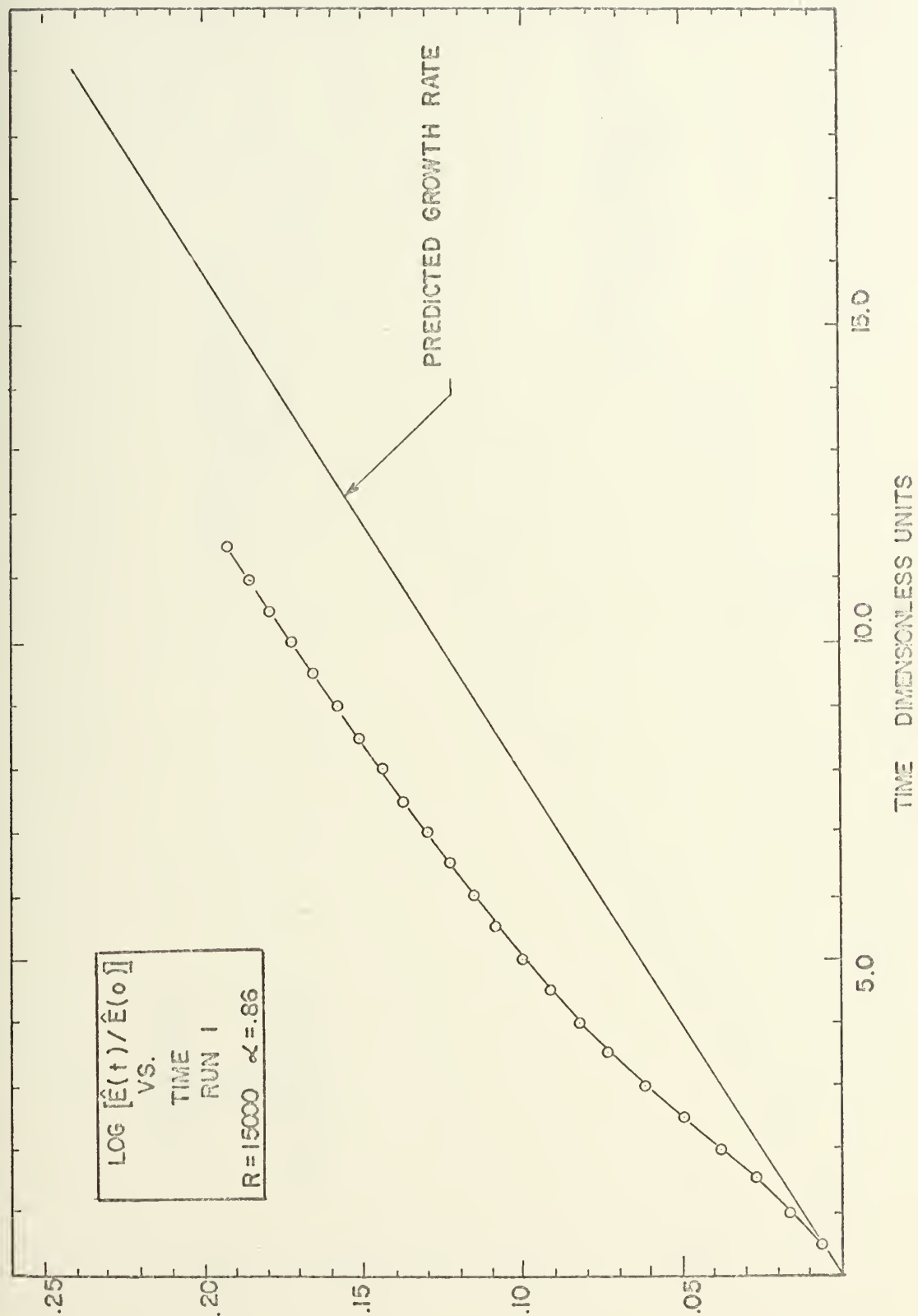


FIGURE 12 TEST FOR LINEAR SOLUTION.

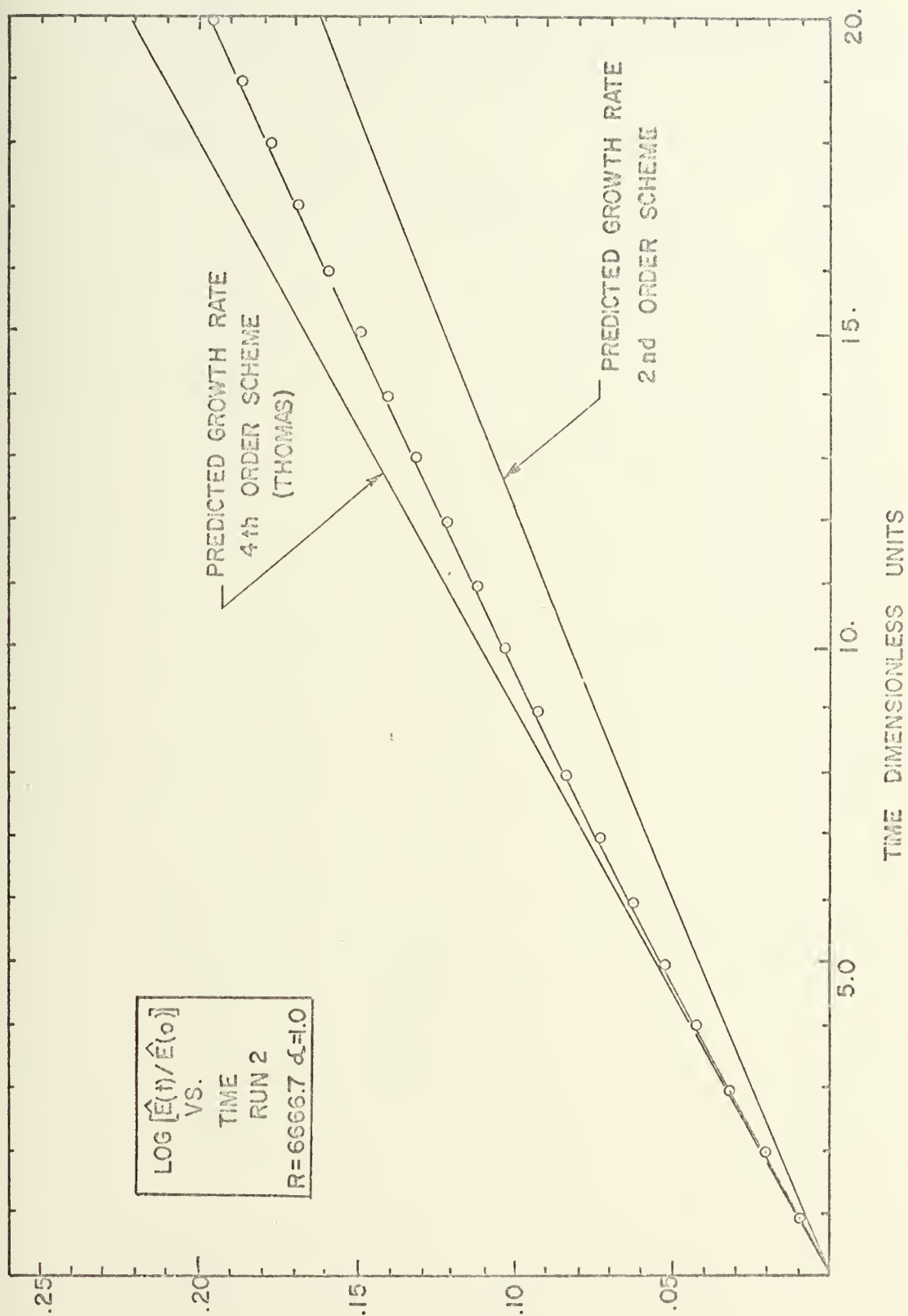


FIGURE 13 TEST FOR LINEAR SOLUTION.

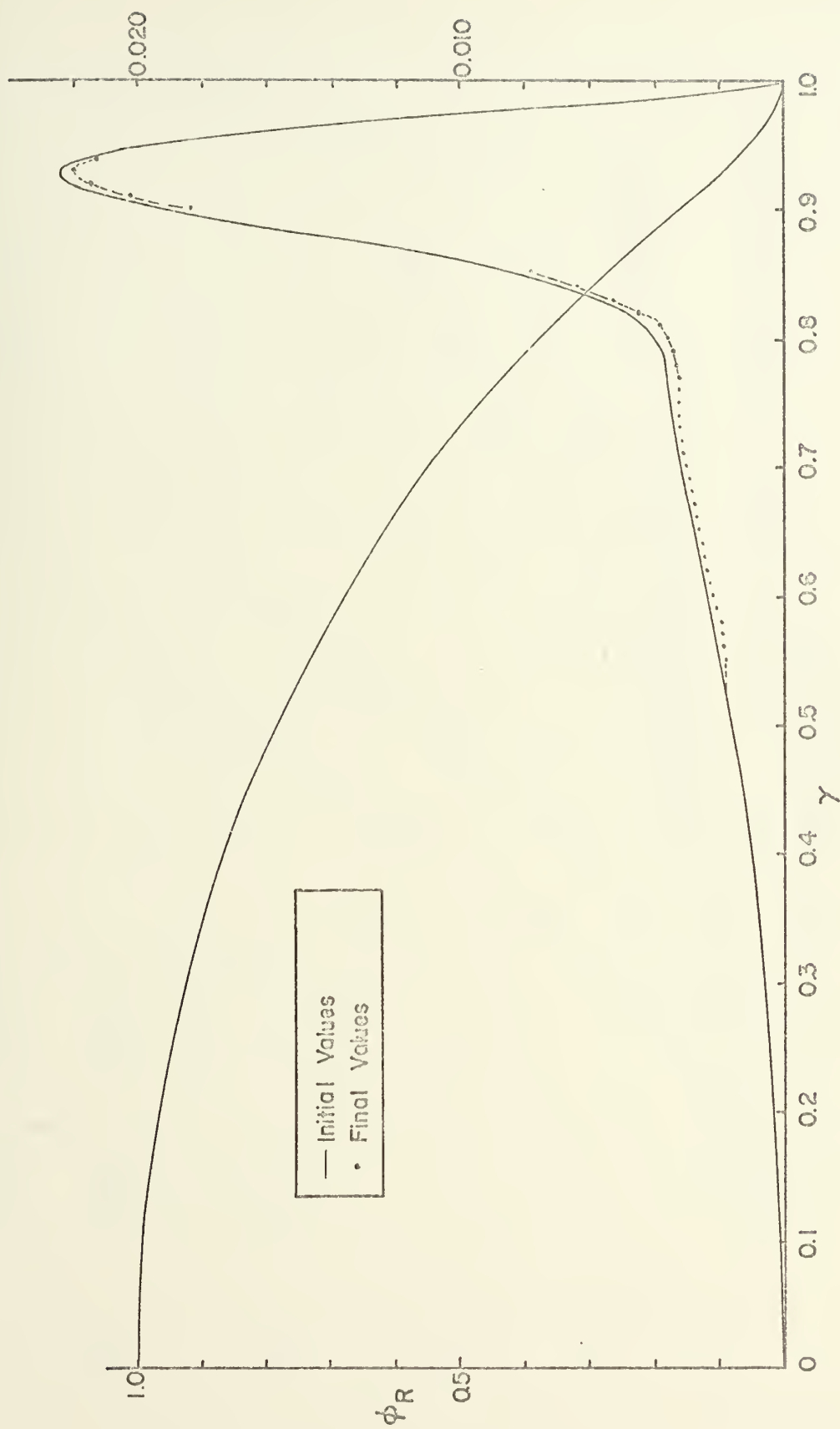


FIGURE 14 RUN NO.2 DISTORTION OF EIGENVECTOR AFTER 1000 STEPS.

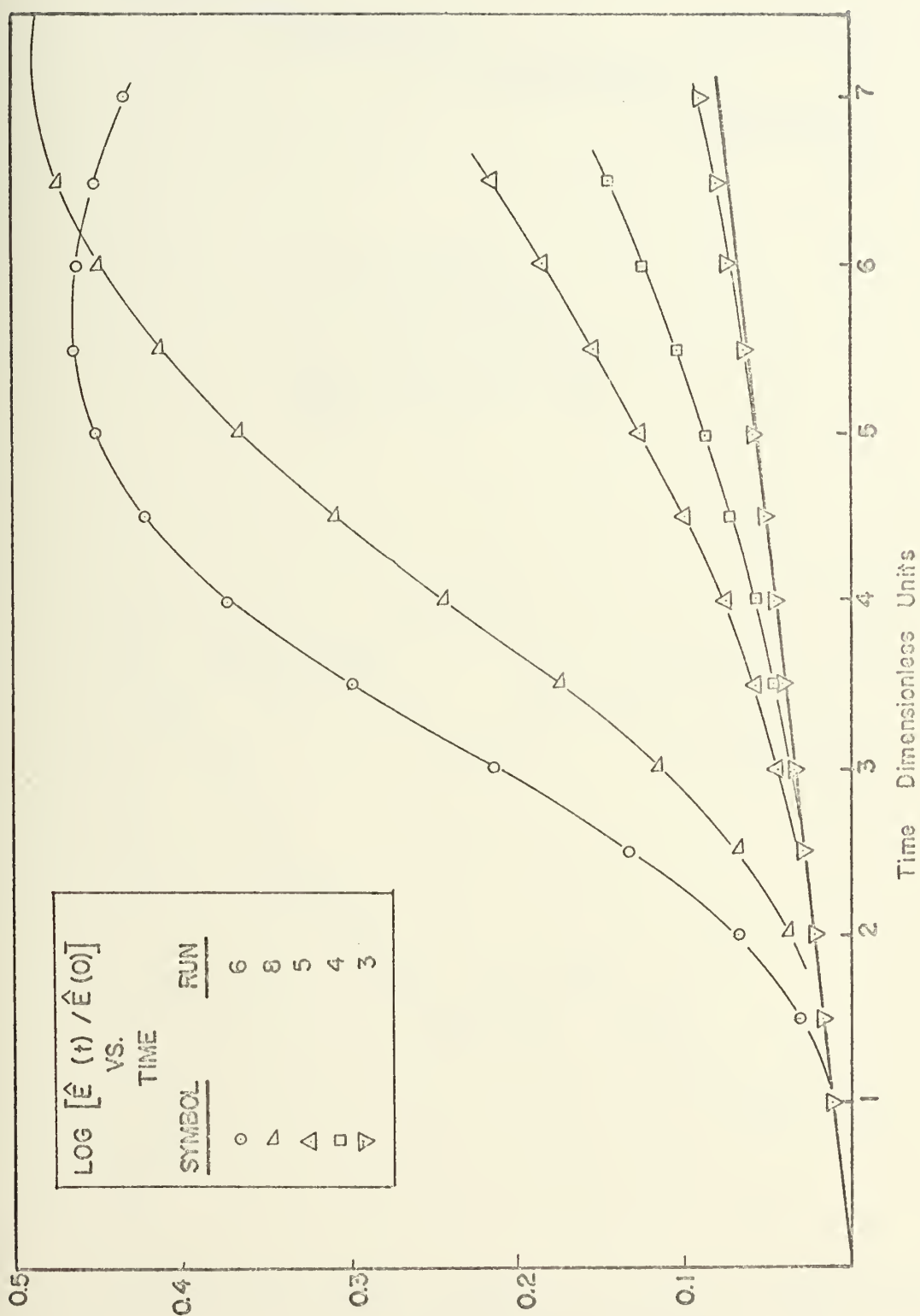


FIGURE 15
EFFECT OF AMPLITUDE ON INITIAL GROWTH RATE

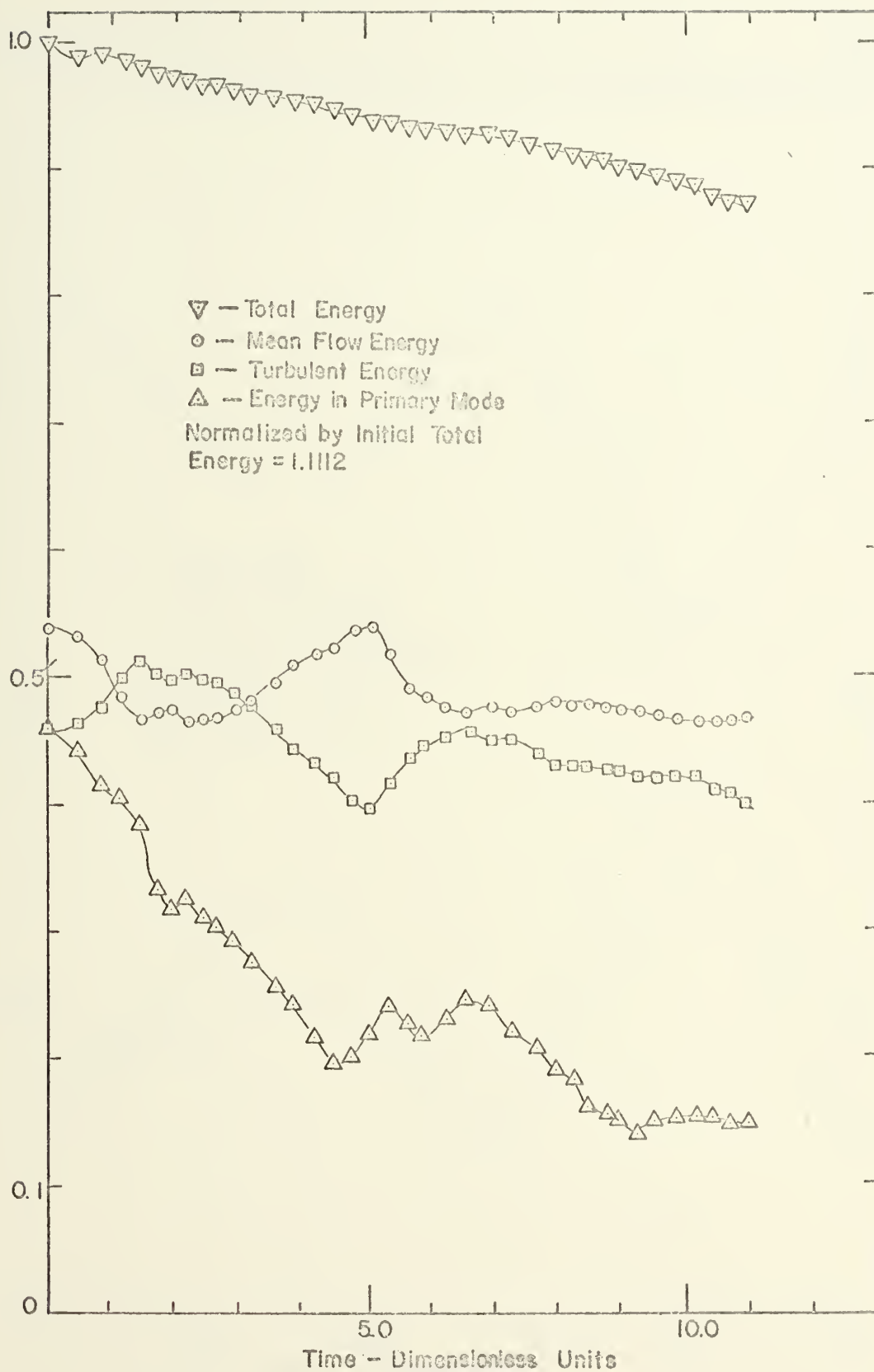


FIGURE 16 ENERGIES VS. TIME — RUN 7

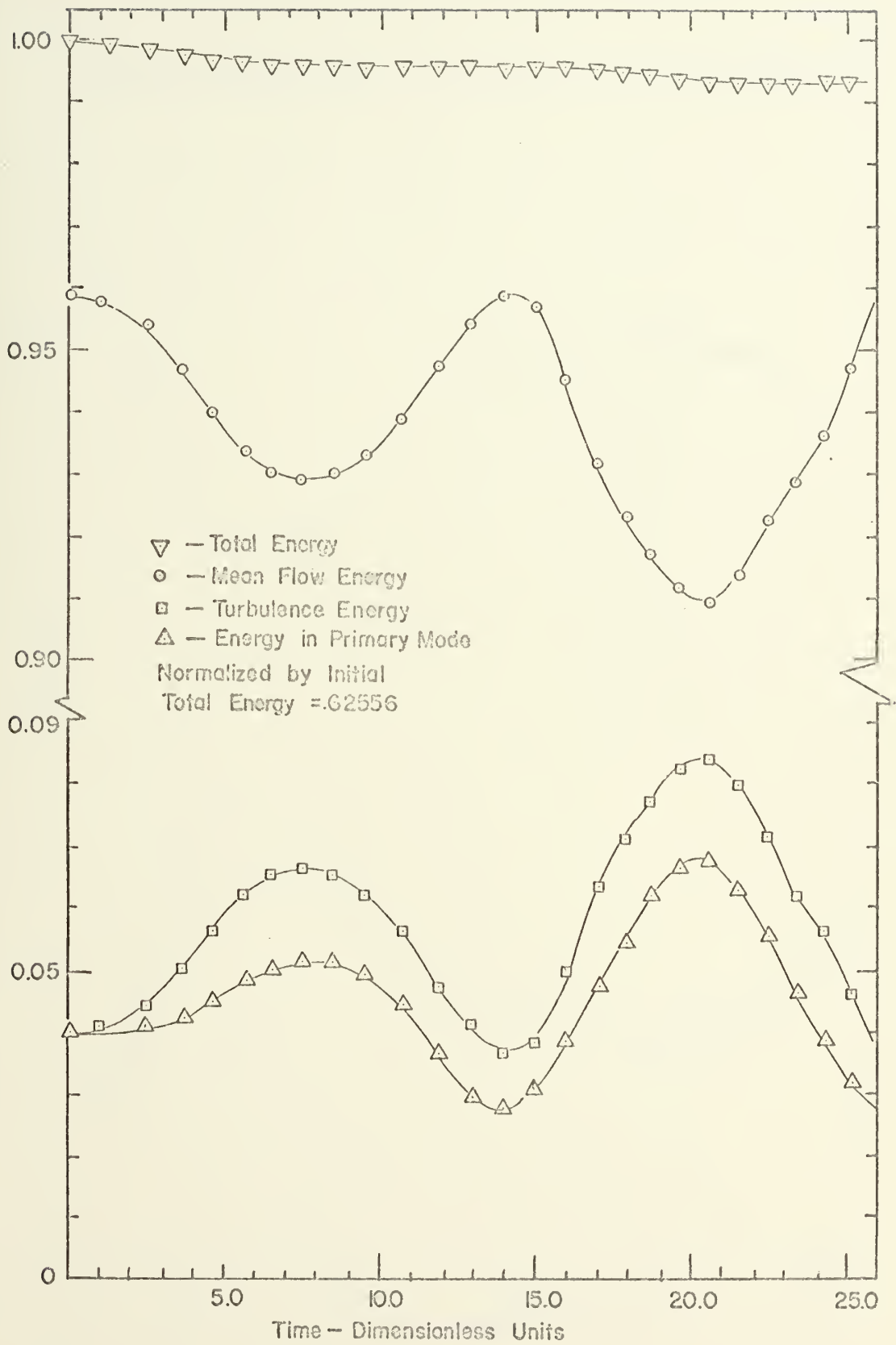


FIGURE 17A ENERGIES VS. TIME— RUN 8

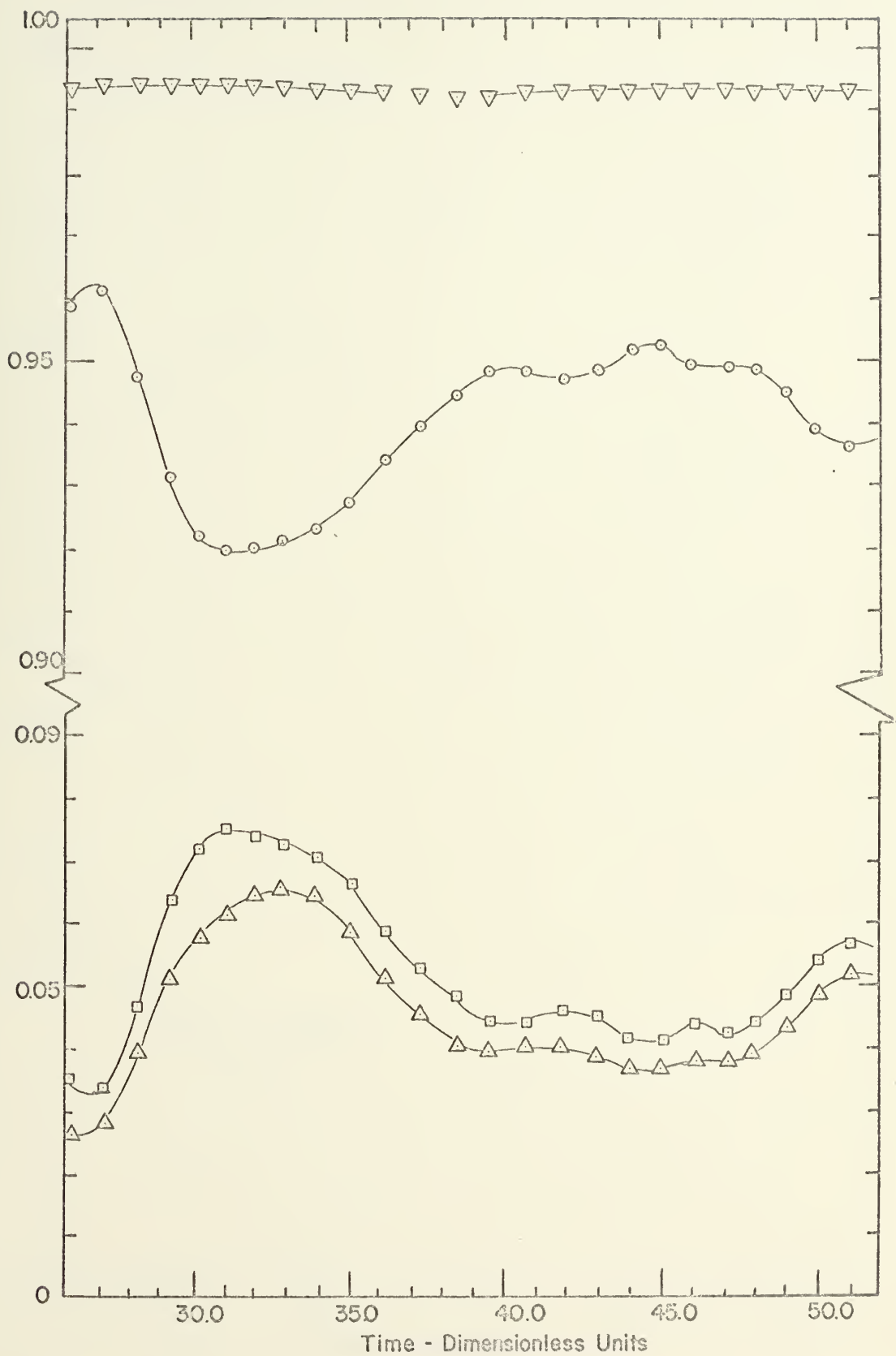


FIGURE 17B ENERGIES VS. TIME - RUN 8

Cont.

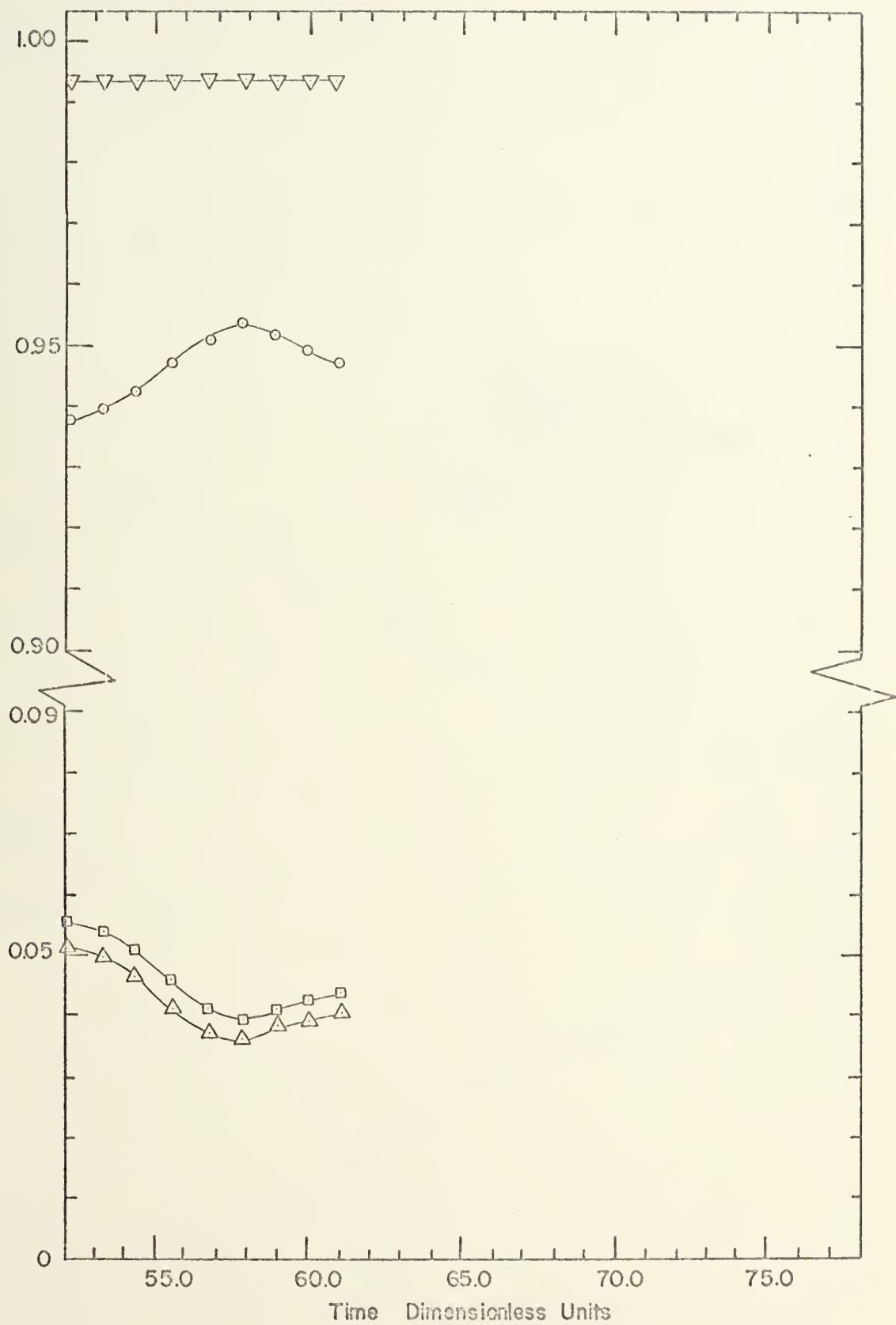


FIGURE 17C ENERGIES VS. TIME — RUN 8 Cont.

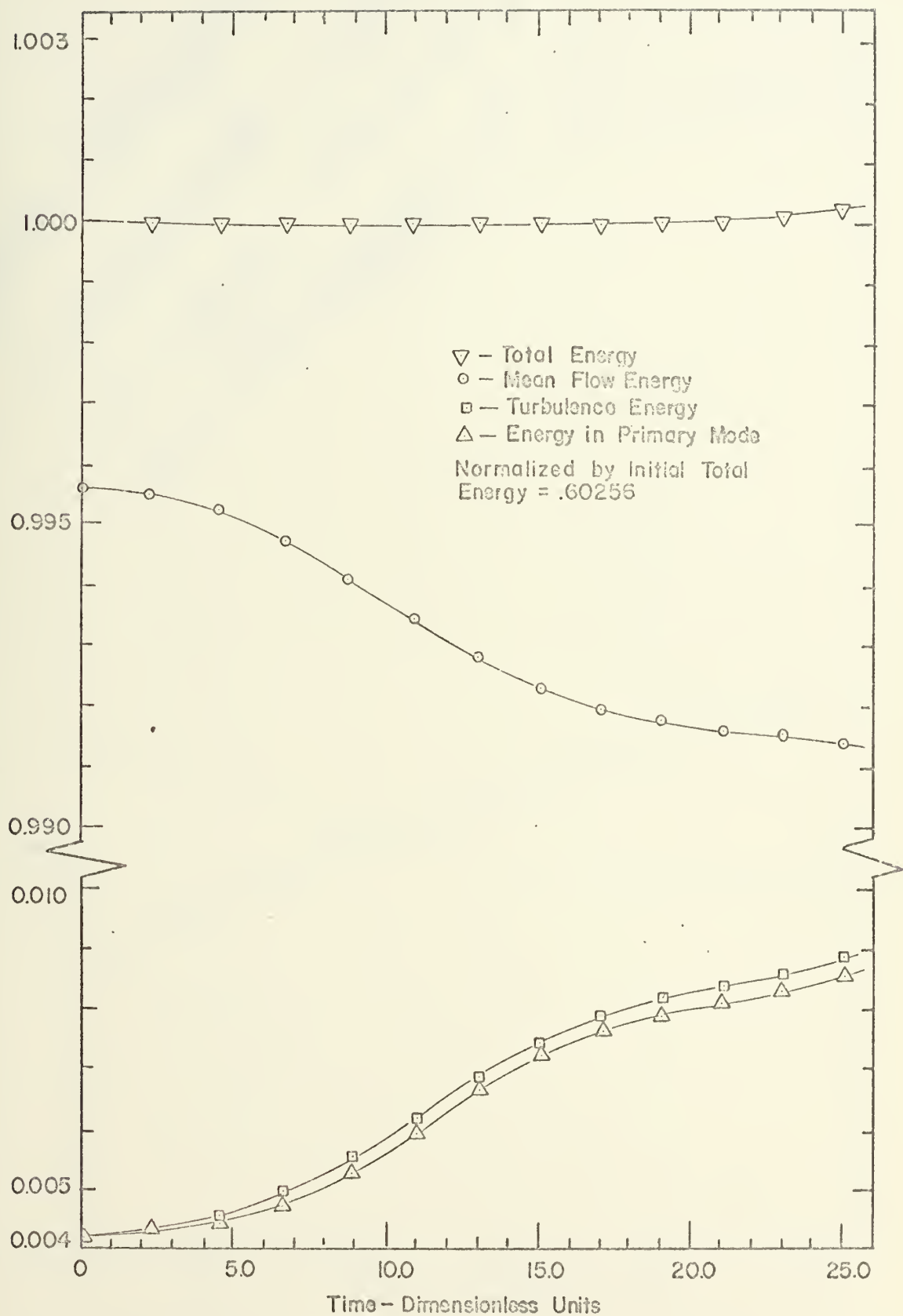


FIGURE 18A ENERGIES VS. TIME — RUN 9

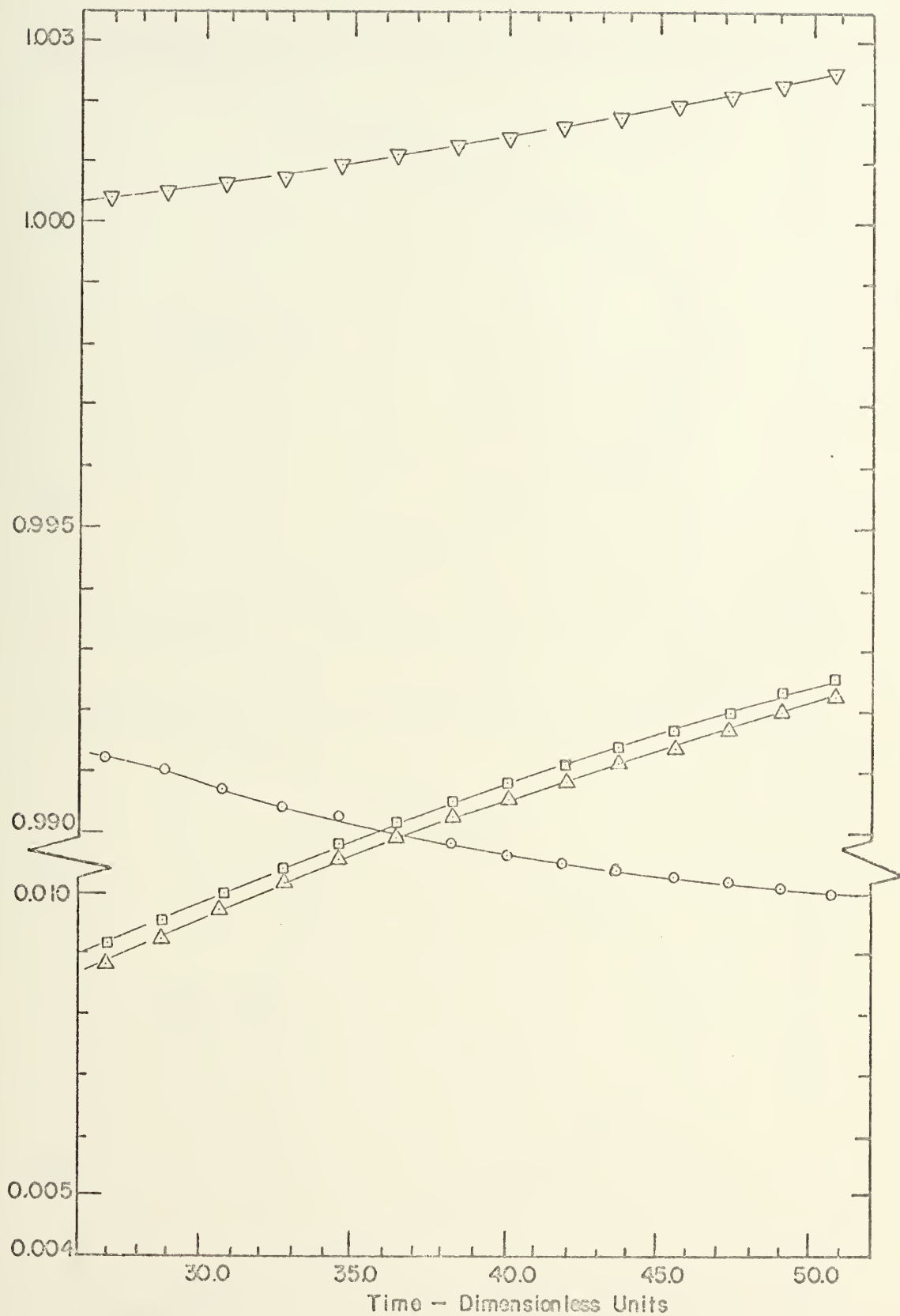


FIGURE 18B ENERGIES VS. TIME — RUN 9 Cont.

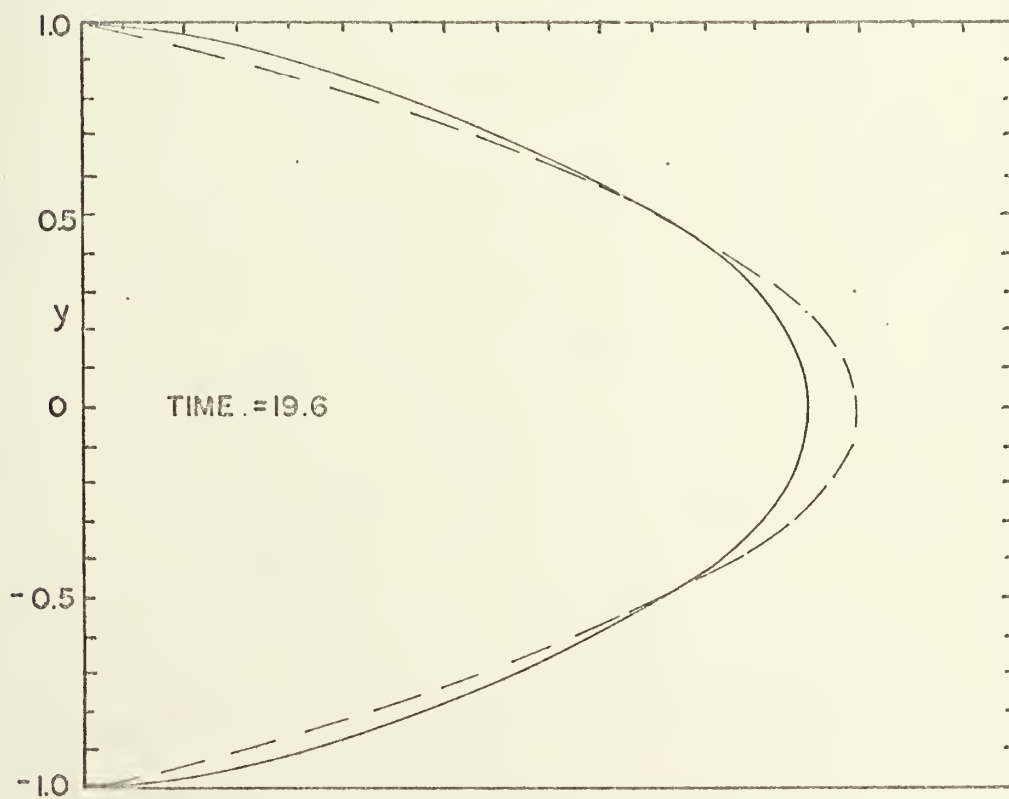
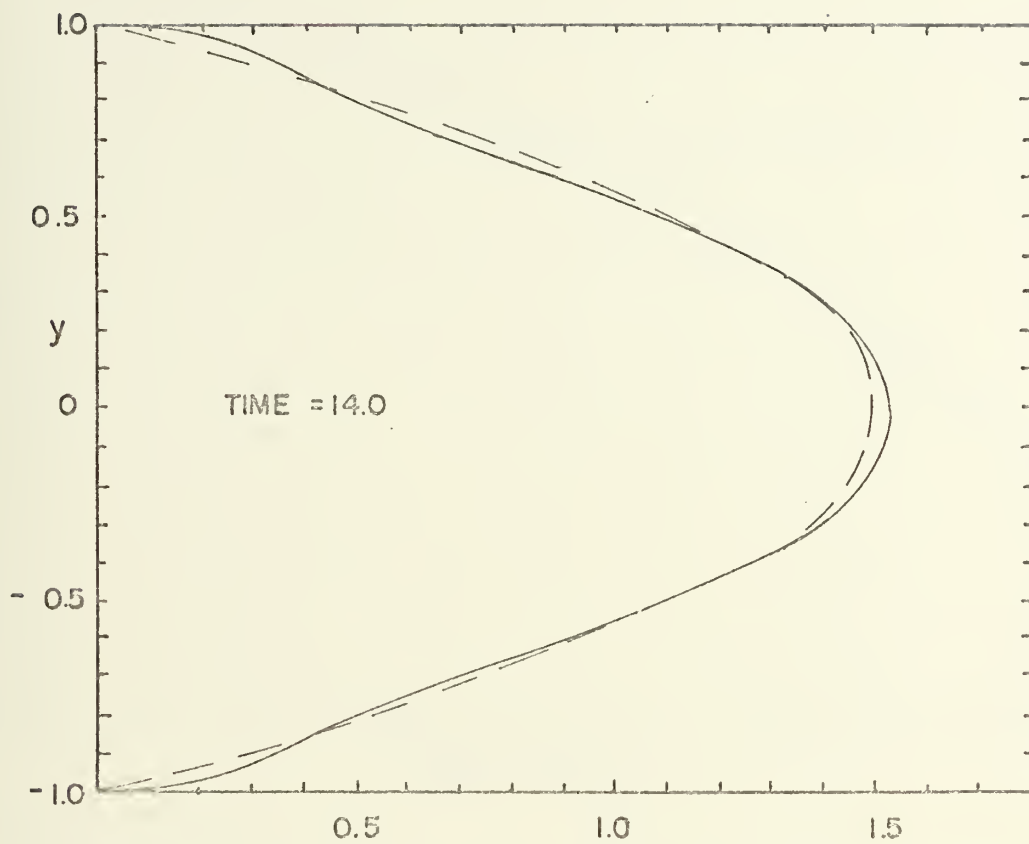


FIGURE 19 MEAN VELOCITY PROFILES , RUN 8

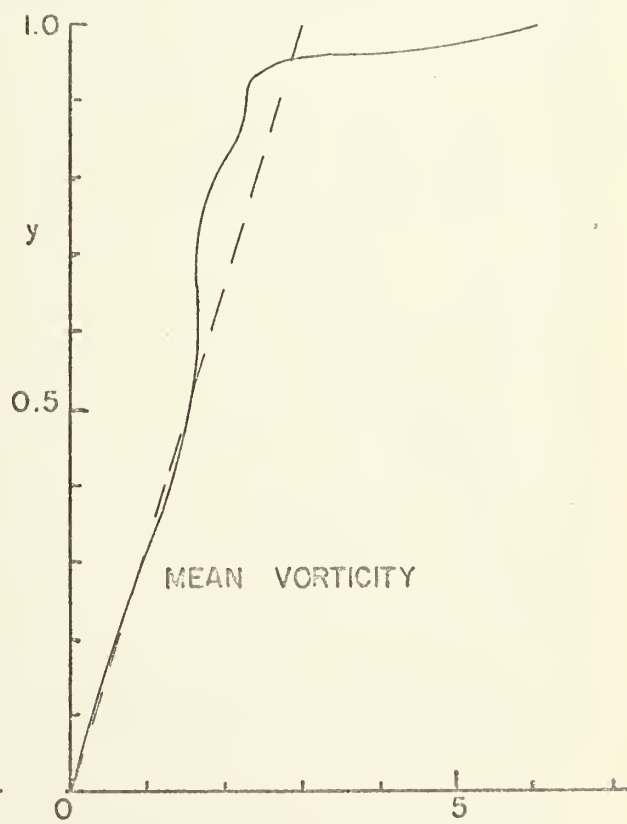
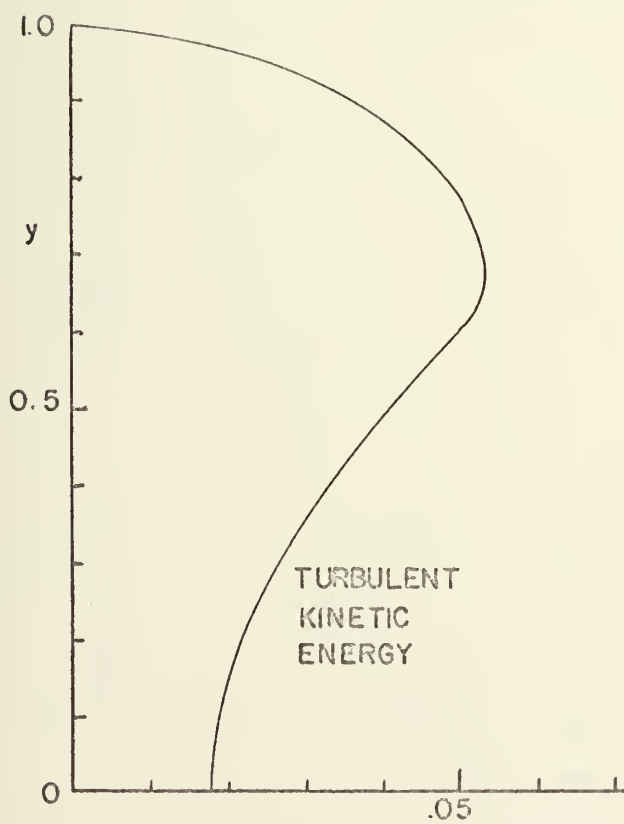
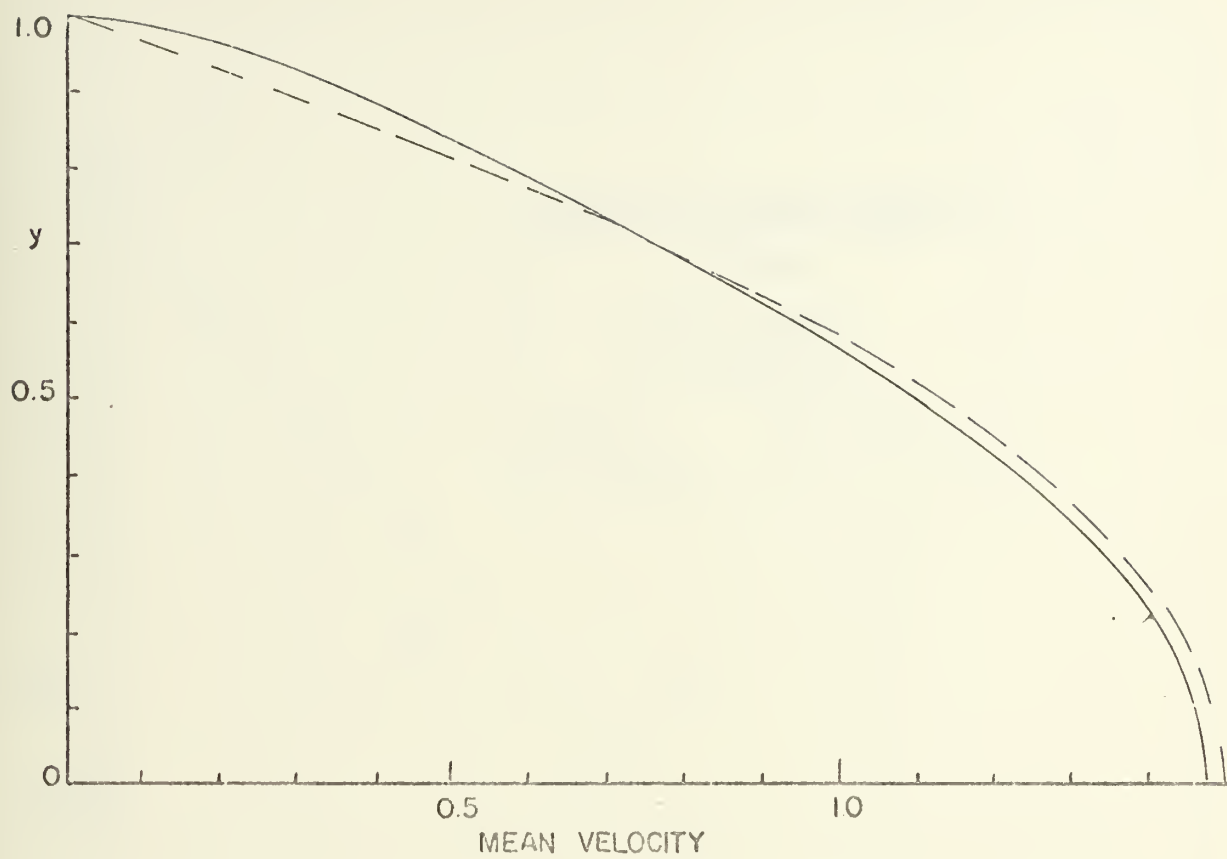


FIGURE 20. RUN 8. TIME = 53.2

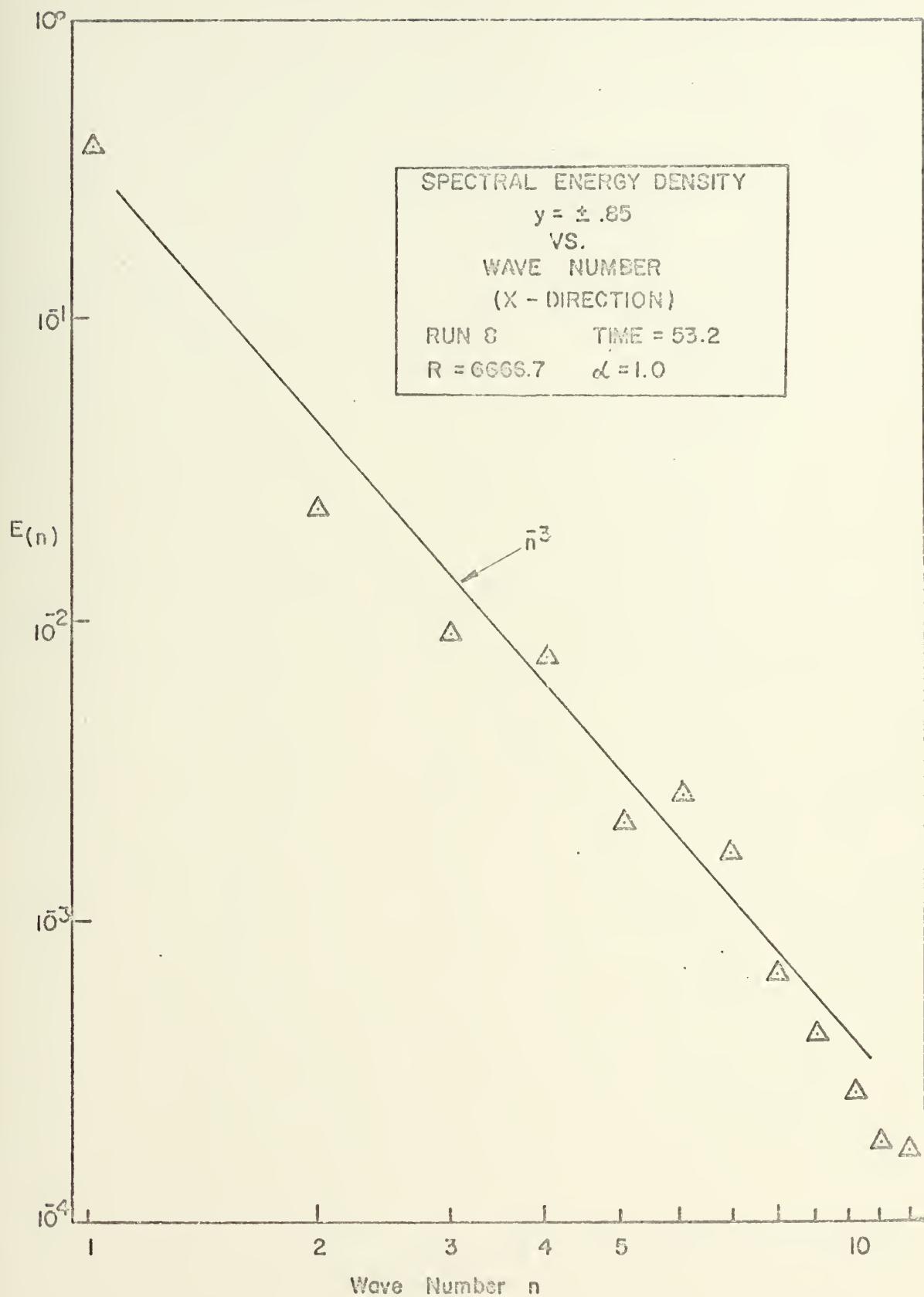


FIGURE 21

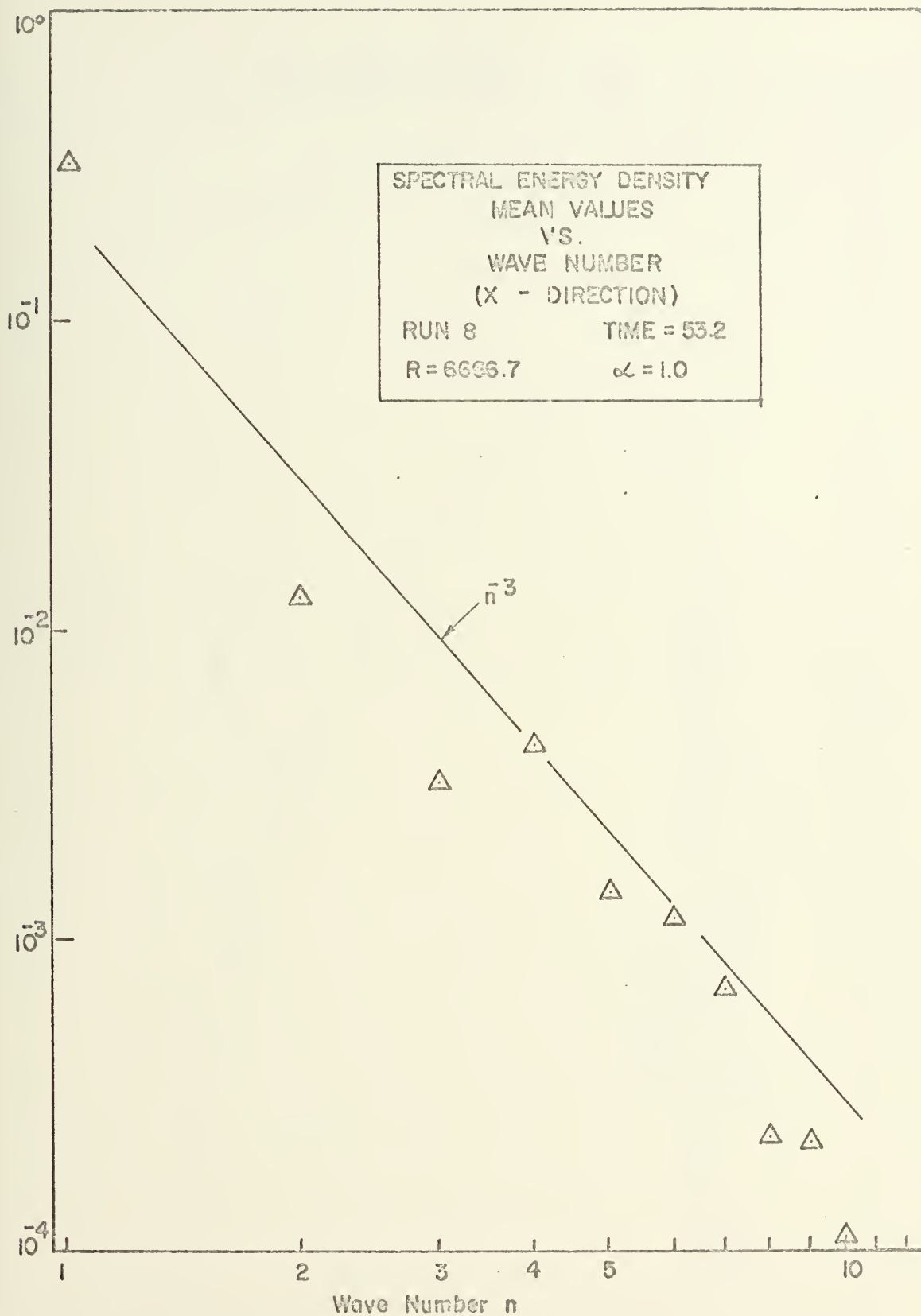


FIGURE 22

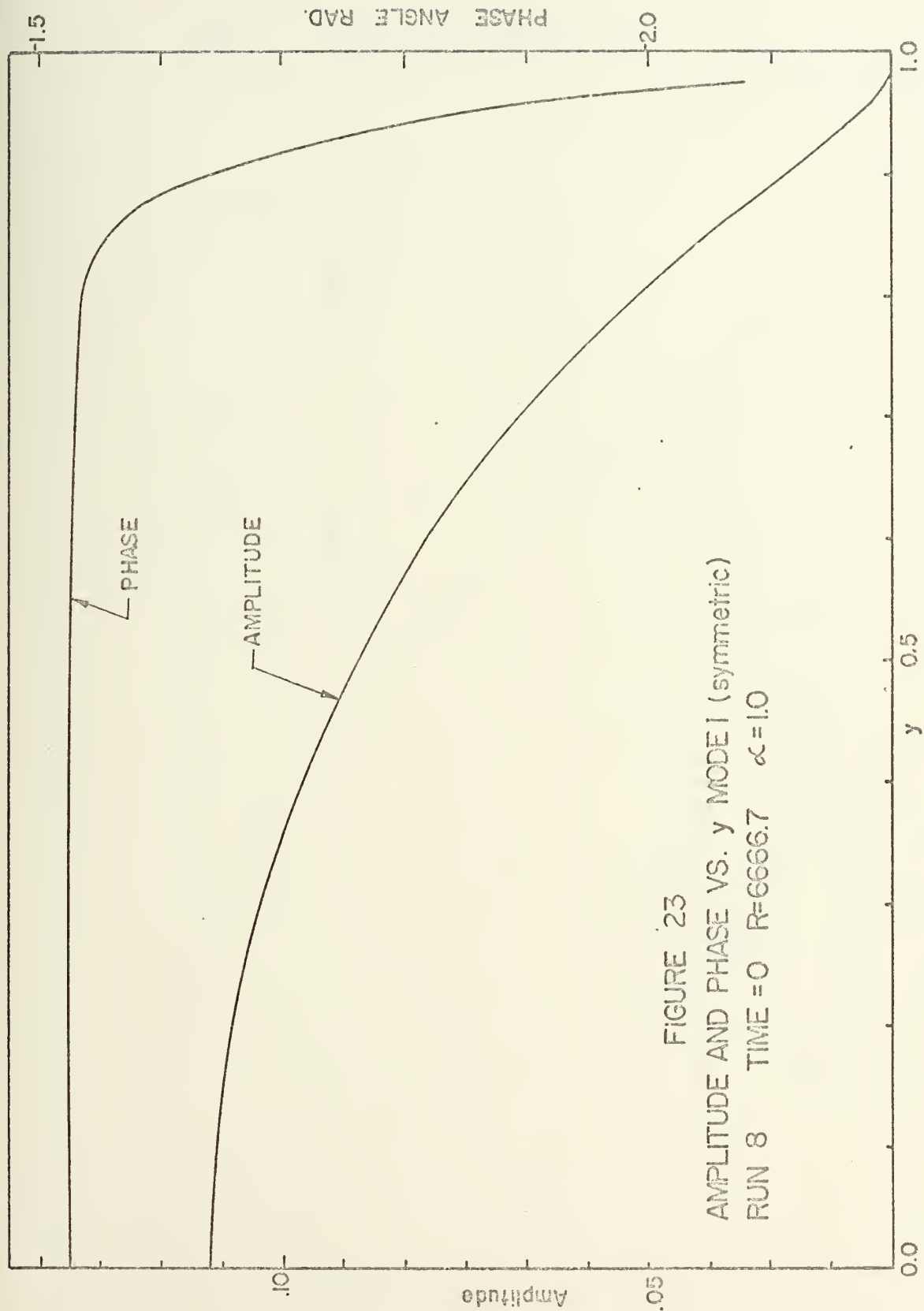
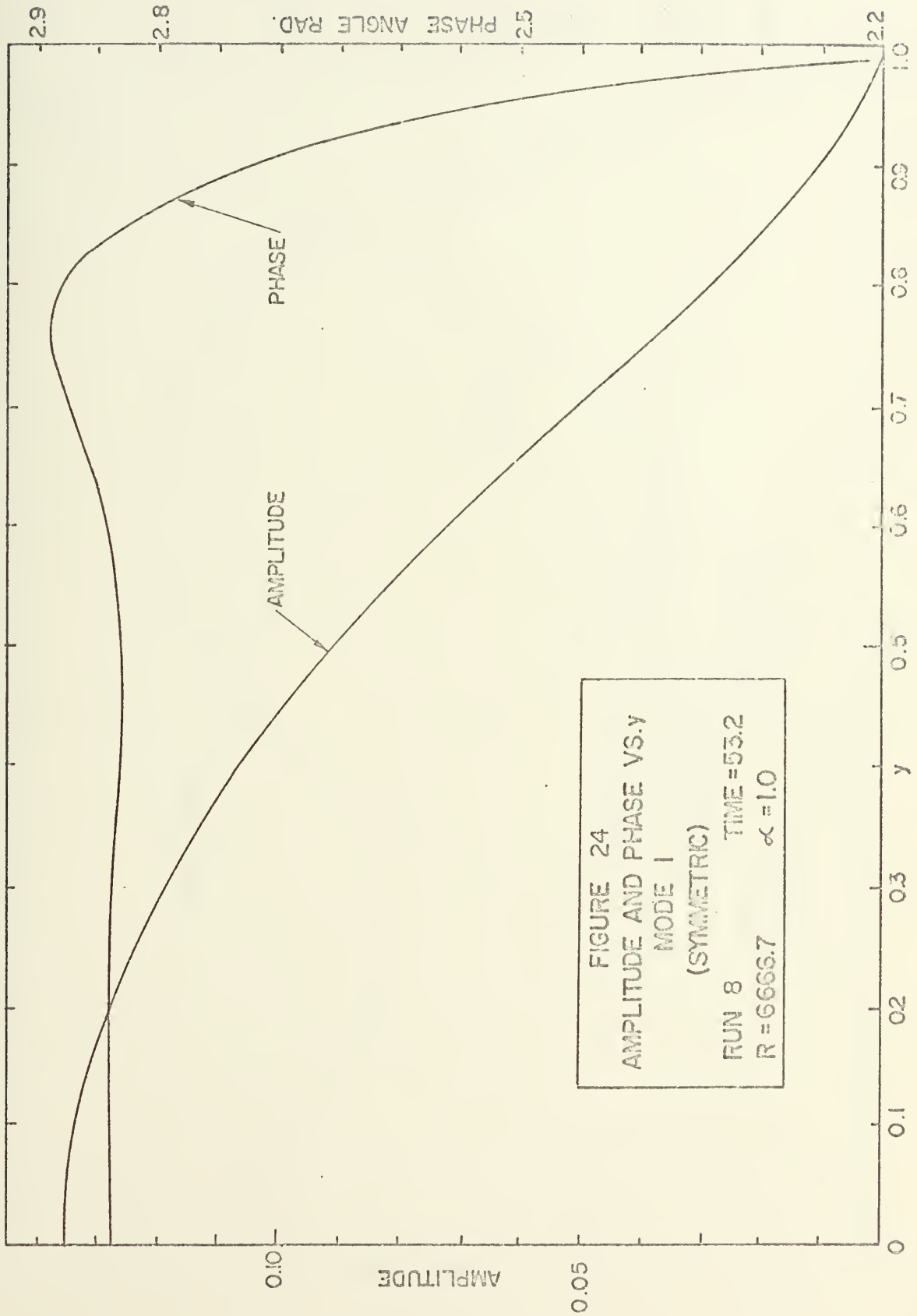
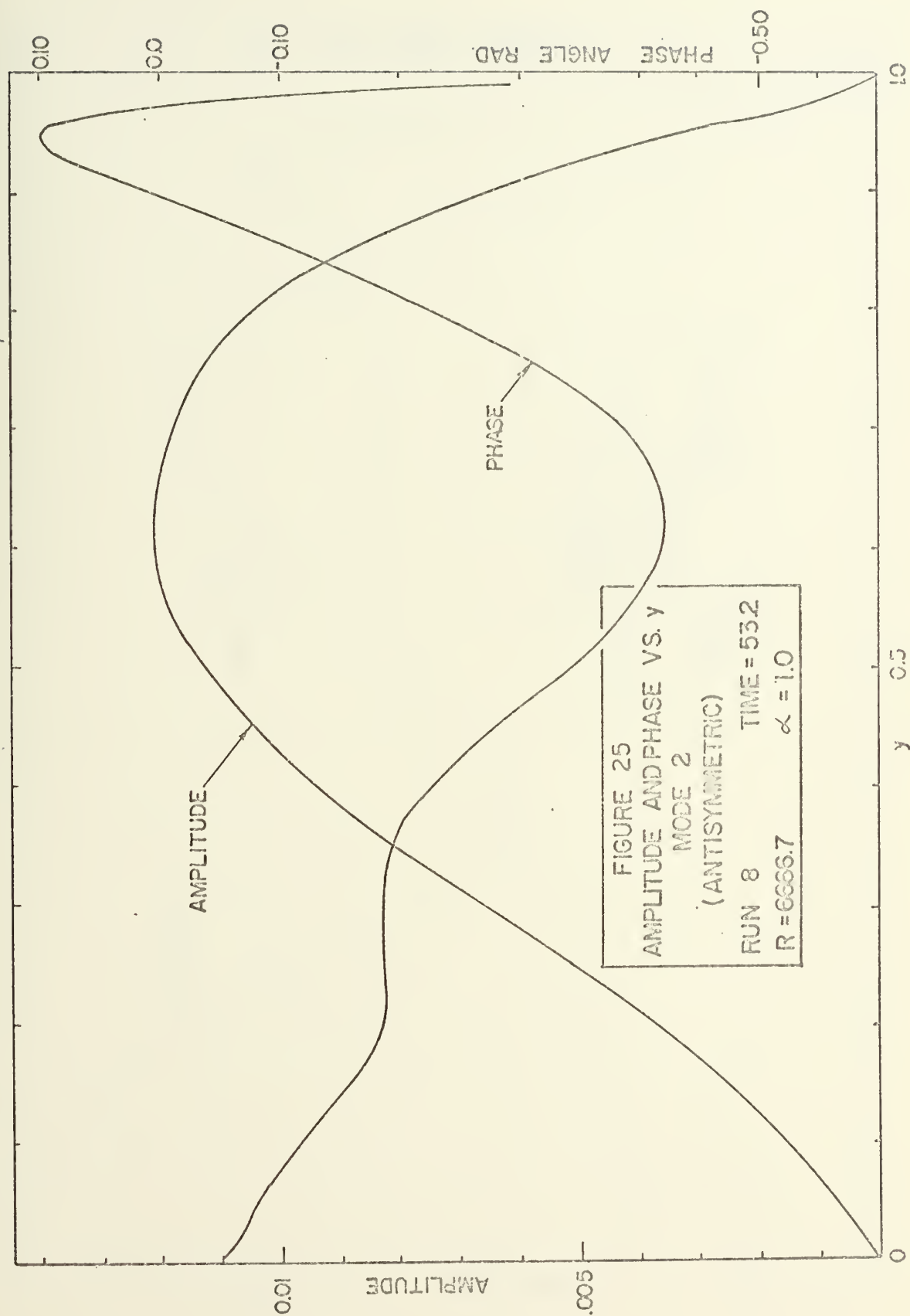
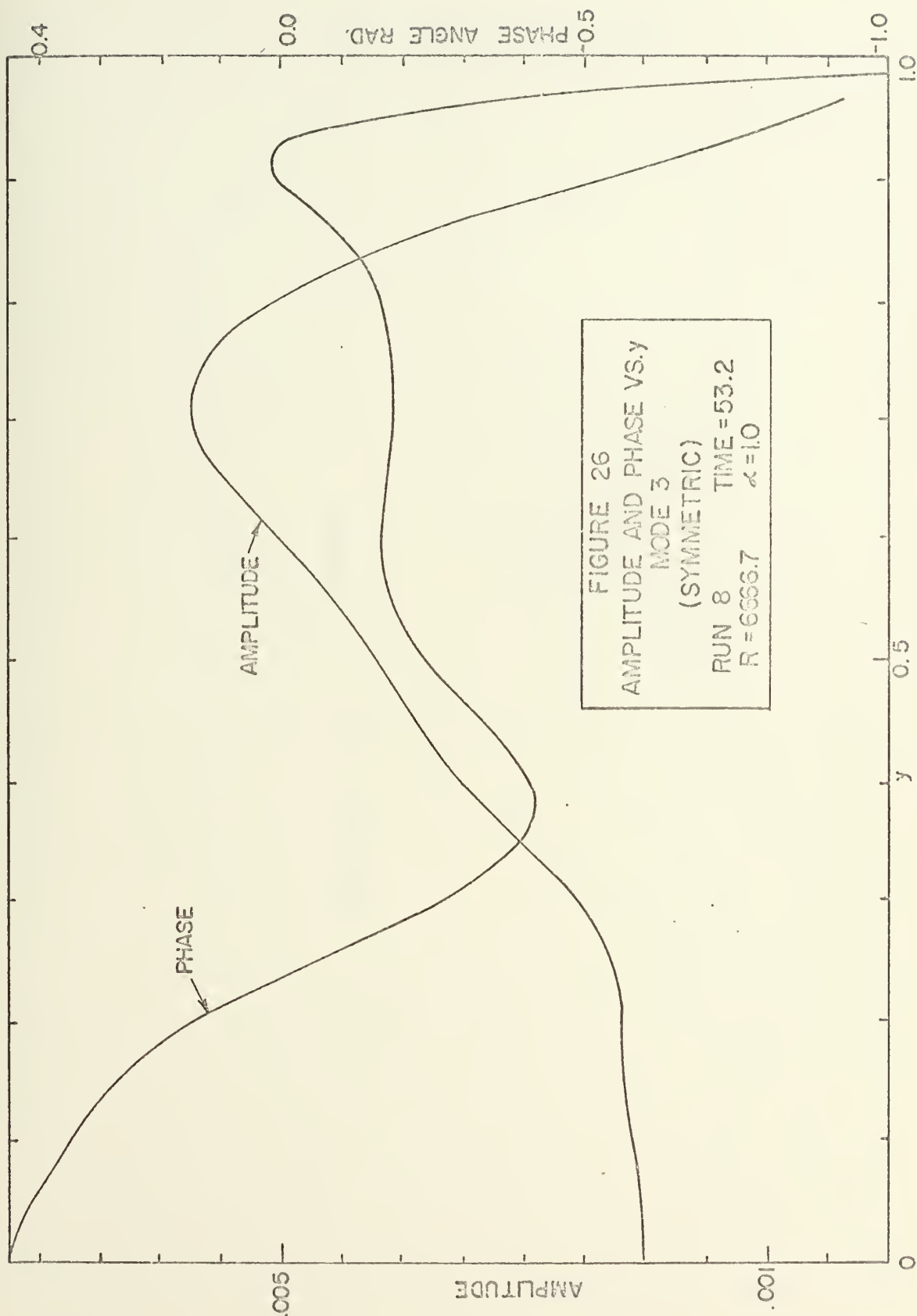


FIGURE 23
 AMPLITUDE AND PHASE VS. y MODEL (symmetric)
 RUN 8 TIME = 0 R=6666.7 $\alpha=1.0$









VI. CONCLUSIONS

The finite-difference representation of the vorticity transport equations, and the explicit treatment of the boundary values of the vorticity are consistent, stable and accurate. This has been demonstrated, in the linear range, by comparison with the established results of the linear theory.

The application of the discrete Fourier transform to the solution of the system of equations, associated with the representation of the Poisson equation, has produced significant improvements in both the speed and the accuracy of the calculations. Numerical tests indicate that the usual iterative schemes are inadequate if the number of mesh points is large.

Extensive calculations based on a consistent second-order representation of the linear eigenvalue problem provided a measure of the effect of mesh size on the accuracy of the representation of the large-scale unstable motions. The results indicate that the mesh sizes employed in previous investigations were often inadequate to represent linear instabilities.

Calculations in the non-linear range, at a moderate Reynolds number, indicate the existence of an equilibrium amplitude of the disturbance motion. In a long-term numerical integration, an approximate value of the equilibrium amplitude has been obtained. At the equilibrium state, the mean intensity of the two-dimensional turbulence is somewhat greater than measured values in real turbulent flows. This reflects the reduced dissipation due to the constraints on energy cascades in two-dimensional turbulence. The calculated spectral densities of kinetic energy are

consistent with the -3 power law predicted by Kraichnan for the two-dimensional turbulence.

The present program provides a means, of demonstrated accuracy, for the extensive investigation of finite-amplitude instability and two-dimensional turbulence.

VII. RECOMMENDATIONS FOR FUTURE WORK

The computer programs developed in the course of this investigation for both the solution of the linear eigenvalue problem and the numerical integration have yet to be fully exploited. A number of interesting applications remain. Among them are:

1. More extensive calculations for the solutions of the linear eigenvalue problem, in particular for the asymmetric modes. This will require only minor modifications of the program.
2. The development of an iterative procedure for the refinement of the solution for the eigenvector associated with the least stable mode. This will facilitate the investigation of finite-amplitude instabilities at sub-critical values of the Reynolds number.
3. A continuation of the integration for run number nine. The results to date show the disturbance increasing smoothly and monotonically at a decreasing rate. If, as seems likely, the energy levels off at the values associated with run eight, the indication of the equilibrium state will be more emphatic.
4. A more extensive investigation of the structure of the two-dimensional turbulent motion. This could be useful for the testing and development of heuristic models, in particular, the promising model developed by Gawain and Pritchett (1970).
5. Finally, some efforts should be made to further improve the speed of the calculations. A computer analysis of the operations in the program for the numerical integration indicates that substantial improvements in speed could be achieved by coding just Subroutine ADVANC in assembly language.

APPENDIX A

DERIVATION OF DISCRETE RELATIONS FOR THE SPECTRAL DENSITIES OF SQUARED VORTICITY AND KINETIC ENERGY

Associated with discrete Fourier transform pair, equations (4.46),
is the convolution

$$\frac{1}{M} \sum_{n=1}^M T_n T_n^* e^{-i \theta_{n,s}} = \sum_{K=1}^M F_K F_{K-s+1}^* \quad (\text{A.1})$$

where $\theta_{n,s}$ is as given by equation (4.47). Equation (A.1) can be derived by substituting the appropriate transform or inverse relation, and reversing the order of the summation.

For $s = 0$ we have the spectral density relation

$$\frac{1}{M} \sum_{n=1}^M T_n T_n^* = \sum_{K=1}^M F_K F_K^* \quad (\text{A.2})$$

The mean value of squared vorticity is given by

$$a_J = \frac{1}{M} \sum_{K=1}^M \Gamma_{K,J} \Gamma_{K,J}^* \quad (\text{A.3})$$

Then from equations (A.3), (4.49) and (A.2),

$$a_J = \frac{1}{M^2} \sum_{n=1}^M G_{n,J} G_{n,J}^*$$

Since $\Gamma_{K,J}$ is real,

$$a_J = \frac{1}{M^2} \left\{ G_{1,J}^2 + 2 \sum_{n=2}^{M/2} G_{n,J} G_{n,J}^* + G_{M/2+1,J}^2 \right\} \quad (\text{A.4})$$

Thus the quantities $G_{1,J}^2, 2G_{2,J} G_{2,J}^*, 2G_{3,J} G_{3,J}^*, \dots$, etc. are the spectral components of mean squared vorticity. Notice that, in the present notation the first spectral term, $n=1$, refers to the contribution

of the disturbance to the mean flow. If the laminar flow vorticity is included then the first term becomes

$$(G_{1,J} + 3y_J)^2$$

Of interest also are the spectral components of the normalized sum of a_J over y ,

$$\frac{1}{N-1} \left\{ \frac{a_1}{2} + \sum_{J=2}^{N-1} a_J + \frac{a_N}{2} \right\}$$

which are obtained by performing the same operation on the various terms on the right of equation (A.3).

Expressions for the spectral components of kinetic energy, at a given value of J , or their normalized sums over y , can be derived in a similar way. The components of turbulent velocity can be expressed as

$$\begin{aligned} \hat{u}_{K,J} &= \frac{1}{M} \sum_{n=1}^M U_{n,J} e^{-i \theta_{n,K}} \\ \hat{v}_{K,J} &= \frac{1}{M} \sum_{n=1}^M V_{n,J} e^{-i \theta_{n,K}} \end{aligned} \tag{A.5}$$

where, from equations (2.25) and (4.49) $U_{n,J}$, and $V_{n,J}$ are given by

$$\begin{aligned} U_{n,J} &= - \frac{F_{n,J+1} - F_{n,J-1}}{2\delta y} \\ V_{n,J} &= - \frac{i \sin \theta_{n,2}}{\delta x} F_{n,J} \end{aligned} \tag{A.6}$$

Thus from equations (4.24) and (A.2) the mean value of turbulent kinetic energy is given by

$$\hat{E}_J = \frac{1}{2M} \sum_{n=2}^M U_{n,J} U_{n,J}^* + \frac{1}{2M} \sum_{n=2}^M V_{n,J} V_{n,J}^*$$

Since $u_{K,J}$ and $v_{K,J}$ are real

$$\hat{E}_J = \frac{1}{2M} \left\{ 2 \sum_{n=2}^{M/2} \left(U_{n,J} U_{n,J}^* + V_{n,J} V_{n,J}^* \right) + U_{M/2+1,J}^2 + V_{M/2+1,J}^2 \right\} \quad (A.7)$$

Finally, the spectral components for

$$\hat{E} = \frac{1}{N-1} \sum_{J=2}^{N-1} \hat{E}_J$$

are obtained by performing the same operation on the terms on the right in equation (A.7).

APPENDIX B

LISTING OF THE FORTRAN CODE FOR THE NUMERICAL INTEGRATION

[illegible]

DIMENSIONS OF ARRAYS

THE FOLLOWING ARRAYS CONTAIN FIXED QUANTITIES AND SHOULD NEVER

УДК 62-50

OTHER ARRAYS MAY BE USED FOR TEMPORARY STORAGE AT CERTAIN PARTS

[illegible]

FUNCTIONS

ESTABLISHED VALUES OF VARIOUS QUANTITIES WHICH

1
 2
 3
 4
 5
 6
 7
 8
 9
 10
 11
 12
 13
 14
 15
 16
 17
 18
 19
 20
 21
 22
 23
 24
 25
 26
 27
 28
 29
 30
 31
 32
 33
 34
 35
 36
 37
 38
 39
 40
 41
 42
 43
 44
 45
 46
 47
 48
 49
 50
 51
 52
 53
 54
 55
 56
 57
 58
 59
 60
 61
 62
 63
 64
 65
 66
 67
 68
 69
 70
 71
 72
 73
 74
 75
 76
 77
 78
 79
 80
 81
 82
 83
 84
 85
 86
 87
 88
 89
 90
 91
 92
 93
 94
 95
 96
 97
 98
 99
 100
 101
 102
 103
 104
 105
 106
 107
 108
 109
 110
 111
 112
 113
 114
 115
 116
 117
 118
 119
 120
 121
 122
 123
 124
 125
 126
 127
 128
 129
 130
 131
 132
 133
 134
 135
 136
 137
 138
 139
 140
 141
 142
 143
 144
 145
 146
 147
 148
 149
 150
 151
 152
 153
 154
 155
 156
 157
 158
 159
 160
 161
 162
 163
 164
 165
 166
 167
 168
 169
 170
 171
 172
 173
 174
 175
 176
 177
 178
 179
 180
 181
 182
 183
 184
 185
 186
 187
 188
 189
 190
 191
 192
 193
 194
 195
 196
 197
 198
 199
 200
 201
 202
 203
 204
 205
 206
 207
 208
 209
 210
 211
 212
 213
 214
 215
 216
 217
 218
 219
 220
 221
 222
 223
 224
 225
 226
 227
 228
 229
 230
 231
 232
 233
 234
 235
 236
 237
 238
 239
 240
 241
 242
 243
 244
 245
 246
 247
 248
 249
 250
 251
 252
 253
 254
 255
 256
 257
 258
 259
 260
 261
 262
 263
 264
 265
 266
 267
 268
 269
 270
 271
 272
 273
 274
 275
 276
 277
 278
 279
 280
 281
 282
 283
 284
 285
 286
 287
 288
 289
 290
 291
 292
 293
 294
 295
 296
 297
 298
 299
 300
 301
 302
 303
 304
 305
 306
 307
 308
 309
 310
 311
 312
 313
 314
 315
 316
 317
 318
 319
 320
 321
 322
 323
 324
 325
 326
 327
 328
 329
 330
 331
 332
 333
 334
 335
 336
 337
 338
 339
 340
 341
 342
 343
 344
 345
 346
 347
 348
 349
 350
 351
 352
 353
 354
 355
 356
 357
 358
 359
 360
 361
 362
 363
 364
 365
 366
 367
 368
 369
 370
 371
 372
 373
 374
 375
 376
 377
 378
 379
 380
 381
 382
 383
 384
 385
 386
 387
 388
 389
 390
 391
 392
 393
 394
 395
 396
 397
 398
 399
 400
 401
 402
 403
 404
 405
 406
 407
 408
 409
 410
 411
 412
 413
 414
 415
 416
 417
 418
 419
 420
 421
 422
 423
 424
 425
 426
 427
 428
 429
 430
 431
 432
 433
 434
 435
 436
 437
 438
 439
 440
 441
 442
 443
 444
 445
 446
 447
 448
 449
 450
 451
 452
 453
 454
 455
 456
 457
 458
 459
 460
 461
 462
 463
 464
 465
 466
 467
 468
 469
 470
 471
 472
 473
 474
 475
 476
 477
 478
 479
 480
 481
 482
 483
 484
 485
 486
 487
 488
 489
 490
 491
 492
 493
 494
 495
 496
 497
 498
 499
 500
 501
 502
 503
 504
 505
 506
 507
 508
 509
 510
 511
 512
 513
 514
 515
 516
 517
 518
 519
 520
 521
 522
 523
 524
 525

TIME
STAMP
BY
DATE

FRANKEL CENTRAL BY DIFFERENCE

ED
W
S
Y
S
T
E
M
S
I
N
F
O
R
M
A
T
I
O
N
T
E
C
H
N
O
L
O
G
Y
I
N
T
E
L
L
I
G
E
N
C
E
A
G
E
N
C
I
E
S
I
N
T
E
R
N
A
T
I
O
N
A
L
C
O
O
P
E
R
A
T
I
O
N
S
I
N
T
E
L
L
I
G
E
N
C
E
A
G
E
N
C
I
E
S
I
N
T
E
R
N
A
T
I
O
N
A
L
C
O
O
P
E
R
A
T
I
O
N
S

COMPUTES MEAN VALUES OF DISTURBANCE STREAM

[illegible]

THE FIRST STEPS TO A BETTER FUTURE

1
 2
 3
 4
 5
 6
 7
 8
 9
 10
 11
 12
 13
 14
 15
 16
 17
 18
 19
 20
 21
 22
 23
 24
 25
 26
 27
 28
 29
 30
 31
 32
 33
 34
 35
 36
 37
 38
 39
 40
 41
 42
 43
 44
 45
 46
 47
 48
 49
 50
 51
 52
 53
 54
 55
 56
 57
 58
 59
 60
 61
 62
 63
 64
 65
 66
 67
 68
 69
 70
 71
 72
 73
 74
 75
 76
 77
 78
 79
 80
 81
 82
 83
 84
 85
 86
 87
 88
 89
 90
 91
 92
 93
 94
 95
 96
 97
 98
 99
 100
 101
 102
 103
 104
 105
 106
 107
 108
 109
 110
 111
 112
 113
 114
 115
 116
 117
 118
 119
 120
 121
 122
 123
 124
 125
 126
 127
 128
 129
 130
 131
 132
 133
 134
 135
 136
 137
 138
 139
 140
 141
 142
 143
 144
 145
 146
 147
 148
 149
 150
 151
 152
 153
 154
 155
 156
 157
 158
 159
 160
 161
 162
 163
 164
 165
 166
 167
 168
 169
 170
 171
 172
 173
 174
 175
 176
 177
 178
 179
 180
 181
 182
 183
 184
 185
 186
 187
 188
 189
 190
 191
 192
 193
 194
 195
 196
 197
 198
 199
 200
 201
 202
 203
 204
 205
 206
 207
 208
 209
 210
 211
 212
 213
 214
 215
 216
 217
 218
 219
 220
 221
 222
 223
 224
 225
 226
 227
 228
 229
 230
 231
 232
 233
 234
 235
 236
 237
 238
 239
 240
 241
 242
 243
 244
 245
 246
 247
 248
 249
 250
 251
 252
 253
 254
 255
 256
 257
 258
 259
 260
 261
 262
 263
 264
 265
 266
 267
 268
 269
 270
 271
 272
 273
 274
 275
 276
 277
 278
 279
 280
 281
 282
 283
 284
 285
 286
 287
 288
 289
 290
 291
 292
 293
 294
 295
 296
 297
 298
 299
 300
 301
 302
 303
 304
 305
 306
 307
 308
 309
 310
 311
 312
 313
 314
 315
 316
 317
 318
 319
 320
 321
 322
 323
 324
 325
 326
 327
 328
 329
 330
 331
 332
 333
 334
 335
 336
 337
 338
 339
 340
 341
 342
 343
 344
 345
 346
 347
 348
 349
 350
 351
 352
 353
 354
 355
 356
 357
 358
 359
 360
 361
 362
 363
 364
 365
 366
 367
 368
 369
 370
 371
 372
 373
 374
 375
 376
 377
 378
 379
 380
 381
 382
 383
 384
 385
 386
 387
 388
 389
 390
 391
 392
 393
 394
 395
 396
 397
 398
 399
 400
 401
 402
 403
 404
 405
 406
 407
 408
 409
 410
 411
 412
 413
 414
 415
 416
 417
 418
 419
 420
 421
 422
 423
 424
 425
 426
 427
 428
 429
 430
 431
 432
 433
 434
 435
 436
 437
 438
 439
 440
 441
 442
 443
 444
 445
 446
 447
 448
 449
 450
 451
 452
 453
 454
 455
 456
 457
 458
 459
 460
 461
 462
 463
 464
 465
 466
 467
 468
 469
 470
 471
 472
 473
 474
 475
 476
 477
 478
 479
 480
 481
 482
 483
 484
 485
 486
 487
 488
 489
 490
 491
 492
 493
 494
 495
 496
 497
 498
 499
 500
 501
 502
 503
 504
 505
 506
 507
 508
 509
 510
 511
 512
 513
 514
 515
 516
 517
 518
 519
 520
 521
 522
 523
 524
 525


```

PRINT
PLOT
SPCTRM

MODES

PLOTSP

CPLOT
OUTPUT

LOAD
RELOAD
DHARM

LOGICAL
ICOUNT
ISCIP
MCOMP
MSCIP
KSTEP
KINT

READ(5,11)NPROB,NCYCLS

```



```

1  ITAPE=10
2  CALL ERRSET(255,1000,-1,1)
3  IF(NC=0) GO TO 2
4  IF(NC=5,12) N.M,ISCIP,MSCIP
5  IREAD(5,13) RMYND,FRACEL,XLAMD
6  IREAD(5,15) DOT,BLANK,XXX
7  INITAR=0
8  ISTEP=C
9  KMCMP=C
10 TIT=0
11 NC=0
12 CALL SETUP
13 WRITE(6,14)NPROB,NCYCLS,N,M,NITWAX,ISCIP,MSCIP
14 GO TO 1
15 CALL LOSTART
16 MCOMP=ITITLE(5,15)
17 WRITE(6,16)
18 IF(IG=1) PRINT
19 CALL
20 ICOUNT=ISTART,NCYCLS
21 ICOUNT,NE,MCOMP) GO TO 5
22 IF(MCOMP+MSCIP
23 CALL COUNT,NE,INT) GO TO 7
24 INIT=ISCIP
25 CALL ADVANCE
26 ICOUNT=ISTART,NCYCLS+1
27 ICOUNT,NE,MCOMP) GO TO 5
28 IF(MCOMP+MSCIP
29 CALL COUNT,NE,INT) GO TO 7
30 INIT=ISCIP
31 CALL ADVANCE
32 ICOUNT=ISTART,NCYCLS+1
33 ICOUNT,NE,MCOMP) GO TO 5
34 IF(MCOMP+MSCIP
35 CALL COUNT,NE,INT) GO TO 7
36 INIT=ISCIP
37 CALL ADVANCE
38 ICOUNT=ISTART,NCYCLS+1
39 ICOUNT,NE,MCOMP) GO TO 5
40 IF(MCOMP+MSCIP
41 CALL COUNT,NE,INT) GO TO 7
42 INIT=ISCIP
43 CALL ADVANCE
44 ICOUNT=ISTART,NCYCLS+1
45 ICOUNT,NE,MCOMP) GO TO 5
46 IF(MCOMP+MSCIP
47 CALL COUNT,NE,INT) GO TO 7
48 INIT=ISCIP
49 CALL ADVANCE
50 ICOUNT=ISTART,NCYCLS+1
51 ICOUNT,NE,MCOMP) GO TO 5
52 IF(MCOMP+MSCIP
53 CALL COUNT,NE,INT) GO TO 7
54 INIT=ISCIP
55 CALL ADVANCE
56 ICOUNT=ISTART,NCYCLS+1
57 ICOUNT,NE,MCOMP) GO TO 5
58 IF(MCOMP+MSCIP
59 CALL COUNT,NE,INT) GO TO 7
60 INIT=ISCIP
61 CALL ADVANCE
62 ICOUNT=ISTART,NCYCLS+1
63 ICOUNT,NE,MCOMP) GO TO 5
64 IF(MCOMP+MSCIP
65 CALL COUNT,NE,INT) GO TO 7
66 INIT=ISCIP
67 CALL ADVANCE
68 ICOUNT=ISTART,NCYCLS+1
69 ICOUNT,NE,MCOMP) GO TO 5
70 IF(MCOMP+MSCIP
71 CALL COUNT,NE,INT) GO TO 7
72 INIT=ISCIP
73 CALL ADVANCE
74 ICOUNT=ISTART,NCYCLS+1
75 ICOUNT,NE,MCOMP) GO TO 5
76 IF(MCOMP+MSCIP
77 CALL COUNT,NE,INT) GO TO 7
78 INIT=ISCIP
79 CALL ADVANCE
80 ICOUNT=ISTART,NCYCLS+1
81 ICOUNT,NE,MCOMP) GO TO 5
82 IF(MCOMP+MSCIP
83 CALL COUNT,NE,INT) GO TO 7
84 INIT=ISCIP
85 CALL ADVANCE
86 ICOUNT=ISTART,NCYCLS+1
87 ICOUNT,NE,MCOMP) GO TO 5
88 IF(MCOMP+MSCIP
89 CALL COUNT,NE,INT) GO TO 7
90 INIT=ISCIP
91 CALL ADVANCE
92 ICOUNT=ISTART,NCYCLS+1
93 ICOUNT,NE,MCOMP) GO TO 5
94 IF(MCOMP+MSCIP
95 CALL COUNT,NE,INT) GO TO 7
96 INIT=ISCIP
97 CALL ADVANCE
98 ICOUNT=ISTART,NCYCLS+1
99 ICOUNT,NE,MCOMP) GO TO 5
100 IF(MCOMP+MSCIP
101 CALL COUNT,NE,INT) GO TO 7
102 INIT=ISCIP
103 CALL ADVANCE
104 ICOUNT=ISTART,NCYCLS+1
105 ICOUNT,NE,MCOMP) GO TO 5
106 IF(MCOMP+MSCIP
107 CALL COUNT,NE,INT) GO TO 7
108 INIT=ISCIP
109 CALL ADVANCE
110 ICOUNT=ISTART,NCYCLS+1
111 ICOUNT,NE,MCOMP) GO TO 5
112 IF(MCOMP+MSCIP
113 CALL COUNT,NE,INT) GO TO 7
114 INIT=ISCIP
115 CALL ADVANCE
116 ICOUNT=ISTART,NCYCLS+1
117 ICOUNT,NE,MCOMP) GO TO 5
118 IF(MCOMP+MSCIP
119 CALL COUNT,NE,INT) GO TO 7
120 INIT=ISCIP
121 CALL ADVANCE
122 ICOUNT=ISTART,NCYCLS+1
123 ICOUNT,NE,MCOMP) GO TO 5
124 IF(MCOMP+MSCIP
125 CALL COUNT,NE,INT) GO TO 7
126 INIT=ISCIP
127 CALL ADVANCE
128 ICOUNT=ISTART,NCYCLS+1
129 ICOUNT,NE,MCOMP) GO TO 5
130 IF(MCOMP+MSCIP
131 CALL COUNT,NE,INT) GO TO 7
132 INIT=ISCIP
133 CALL ADVANCE
134 ICOUNT=ISTART,NCYCLS+1
135 ICOUNT,NE,MCOMP) GO TO 5
136 IF(MCOMP+MSCIP
137 CALL COUNT,NE,INT) GO TO 7
138 INIT=ISCIP
139 CALL ADVANCE
140 ICOUNT=ISTART,NCYCLS+1
141 ICOUNT,NE,MCOMP) GO TO 5
142 IF(MCOMP+MSCIP
143 CALL COUNT,NE,INT) GO TO 7
144 INIT=ISCIP
145 CALL ADVANCE
146 ICOUNT=ISTART,NCYCLS+1
147 ICOUNT,NE,MCOMP) GO TO 5
148 IF(MCOMP+MSCIP
149 CALL COUNT,NE,INT) GO TO 7
150 INIT=ISCIP
151 CALL ADVANCE
152 ICOUNT=ISTART,NCYCLS+1
153 ICOUNT,NE,MCOMP) GO TO 5
154 IF(MCOMP+MSCIP
155 CALL COUNT,NE,INT) GO TO 7
156 INIT=ISCIP
157 CALL ADVANCE
158 ICOUNT=ISTART,NCYCLS+1
159 ICOUNT,NE,MCOMP) GO TO 5
160 IF(MCOMP+MSCIP
161 CALL COUNT,NE,INT) GO TO 7
162 INIT=ISCIP
163 CALL ADVANCE
164 ICOUNT=ISTART,NCYCLS+1
165 ICOUNT,NE,MCOMP) GO TO 5
166 IF(MCOMP+MSCIP
167 CALL COUNT,NE,INT) GO TO 7
168 INIT=ISCIP
169 CALL ADVANCE
170 ICOUNT=ISTART,NCYCLS+1
171 ICOUNT,NE,MCOMP) GO TO 5
172 IF(MCOMP+MSCIP
173 CALL COUNT,NE,INT) GO TO 7
174 INIT=ISCIP
175 CALL ADVANCE
176 ICOUNT=ISTART,NCYCLS+1
177 ICOUNT,NE,MCOMP) GO TO 5
178 IF(MCOMP+MSCIP
179 CALL COUNT,NE,INT) GO TO 7
180 INIT=ISCIP
181 CALL ADVANCE
182 ICOUNT=ISTART,NCYCLS+1
183 ICOUNT,NE,MCOMP) GO TO 5
184 IF(MCOMP+MSCIP
185 CALL COUNT,NE,INT) GO TO 7
186 INIT=ISCIP
187 CALL ADVANCE
188 ICOUNT=ISTART,NCYCLS+1
189 ICOUNT,NE,MCOMP) GO TO 5
190 IF(MCOMP+MSCIP
191 CALL COUNT,NE,INT) GO TO 7
192 INIT=ISCIP
193 CALL ADVANCE
194 ICOUNT=ISTART,NCYCLS+1
195 ICOUNT,NE,MCOMP) GO TO 5
196 IF(MCOMP+MSCIP
197 CALL COUNT,NE,INT) GO TO 7
198 INIT=ISCIP
199 CALL ADVANCE
200 ICOUNT=ISTART,NCYCLS+1
201 ICOUNT,NE,MCOMP) GO TO 5
202 IF(MCOMP+MSCIP
203 CALL COUNT,NE,INT) GO TO 7
204 INIT=ISCIP
205 CALL ADVANCE
206 ICOUNT=ISTART,NCYCLS+1
207 ICOUNT,NE,MCOMP) GO TO 5
208 IF(MCOMP+MSCIP
209 CALL COUNT,NE,INT) GO TO 7
210 INIT=ISCIP
211 CALL ADVANCE
212 ICOUNT=ISTART,NCYCLS+1
213 ICOUNT,NE,MCOMP) GO TO 5
214 IF(MCOMP+MSCIP
215 CALL COUNT,NE,INT) GO TO 7
216 INIT=ISCIP
217 CALL ADVANCE
218 ICOUNT=ISTART,NCYCLS+1
219 ICOUNT,NE,MCOMP) GO TO 5
220 IF(MCOMP+MSCIP
221 CALL COUNT,NE,INT) GO TO 7
222 INIT=ISCIP
223 CALL ADVANCE
224 ICOUNT=ISTART,NCYCLS+1
225 ICOUNT,NE,MCOMP) GO TO 5
226 IF(MCOMP+MSCIP
227 CALL COUNT,NE,INT) GO TO 7
228 INIT=ISCIP
229 CALL ADVANCE
230 ICOUNT=ISTART,NCYCLS+1
231 ICOUNT,NE,MCOMP) GO TO 5
232 IF(MCOMP+MSCIP
233 CALL COUNT,NE,INT) GO TO 7
234 INIT=ISCIP
235 CALL ADVANCE
236 ICOUNT=ISTART,NCYCLS+1
237 ICOUNT,NE,MCOMP) GO TO 5
238 IF(MCOMP+MSCIP
239 CALL COUNT,NE,INT) GO TO 7
240 INIT=ISCIP
241 CALL ADVANCE
242 ICOUNT=ISTART,NCYCLS+1
243 ICOUNT,NE,MCOMP) GO TO 5
244 IF(MCOMP+MSCIP
245 CALL COUNT,NE,INT) GO TO 7
246 INIT=ISCIP
247 CALL ADVANCE
248 ICOUNT=ISTART,NCYCLS+1
249 ICOUNT,NE,MCOMP) GO TO 5
250 IF(MCOMP+MSCIP
251 CALL COUNT,NE,INT) GO TO 7
252 INIT=ISCIP
253 CALL ADVANCE
254 ICOUNT=ISTART,NCYCLS+1
255 ICOUNT,NE,MCOMP) GO TO 5
256 IF(MCOMP+MSCIP
257 CALL COUNT,NE,INT) GO TO 7
258 INIT=ISCIP
259 CALL ADVANCE
260 ICOUNT=ISTART,NCYCLS+1
261 ICOUNT,NE,MCOMP) GO TO 5
262 IF(MCOMP+MSCIP
263 CALL COUNT,NE,INT) GO TO 7
264 INIT=ISCIP
265 CALL ADVANCE
266 ICOUNT=ISTART,NCYCLS+1
267 ICOUNT,NE,MCOMP) GO TO 5
268 IF(MCOMP+MSCIP
269 CALL COUNT,NE,INT) GO TO 7
270 INIT=ISCIP
271 CALL ADVANCE
272 ICOUNT=ISTART,NCYCLS+1
273 ICOUNT,NE,MCOMP) GO TO 5
274 IF(MCOMP+MSCIP
275 CALL COUNT,NE,INT) GO TO 7
276 INIT=ISCIP
277 CALL ADVANCE
278 ICOUNT=ISTART,NCYCLS+1
279 ICOUNT,NE,MCOMP) GO TO 5
280 IF(MCOMP+MSCIP
281 CALL COUNT,NE,INT) GO TO 7
282 INIT=ISCIP
283 CALL ADVANCE
284 ICOUNT=ISTART,NCYCLS+1
285 ICOUNT,NE,MCOMP) GO TO 5
286 IF(MCOMP+MSCIP
287 CALL COUNT,NE,INT) GO TO 7
288 INIT=ISCIP
289 CALL ADVANCE
290 ICOUNT=ISTART,NCYCLS+1
291 ICOUNT,NE,MCOMP) GO TO 5
292 IF(MCOMP+MSCIP
293 CALL COUNT,NE,INT) GO TO 7
294 INIT=ISCIP
295 CALL ADVANCE
296 ICOUNT=ISTART,NCYCLS+1
297 ICOUNT,NE,MCOMP) GO TO 5
298 IF(MCOMP+MSCIP
299 CALL COUNT,NE,INT) GO TO 7
300 INIT=ISCIP
301 CALL ADVANCE
302 ICOUNT=ISTART,NCYCLS+1
303 ICOUNT,NE,MCOMP) GO TO 5
304 IF(MCOMP+MSCIP
305 CALL COUNT,NE,INT) GO TO 7
306 INIT=ISCIP
307 CALL ADVANCE
308 ICOUNT=ISTART,NCYCLS+1
309 ICOUNT,NE,MCOMP) GO TO 5
310 IF(MCOMP+MSCIP
311 CALL COUNT,NE,INT) GO TO 7
312 INIT=ISCIP
313 CALL ADVANCE
314 ICOUNT=ISTART,NCYCLS+1
315 ICOUNT,NE,MCOMP) GO TO 5
316 IF(MCOMP+MSCIP
317 CALL COUNT,NE,INT) GO TO 7
318 INIT=ISCIP
319 CALL ADVANCE
320 ICOUNT=ISTART,NCYCLS+1
321 ICOUNT,NE,MCOMP) GO TO 5
322 IF(MCOMP+MSCIP
323 CALL COUNT,NE,INT) GO TO 7
324 INIT=ISCIP
325 CALL ADVANCE
326 ICOUNT=ISTART,NCYCLS+1
327 ICOUNT,NE,MCOMP) GO TO 5
328 IF(MCOMP+MSCIP
329 CALL COUNT,NE,INT) GO TO 7
330 INIT=ISCIP
331 CALL ADVANCE
332 ICOUNT=ISTART,NCYCLS+1
333 ICOUNT,NE,MCOMP) GO TO 5
334 IF(MCOMP+MSCIP
335 CALL COUNT,NE,INT) GO TO 7
336 INIT=ISCIP
337 CALL ADVANCE
338 ICOUNT=ISTART,NCYCLS+1
339 ICOUNT,NE,MCOMP) GO TO 5
340 IF(MCOMP+MSCIP
341 CALL COUNT,NE,INT) GO TO 7
342 INIT=ISCIP
343 CALL ADVANCE
344 ICOUNT=ISTART,NCYCLS+1
345 ICOUNT,NE,MCOMP) GO TO 5
346 IF(MCOMP+MSCIP
347 CALL COUNT,NE,INT) GO TO 7
348 INIT=ISCIP
349 CALL ADVANCE
350 ICOUNT=ISTART,NCYCLS+1
351 ICOUNT,NE,MCOMP) GO TO 5
352 IF(MCOMP+MSCIP
353 CALL COUNT,NE,INT) GO TO 7
354 INIT=ISCIP
355 CALL ADVANCE
356 ICOUNT=ISTART,NCYCLS+1
357 ICOUNT,NE,MCOMP) GO TO 5
358 IF(MCOMP+MSCIP
359 CALL COUNT,NE,INT) GO TO 7
360 INIT=ISCIP
361 CALL ADVANCE
362 ICOUNT=ISTART,NCYCLS+1
363 ICOUNT,NE,MCOMP)
```


STOP
END

CCCC1970
CCCC1980


```

MM(2)=0
MM(3)=0
M=2**M
MH=M/2+1
MHP=MH+1
MP1=M+1
MP2=M+2
MP3=M+3
MP4=M+4
MM1=M-1
XN=DELLOCAT(N)
XM1=DELLOCAT(M)
XM=DELLOCAT(M)
DX2=2.DC*H/XM
DX3=2.DC*DX
DX4=4.DC*DX
DX8=8.DC*DX
DY2=2.DC/XM1
DY3=2.DC*DY
R=DX/DY
PSQR=PSQR+1.DC
REY=1.DC/REYNLD
TERL=M=1.DC/2.DC*DY2
ATERM=XV*DX2*DY2
EA=1.DC/(DY2**2)
EB=1.DC/(8.DC*DI/XM)
EC=ETA=2.DC*PI/XM
THETE(S,100)P;RQR,RQR
WRITE(8X,F12.8,3X,F12.9)
100
CCCCC
SET UP PERIODIC COUNTERS, IAC 81AP.
SET UP INDEXING COUNTERS, IAC 81AP.
JC=0
DO 10 I=1,M
IPQ(I)=I+1
IMQ(I)=I-1
IAQ(I)=I+JC
JC=JC+1
CONTINUE
10 IPQ(M)=1

```



```

SUBROUTINE START /
COMMON / FIELDS / PHI,GAMA,EG,GAMOLD
COMMON / VECTOR / T,A,S,XALPHA,PHMEAN,GAMEAN,UMEAN,TEMP,TURBKE,
1 COMMON / APPAYS / U,PHILAM,EE,E-A,GAP,X,Y
COMMON / PARAMS / IPO,IMD,INV,IAP,MM(3)
2 COMMON / PARAMS / NM1,NP1,NP2,NM1,NM2,NM3,NM4,NH,MPI,MD2,MD3,MM1,
3 M2M,MH,MHP,NDBR,TCOUNT,TTEL,TINT,KCTEB,ISTART,
ISCI,P,WSCIP,I-APF,NITER,NITOT,NITMAX,IFIG,MCMMD,
KIN
COMMON / FACTOR / DX,DX2,DXSOR,DXSQR4,DXSQR8,DY,DY2,DYSQR,P,PSQR,
1 RSORP,REYNLD,PEY,FERA,CEL,XLAMDA,TIME,DT,DTT,DT,H,
2 EKMEAN,EKTURP,IVBAR,ATERM,ALPHA,XM,XN
3 XNMI,UMNLC,UELO,TOL,FA,EA,E2,E3,E4,E5,E6
COMMON / SYMBOL / CCT,RLANK,XX
DOUBLE PRECISION / DX,DX2,DXSOR,DXSOR4,DXSOR8,DY,DY2,DYSQR,R,PSQR,
1 RSORP,REYNLD,PEY,FERA,CEL,XLAMDA,TIME,DT,DTT,DT,H,XM,XN
2 EKMEAN,EKTURP,IVBAR,ATERM,ALPHA,XM,XN
3 XNMI,UMNLC,UELO,TOL,FA,EA,E2,E3,E4,E5,E6
DIMENSION PHI(64,201),GAMA(64,201),T(201),TEMP(201),TURBKE(201),GAMOLD(64,201)
DOUBLE PRECISION UVEAN(201),GAMA(201),X(54),Y(201),EE(32),
1 PHILAM(201),T(201),A(128),XALPHA(54),
2 E-A(201),GA(201)
3 IPO(64),IMD(64),INV(32),IAP(64),IAD(64)
DOUBLE PRECISION PI,THETA,C,P,XL
** ** ** ** ** ** ** ** ** ** ** ** ** ** ** ** ** ** ** ** ** ** ** ** ** ** ** ** ** ** ** ** ** ** ** ** ** ** ** ** ** ** ** ** ** ** ** ** **
BOUNDARY VALUES OF STREAM FUNCTION
PI=3.1415926535898
DO 10 I=1,M
PHI(I,1)=0.
PHI(I,N)=0.
10 CONTINUE
ESTABLISH INITIAL VALUES OF STREAM FUNCTION
USE APPAYS UMEAN AND TEMP FOR TEMPORARY STORAGE
DO 60 J=1,NH
READ(5,11) PHMEAN(J),GAMEAN(J)
11 FORMAT(2F10.0)
CONTINUE
NH=NH-1
DO 65 J=1,NHM

```

000000

000000


```

JC=N-J+1
PHMEAN(JC)=PHMEAN(J)
GAMMEAN(JC)=GAMMEAN(J)
CONTINUE
65 EQPMAT(1,OX,3(F12.6,3X))
12 EPS=.1*DO/DSQRT(2.00)
DO 70 J=1,N
C=PHMEAN(J)
R=GAMMEAN(J)
DO 70 I=1,M
THETA=PI/H*X(I)
PHI(I,J)=EPS*(C*DCOS(THETA)+B*DSIN(THETA))
70 CONTINUE
WRITE(6,12) Y(J),C,R
71 CONTINUE

      COMPUTE INITIAL VALUES OF VORTICITY
DO 13 I=1,M
IP=IPQ(I)
IM=IMQ(I)
GAMA(I,N)=(8.00*PHI(I,NM1)-PHI(I,2))-PHI(I,3)*ATEPM
GAMA(I,1)=(8.00*PHI(I,2)-PHI(I,3))*ATEPM
GAMOLD(I,1)=GAMA(I,1)
GAMOLD(I,N)=GAMA(I,N)
DO 15 J=2,NM1
GAMA(I,J)=(PCOR*(PHI(I,J+1)+PHI(I,J-1))+PHI(IP,J)+PHI(IM,J)
1 GAMOLD(I,J)=GAMA(I,J)
15 GAMOLD(I,J)=GAMA(I,J)
CONTINUE
CALL MEANS
CALL TIMER
RETURN
END

```

CC

```

SUPROUTINE TITLE /
COMMON / FIELDS /
COMMON / VECTOR /
1 COMMON / ARAYS /
COMMON / PARAMS /
1 2 3 COMMON / FACTOR /
1 2
PHI,GAMA,EG,GAMOLD
T,A,S,XALPHA,PHMEAN,GAMMEAN,TEMP,TURBKE,
U,PHILAM,ETA,GAS,X,Y
IPQ,IMQ,INV,IAC,IAB,VM(3)
NM,NM1,NM2,NM3,NM4,NH,MD1,MD2,MD3,MM1,
M2M,MH,MUP,NPCB,ICOUNT,ITEL,INT,KSTEB,ISTABT,
ISCTP,MSCIP,ITAPE,NI TEP,NI TMAX,IFIG,MCOMP,
KINT
DX,CX2,PXSQR,PXSQR4,PXSQR6,PXSQR8,PXSQR,E,RSQR,
PSQRP,PSYNLD,PEY,ERACCEL,XLAMDA,TIME,DT,PI,H,
EKMEAN,EKTUPR,UVRAP,ATEPM,B-ERM,ALPHA2,BETA,XW,XN

```



```

SUBROUTINE STEP / PHI, GAMA, EG, GAMOLD
COMMON / FIELDS / T, A, S, XALPHA, PHMEAN, GAMEAN, UMEAN, TEMP, TURBKE,
COMMON / VECTOR / U, PHILAM, FE, -A, G, X, Y
1 COMMON / ARRAYS / IPO, IMO, INV, IAO, IAD, MM(3)
COMMON / PARAMS / N, M, NPI, NP2, NM2, NM3, NM4, NH, MPI, MP2, MP3, MMI,
2 M2M, MH, MDP, MDCP, ICOUNT, ITEL, INT, KCTF, ISTART,
3 ISTOP, MSCIP, ITAPE, NITER, NITOT, NITMAX, IEIG, MCMP,
4 KINT
COMMON / FACTOR / DX, DX2, XSQR, DXSQR4, DXSQRP, DY, DY2, DYSQR, R, RSQR,
5 RSQRP, REYNLD, REY, EDCCEL, XLAMDA, TIME, DT, DTT, PI, H,
6 EKMEAN, EKUTUP, UVPAP, ATERM, RTERM, ALPHA, PETA, XM, XN
COMMON / SYMBOL / XNM1, UVMFLO, UFLD, TOL, FA, FR, FC, FI, F2, F3, F4, F5, FA
DOUBLE PRECISION / DDT, BLANK, XX
1 DOUBLE PRECISION / DX, DX2, XSQR, DXSQR4, DXSQRP, DY, DY2, DYSQR, R, RSQR,
2 RSQRP, REYNLD, REY, EDCCEL, XLAMDA, TIME, DT, DTT, PI, H,
3 EKMEAN, EKUTUP, UVPAP, ATERM, RTERM, ALPHA, PETA, XM, XN
1 DIMENSION PHI(64,201), GAMA(64,201), EG(64,201), GAMOLD(64,201)
DOUBLE PRECISION / UMEAN(201), TEMP(201), TURBKE(201), U(201),
1 PHILAM(201), T(201), A(128), S(32), XALPHA(64),
2 PHMEAN(201), GAMEAN(201), X(64), Y(201), FE(32),
3 ETA(201), GA(201)
1 DIMENSION IPO(64), IMO(64), INV(32), IAO(64), IAD(64)
DOUBLE PRECISION / GJ, GJ1, GJ2, GJ3, Q
DOUBLE PRECISION / CRIT, TST, PUNT, GAMAIJ
* * * * *
REAL*8 LAMDA, LAMDA3, LAMDAC, LAMDAR, LAMDAE
THIS ROUTINE COMPUTES NEW VALUES OF VORTICITY AT TIME+DT BY
MODIFIED EULER IMPLICIT TIME DIFFERENCING.
ARRAY EG IS USED TO STORE TERMS EVALUATED AT TIME T.
IF(KINT.EQ.1) GO TO 6
IF(ICOUNT.EQ. 0) GO TO 6
DO 5 I=1, M
DO 5 J=1, N
GAMA(I,J)=.5*(GAMA(I,J)+GAMOLD(I,J))
GAMOLD(I,J)=GAMA(I,J)
CONTINUE
CALL PRESUR
TIME=TIME-DT/2.00
CALL TIMER
6 LAMDAE=RSQRP*DT/(REYNLD*DXSOR)

```

000 000000


```

2      +GAMA(I,JM)*(PHI(IP,JM)-PHI(IM,JM))
3      +GAMA(IP,J)*(PHI(IP,JP)-PHI(IP,JM))
      GJ=(GJ1+GJ2+GJ3)/12.DO
      GJ=P*GJ
      Q=RSQR*(GAMA(I,JP)+GAMA(I,JM))+GAMA(IP,J)+GAMA(IM,J)
      Q=Q*REY
      GAMA(I,J)=LAMDAC*(GJ+Q)-LAMDAC*U(J)*(GAMA(IP,J)-GAMA(IM,J))
      -LMDAE*(PHI(IP,J)-PHI(IM,J))+EG(I,J)
1      CONTINUE
20     CALL PRESUP

      SECOND SWEEP. START Y PASS AT UPPER WALL

DO 30 I=1,M
IP=IPD(I)
IM=IMD(I)
J=NM1
DO 30 JC=2,NM1
JP=J+1
JM=J-1
GJ1= (PHI(IM,J)-PHI(IP,J))*(GAMA(I,JP)-GAMA(IM,JM))
      + (PHI(IP,JP)-PHI(IP,JM))*(GAMA(IP,JP)-GAMA(IP,JM))
1     GJ2= GAMA(IP,JP)*(PHI(IP,JP)-PHI(IP,JM))
      +GAMA(IP,JM)*(PHI(IP,JP)-PHI(IP,JM))
12    GJ3= GAMA(IM,JP)*(PHI(IM,JP)-PHI(IM,JM))
      +GAMA(IM,JM)*(PHI(IM,JP)-PHI(IM,JM))
3     GJ=(GJ1+GJ2+GJ3)/12.DO
      GJ=P*GJ
      Q=RSQR*(GAMA(I,JP)+GAMA(I,JM))+GAMA(IP,J)+GAMA(IM,J)
      Q=Q*REY
      TST=GAMA(I,J)
      GAMA(I,J)= LAMDAC*(GJ+Q)-LAMDAC*U(J)*(GAMA(IP,J)-GAMA(IM,J))
      -LMDAE*(PHI(IP,J)-PHI(IM,J))+EG(I,J)
1      TEST FOR CONVERGENCE

      CRIT=DARS(1.-GAMA(I,J)/GAMAIJ)
      PUNT=PUNT+CRIT
29     GAMA(I,J)=GAMAIJ
30     J=J-1
      CONTINUE
      NITER=NITER+2
      TST=PUNT/(XM*NM2)
      IF(TST.LT. TOL) GO TO 31

```



```

IF(NITER.GT.NITMAX) GO TO 31
CALL PRESUR
GO TO 15
TIMET=TIME+DT
NIT=NITOT+NITER
IF(ICOUNT.EQUALS KSTEP THEN SUBROUTINE SPECTRM WILL BE BYPASSED
SO THAT COUNT NO SPECTRA WILL BE CALCULATED DURING THE ITERATIONS
IN SUBROUTINE STEP
KSTEP=KSTEP+1
CALL PRESUR
KSTEP=KSTEP-1
RETURN
END

```


000067221
000067222
000067223
000067224
000067225

```
DTT=XLAMDA#DX#DY#REYNLD/4.D0  
DT=DMIN1(DT,DTT)  
IF(DT.EQ.DTT) ITEL=0  
RETURN  
END
```



```

LAMDAB=3.D0*LAMDAD
DO 10 I=1,M
  IP=IPC(I)
  IMM=IMC(I,M)
  IPP=IPC(IP)
  DO 10 J=2,NM1
    JP=J+1
    JM=J-1
    GJ1= (PHI(IM,J)-PHI(IP,JM))* (GAMA(IP,J)-GAMA(IM,JM))
    1 GJ2= (GAMA(IP,JP)-PHI(IP,JM))* (GAMA(IP,J)-GAMA(IM,J))
    1 2 GJ3= (GAMA(IP,JP)-PHI(IP,JM))* (PHI(IP,JM)-PHI(IM,JM))
    1 2 3 GJ3= (GAMA(IM,JP)-PHI(IM,JM))* (PHI(IM,JM)-PHI(IP,JM))
    1 2 3 GJ3= (GAMA(IM,JP)-PHI(IM,JM))* (PHI(IM,JM)-PHI(IP,JM))
    GJ=(GJ1+GJ2+GJ3)/12.D0
    QJ=RSQRE*(GAMA(IP,JP)+GAMA(IM,JM))+GAMA(IP,J)+GAMA(IM,J)
    Q=Q*REY
    FG(I,J)=LAMDAB*GAMOLD(I,J)+LAMDAB*(GJ+Q)
    1 -LAMDAB*U(J)*(GAMA(IP,J)-GAMA(IM,J))
    2 -LAMDAB*(PHI(IP,J)-PHI(IM,J))
10 CONTINUE
DO 20 I=1,M
  DO 20 J=2,NM1
    GAMOLD(I,J)=GAMA(I,J)
    GAMOLD(I,J)=FG(I,J)
20 CONTINUE
CALL PRIME SUP
TIME=TIME+DT
NITE=0
GO 40
30 CALL STEP
40 KSTEP=KSTEP+KINT
40 RETURN
END

```

C

00000000

END


```

      ETA(4)=A3*PHI(IM2,J)+A4*PHI(IM2P,J)
      WRITE(6,12) J,ETA(1),ETA(2),Y(J),ETA(3),ETA(4),J
10    CONTINUE
11    FORMAT('HO,5X,'J',4X,'REAL',MODE',I3,',IMAG',6X,'J',
12    'REAL',MODE',I3,',IMAG',6X,'J',
      EQPMAT(4X,I3,2(3X,E10.6),6X,E7.4,6X,2(E10.6,3X),I3)
20    GO TO 40
      WRITE(6,21) IMOD1,IMOD2
      DO 30 J=1,N
      DETA(1)=PHI(IM1,J)*2+PHI(IM1P,J)**2
      DETA(2)=DSQRN2(PHI(IM1,J),PHI(IM1P,J))
      DETA(3)=PHI(IM2,J)*2+PHI(IM2P,J)**2
      DETA(4)=DSQRN2(PHI(IM2,J),PHI(IM2P,J))
      DETA(5)=ATTAN2(PHI(1),ETA(2),Y(J),ETA(3),ETA(4),J
      CONTINUE
20    EQPMAT('HO,5X,'J',4X,'MAG',MODE',I3,',PHAS',11X,'Y',6X,
21    'REAL',MODE',I3,',PHAS',6X,'J',
40    RETURN
      END

```



```

SURROUTINE SPECTRM(INDEX)
COMMON / FIELDS / PHI, GAMMA, EG, GAMMA, GAMMA, GAMMA, UMEAN, TEMP, TURBKE,
COMMON / VECTOR / T, A, S, XALPHA, PHMEAN, GAMMA, X, Y
1 COMMON / ARRAYS / IPO, INP, INV, TAC, IAD, MM(3)
COMMON / PARAMS / NM, MPI, NP2, NM2, NM3, NM4, NH, MPI, MP2, MP3, MM1,
M2M, MH, MHP, NDBP, ICOUNT, TTCL, INT, K2-EB, TSTART,
ISCIPI, MSCIP, IADG, NI-ER, MITT, NI-NAX, TEG, MCOMB,
KINT
COMMON / FACTOR / DX, DX2, DXSOR, DXSOR2, DY, DY2, DYSOR, R, RSOR,
RSORP, PEYNLD, PEY, ESACEL, XLAMPD, TIME, DT, DTI, PI, XM,
EKMEAN, EKTOP, UVRAB, ATERM, BTERM, ALPHA, ETA, XM,
XNM1, UMELO, UELC, TOL, EA, ER, EC, FI, F2, E3, E4, E5, E6
COMMON / SYMBOL / DT, PLANK, XX
DOUBLE PRECISION
DIMENSION PHI(64,201), GAMMA(64,201), GAMMAD(64,201),
DOUBLE PRECISION
PHILAM(201), T(201), A(128), XLAMPD(44),
ETA(201), GAMMA(201), X(64), Y(201), EF(32),
IPC(64), INV(32), IAD(64), IAP(64)
DIMENSION
* * * * *
THIS ROUTINE COMPUTES THE KINETIC ENERGY OF THE DISTURBANCE
NOTION AS A FUNCTION OF Y AND WAVE NUMBERS IN THE X DIRECTION.
WAVE OR MODE NUMBERS ONE CORRESPONDS TO THE MEAN VALUE OF THE
DISTURBANCE. THE SPECTRUM OF THE TURBULENT ENERGY IS CONTAINED
IN MODE NUMBERS TWO THROUGH NH.
ARRAY EG IS USED FOR STORAGE OF THE SPECTRAL VALUES
IF(ICOUNT.EQ.KSTEP) RETURN
IF(IG=1)
IF(INDEX.LT.0) GO TO 60
L=MH+1
DO 10 J=2,NM1
JM=J-1
JP=J+1
EG(1,J)=EG*(PHI(1,JM)-PHI(1,JP))**2
EG(L,J)=EG*(PHI(L,JM)-PHI(L,JP))**2
DO 10 I=2,MH
LL=I+1

```

CCCCCCCCCCCC


```

35 GA(J)=G(I2,J)
36 CONTINUE
37 FORMAT(6,10X,'I1,I2',20X,'ENERGY IN MODE ',I2)
38 CALL PLOTSP(ETA,GA,N)
39 I1=4
40 I2=5
41 GO TO 100
42 CONTINUE
43 SIMILAR OPERATIONS FOR THE SPECTRUM OF SQUARED VORTICITY
44
45 F6=1.DC/XM**2
46 DO 50 J=1,N
47   PHI(I,J)**2
48   EG(MHP,J)=F6*PHI(M,J)**2
49   DO 50 I=2,MH
50     LL=IAO(I)
51     EG(I,J)=F6*(PHI(LL-1,J)**2+PHI(LL,J)**2)
52   CONTINUE
53 DO 60 I=1,MHP
54   J=1,N
55   T(J)=EG(I,J)
56 CONTINUE
57 CALL ASUM(T,N,SUM)
58 ETA(I)=SUM/XNM1
59 GA(I)=EG(I,NH)
60 CONTINUE
61 TITLE
62 L=ICOR(6,61),L
63 VORTICITY SPECTRUM FOR CYCLE NUMBER ',I5)
64 WRITE(6,10X,'I1,I2',20X,'ENERGY IN MODE ',I2)
65 CALL PLOTSP(ETA,GA,MHP)
66 DO 70 I=1,MHP
67   EG(I)=EG(I,16)
68   GA(I)=EG(I,186)
69 CONTINUE
70 WRITE(6,23) Y(16),Y(186)
71 CALL PLOTSP(ETA,GA,MHP)
72 RETURN
73 ENDO

```



```

51  ALINE(JA)=XXX
    ALINE(JR)=XXX
    WRITE(6,51) APLCT(I),ALINE,I,RPLOT(I),PLINE
    FORMAT(1X,F10.4,2X,49A1,2X,I3,2X,F10.4,2X,49A1)
    ALINE(JA)=BLANK
    ALINE(JR)=BLANK
    ALINE(I)=DOT
    ALINE(I)=DOT
50  CONTINUE
    SET UP BOTTOM HORIZONTAL AXIS
    GO TO 60
    GO TO 1,4C
    ALINE(I)=DOT
    ALINE(I)=DOT
    CONTINUE
    WRITE(6,61) ALINE,BLINE
    FORMAT(1X,49A1,20X,49A1//)
    RETURN
61  END

```

UUU


```

SUBROUTINE MEANS /
COMMON / FIELDS /
COMMON / VECTOR /
1 COMMON / ARRAYS /
COMMON / PARAMS /
123
COMMON / FACTOR /
123
COMMON / SYMBOL /
COMMON / PRECISION /
123
DIMENSION PHI(64,201), GAMMA(64,201), T(201), TCOMP(201), TURPKF(201),
DOUBLE PRECISION UMEAN(201), GAMMEAN(201), X(201), Y(201), FF(32),
123
DIMENSION
* * * * *
THIS ROUTINE COMPUTES THE MEAN VALUES OF PHI AND GAMMA
ARRAY A IS USED FOR TEMPORARY STORAGE.
DO 10 J=1,N
DO 20 I=1,M
A(I)=PHI(I,J)
20 CONTINUE SUM(A,M,SUM)
PHI MEAN(J)=SUM/XM
DO 30 I=1,M
A(I)=GAMMA(I,J)
30 CONTINUE SUM(A,M,SUM)
GAMMEAN(J)=SUM/XM+3.DO*Y(J)
10 CONTINUE
END

```

CCCCC

20 EG(I,J)=GAMA(I,J)-GAMEAN(J)
25 CONTINUE
30 RETURN
35 END

00013350
00013350
00013350
00013350


```

30 DO J=2,NM1
  UMEAN(J)=(PHMEAN(J-1)-PHMEAN(J+1))/DY2+U(J)
CONTINUE
  UMEAN(1)=C.
  UMEAN(N)=O.
  CALL ASUM(UMEAN,NM1,SUM)
  UMELO=SUM/XNM1
  UELC=(2.00+PHMEAN(2)-PHMEAN(NM1)+PHILAM(2)-PHILAM(NM1))/4.00
  UELC=0.10G(EKTTURR)
RETURN
END

```

```

SUBROUTINE ASUM(A,NM,SUM)
DOUBLE PRECISION A(1)
DOUBLE PRECISION SUMM
THIS ROUTINE COMPUTES THE SUM OF THE FIRST NM ELEMENTS OF A,
AND STORES THE RESULT IN SUM
SUM=0.00
DO 10 I=1,NM
  SUMM=SUMM+A(I)
CONTINUE
SUM=SUMM
RETURN
END

```

CCCC

C0014470
 C0014480
 C0014490
 C0014500
 C0014510
 C0014520
 C0014530
 C0014540
 C0014550
 C0014560
 C0014570

C0014580
 C0014590
 C0014600
 C0014610
 C0014620
 C0014630
 C0014640
 C0014650
 C0014660
 C0014670
 C0014680


```

0000      FIND LARGEST ELEMENTS IN APL0T AND BPL0T
15      ABIG=0.
      BBIG=0.
      DO 20 J=1,N
      ABIG=AMAX1(ABIG,ABS(APLOT(J)))
      BBIG=AMAX1(BBIG,ABS(BPLOT(J)))
20      CONTINUE

      SET UP TOP HORIZONTAL AXIS
      DO 30 I=1,49
      ALINE(I)=DOT
      BLINE(I)=DOT
30      CONTINUE
12      FORMAT(1X,49A1,20X,49A1)

      BLANK ALINE AND BLINE AND PUT PLOTTING SYMBOL IN COMPUTED ELEMENT
      DO 40 I=1,49
      ALINE(I)=BLANK
      BLINE(I)=BLANK
40      CONTINUE
      ALINE(1)=DOT
      BLINE(25)=DOT
      J=N
      DO 50 JC=1,N,2
      JC=APLOT(J)/ABIG+.1+.2F.
      JB=BPLOT(J)/BBIG+.1+.2F.
      ALINE(JC)=XXX
      BLINE(JC)=XXX
      WRITE(6,13)APLOT(J),BPL0T(J),ALINE(JC),BLINE(JC),49A1)
13      FORMAT(1X,10.4,2X,49A1,2X,13,3X,F10.4,2X,49A1)
      ALINE(JC)=BLANK
      BLINE(JC)=BLANK
      ALINE(1)=DOT
      BLINE(25)=DOT
      J=J-2
50      CONTINUE

      SET UP BOTTOM HORIZONTAL AXIS
      DO 60 I=1,49
      ALINE(I)=DOT
      BLINE(I)=DOT
60      CONTINUE

```



```

00015660
00015670
00015680
00015690
00015700
00015710
00015720
00015730
00015740
00015750
00015760
00015770
00015780
00015790
00015800
00015810
00015820
00015830
00015840

```

```

14 WRITE(6,14)ALINE,BLINE
   FORMAT(14X,4G41,20X,4G41//)
   IF(III.GT.0)GO TO 100

   PUT TURBKE IN APLDT , GAMFAN IN SPLOT

55 DO _O J=1,N
   APLDT(J)=TURBKE(J)
70 APLDT(J)=GAMFAN(J)
   CONTINUE
   III=1
   TITLE
   WRITE(6,15)
16 FORMAT(1H0,4X,'TURBKE',25X,'GAMEAN',32X,'GAMEAN')
   GO TO 15
100 RETURN
   END

```



```

1200) RV(7),RV(8),RV(9),RV(10),RV(11),
WRITE(6,1200) RV(12),RV(13),RV(14),RV(15),RV(16),
WRITE(6,1200) RV(17),RV(18),RV(19),RV(20),RV(21),
WRITE(6,1050)
M=1
DO 40 K=1,N
DO 40 J=1,M
AJ=A(K,J)+2.50001
JJ=INT(AJ)
LINE(J)=F5.41,41,46
IF(M-INT(M))=M1,115
CONTINUE=1
CONTINUE=1
WRITE(6,2000) LINE
DO 40 I=1,N
DO 40 J=1,M
AJ(I,J)=A(I,J)/SCF +AMIN
CONTINUE=1
FORMAT(1//)
1000) FORMATT(5X,F8.3)
1100) FORMATT(5X,F8.3)
1200) FORMATT(5X,F8.3)
1210) FORMATT(5X,F8.3)
1220) FORMATT(5X,F8.3)
1300) FORMATT(5X,F8.3)
2000) FORMATT(2X,115A1)
END
A=,E8.3,3X,3H B=,E8.3,3X,3H C=,E8.3,3X,3H D=,E8.3,
E=,E8.3,3X,3H F=,E8.3,3X,3H G=,E8.3,3X,3H H=,E8.3,
I=,E8.3,
J=,E8.3,3X,3H K=,E8.3,3X,3H L=,E8.3,3X,3H M=,E8.3,
N=,E8.3,3X,3H O=,E8.3,3X,3H P=,E8.3,3X,3H Q=,E8.3,
R=,E8.3,3X,3H S=,E8.3,3X,3H T=,E8.3,3X,3H U=,E8.3,
V=,E8.3,3X,3H W=,E8.3,3X,3H X=,E8.3,3X,3H Y=,E8.3,
Z=,E8.3,3X,3H
F10.6,5X,7H RANGE(,E1=,6,5X,E15.6,2H ) )

```



```

16 FORMAT(IX,'J= ',I3,IX,'Y= ',E5.3,2X,'O(E10.7,IX) )
17 FORMAT(IH0,'**
100 RETURN

```

```

**
**
**

```

```

0014700
00014800
00014800
00014800
00014800

```



```

SURROUTINE LOAD
COMMON / FIELDS / PHI, GAMA, EG, GAMOLD
COMMON / VECTOR / T, A, S, XALPHA, PHMEAN, GAMMEAN, UMEAN, TEMP, TURRKE,
I U, PHILAM, EE, ETA, GA, X, Y
COMMON / ARAYS / ITC, TMO, INV, IAC, IAP, MM(2)
COMMON / PARAMS / NUMBER(31)
COMMON / FACTOR / EACTO
COMMON / SYMBOL / DOT, PLANK, XXX
COMMON / PRECISION / FACTO(42)
DOUBLE PRECISION PHI(64,201), GAMA(64,201), EG(64,201), GAMOLD(64,201)
DOUBLE PRECISION UMEAN(201), TURRKE(201), TMO(201),
I PHILAM(201), T(201), A(128), S(32), XALPHA(64),
PHMEAN(201), GAMMEAN(201), X(64), Y(201), EE(32),
ETA(201), GA(201), INV(32), TMO(64), IAP(64)
DIMENSION NUMBER(25)
ITAPE=NUMBER
ITAPENO(ITAPE) PHI, GAMA, EG, GAMOLD
IREAD(ITAPE) T, A, S, XALPHA, PHMEAN, GAMMEAN, UMEAN, TEMP
IREAD(ITAPE) TURRKE, U, PHILAM, EE, ETA, GA, X, Y
IREAD(ITAPE) ITC, TMO, INV, IAC, IAP, MM
IREAD(ITAPE) NUMBER
IREAD(ITAPE) EACTO
IREAD(ITAPE) DOT, PLANK, XXX
IREAD(ITAPE) IAP, MM, INV, S, O, TMO
CALL PHAP(A, MM, INV, S, O, TMO)
RETURN

```

```

00017630
00017640
00017650
00017660
00017670
00017680
00017690
00017700
00017710
00017720
00017730
00017740
00017750
00017760
00017770
00017780
00017790
00017800
00017810
00017820
00017830
00017840
00017850
00017860
00017870
00017880
00017890
00017900

```


APPENDIX C

LISTING OF THE FORTRAN CODE FOR THE SOLUTION
OF THE ALGEBRAIC EIGENVALUE PROBLEM


```

COMMON / FIELDS / W,VAL,Y,U
COMMON / SPACES / B,RI,TEMP,VECT
COMMON / ARRAYS / IORD(101),INUM(101)
COMMON / PARAMS / M,N,NM1,NM2,NM3,NM4,NM5,NH,NHM1,NHM2,NHM3,NHM4,
1 NHM5,KCUNT,MODE,NCAL
COMMON / FACTOR / XN,XN1,XNH,XNHM1,DX,DY,DXSQR,DYSQR,RATIO,
1 RATIO1,DT,DTT,ERRACEL,XLAMDA,ALPHA,H,REYNLD,
2 ZETA,OMEGA,OMEGT,C1,C2,D1,D2,GAMA,BETA,DETRM,
3 ZETA,PUNT,CRI,T,P1,P2,P3,P4
COMMON / EXTRA / NUMVEC
DOUBLE PRECISION W(2,100,100),VAL(2,100),Y(201),U(201)
DOUBLE PRECISION B(100,100),RI(100,100),TEMP(2,100),VECT(2,100)
DOUBLE PRECISION XN,XNM1,XNH,XNHM1,DX,DY,DXSQR,DYSQR,RATIO,
1 RATIO1,DT,DTT,ERRACEL,XLAMDA,ALPHA,H,REYNLD,
2 ZETA,OMEGA,OMEGT,C1,C2,D1,D2,GAMA,BETA,DETRM,
3 ZETA,PUNT,CRI,T,P1,P2,P3,P4
XLAMDA=.2D0
ERRACEL=.4D0
NUMVEC=4
N=201
M=64
REYNLD=25000.D0
ALPHA=1.D0
CALL SETUP
CALL EXACT
FORMAT(2F29.14)
11 STOP
END

```

```

SUBROUTINE SETUP
COMMON / FIELDS / W,VAL,Y,U
COMMON / SPACES / B,RI,TEMP,VECT
COMMON / ARRAYS / IORD(101),INUM(101)
COMMON / PARAMS / M,N,NM1,NM2,NM3,NM4,NM5,NH,NHM1,NHM2,NHM3,NHM4,
1 NHM5,KCUNT,MODE,NCAL
COMMON / FACTOR / XN,XN1,XNH,XNHM1,DX,DY,DXSQR,DYSQR,RATIO,
1 RATIO1,DT,DTT,ERRACEL,XLAMDA,ALPHA,H,REYNLD,
2 ZETA,OMEGA,OMEGT,C1,C2,D1,D2,GAMA,BETA,DETRM,
3 ZETA,PUNT,CRI,T,P1,P2,P3,P4
COMMON / EXTRA / NUMVEC
DOUBLE PRECISION W(2,100,100),VAL(2,100),Y(201),U(201)
DOUBLE PRECISION B(100,100),RI(100,100),TEMP(2,100),VECT(2,100)
DOUBLE PRECISION XN,XNM1,XNH,XNHM1,DX,DY,DXSQR,DYSQR,RATIO,
1 RATIO1,DT,DTT,ERRACEL,XLAMDA,ALPHA,H,REYNLD,
2 ZETA,OMEGA,OMEGT,C1,C2,D1,D2,GAMA,BETA,DETRM,
3 ZETA,PUNT,CRI,T,P1,P2,P3,P4

```



```

CC
MISCELLANEOUS PARAMETERS
WRITE(6,99)
H=3.1415926535898D0
NM1=N-1
NM2=N-2
NM3=N-3
NM4=N-4
NM5=N-5
NH=(N+1)/2
NHM1=NH-1
NHM2=NH-2
NHM3=NH-3
NHM4=NH-4
NHM5=NH-5
XN=DFLOAT(N)
XNM1=DFLOAT(NM1)
XNH=DFLOAT(NH)
XNHM1=DFLOAT(NHM1)
DX=2.0D0/XNM1
DY=2.0D0/XNM1
DXSQR=DX*DX
DYSQR=DY*DY
RATIO=DYSQR/DXSQR
RATIOP=RATIO+1.0D0
DT=FRACEL*DSQR(DX*DY)/1.5D0
DT=XLAMDA*DX*DY*REYNLD/4.0D0
DT=DMIN1(DT,DTT)
ITEL=1
IF(DT.EQ.DTT) ITEL=-1
VORTICITY BOUNDARY CONDITIONS
P1=8.0D0
P2=-3.0D0
P3=8.0D0/9.0D0
P4=-1.25D0
P1=4.0D0
P2=-.5D0
P3=0.0D0
P4=0.0D0
TITLE
WRITE(6,13) N,M,ITEL
WRITE(6,14) DX,DXSQR,RATIO
WRITE(6,15) DY,DYSQR,RATIOP
WRITE(6,16) DT,FRACEL,XLAMDA

```



```

C1=-TEMP(1,1)/ALPHA
C2=-TEMP(2,1)/ALPHA
D1=1.00
D2=0.00
WRITE(6,1)
FORMAT(10X, '*** CONTINUOUS CASE ***' DATA FOR LEAST STABLE MODE
1 //)
WRITE(6,2) CMEGA,OMEGT,ZETA
WRITE(6,3) C1,D2
WRITE(6,4) C1,C2
WRITE(6,5) GAMMA,BETA,ALPHA
FORMAT(10X, 'D1 =',F13.8,3X, 'OMEGT =',F13.8,3X, 'ZETA =',F13.8)
FORMAT(10X, 'D2 =',F13.8,3X, 'C1 =',F13.8,3X, 'C2 =',F13.8)
FORMAT(10X, 'GAMMA =',F13.8,3X, 'BETA =',F13.8,3X, 'ALPHA =',F13.8//)
IF(NUMVEC.GE.0) CALL OUTPUT(NUMVEC)
RETURN
END

SUBROUTINE DISCRT
COMMON / FIELDS / W,VAL,X,Y,U
COMMON / SPACES / R,R1,TEMP,VECT
COMMON / ARRAYS / TORDD(101),INUM(101)
COMMON / PARAMS / P,N,NML,NM2,NM3,NM4,NM5,NH,NHM1,NHM2,NHM3,NHM4,
NH*5,KOUNT,MODE,VCAL
XN,XNM1,XNH,XNH*5,DOX,DY,DXSQ,DYSQR,RATIO,
RATIO*2,T,DTT,ESACEL,XLAVPA,ALPHA,H,REYNLD,
ZETA,PUNT,GAMMA,OMEGT,C1,C2,D1,D2,GAMA,BETA,DETRM,
FAC,PUNT,CRIT,P1,P2,P3,P4
COMMON / EXTRA / NUMVEC
COMMON / PRECISION / NW(2,100),VAL(2,100),Y(201),U(201)
COMMON / PRECISION / R(2,100),I(100),I(100),DX,DY,DXSQ,DYSQR,RATIO,
XN,XNM1,XNH,XVPA,DOX,DY,DXSQ,DYSQR,RATIO,
RATIO*2,T,DTT,ESACEL,XLAVPA,ALPHA,H,REYNLD,
ZETA,PUNT,GAMMA,OMEGT,C1,C2,D1,D2,GAMA,BETA,DETRM,
FAC,PUNT,CRIT,P1,P2,P3,P4
DOUBLE PRECISION XX,VY
OMEGA=-2.00-4.00*PI*OMEGA*DX/2.00)*2
OMEGT=OMEGA+2.00*PI*OMEGA*DX/2.00
ZETA=DSIN(ALPHA*DX)/DX
CALL SETVAL
FAC=2.00*RATIO/(REYNLD*DYSQR)
IF(NCAL.EQ.0) GO TO 100
DO 20 J=1,NCAL
C1=TEMP(1,J)
C2=TEMP(2,J)
PUNT=C1-FAC

```



```

CRIT=C2
DO 10 I=1,100
  XX=CRIT*DT
  YY=PUNT*DT
  D1=XX/(DSINH(YY)*DCOS(XX))*(C1-FAC*DCOSH(YY)*DCOS(XX))
  D2=XX/(DSINH(XX)*DCOSH(YY))*(C2-FAC*DSINH(YY)*DSIN(XX))
  PUNT=1.00-DABS(PUNT/D1)
  CRIT=1.00-DABS(CRIT/D2)
  IF((PUNT .LT. .00001) .AND. (CRIT .LT. .00001)) GO TO 15
  PUNT=D1
  CRIT=D2
  CONTINUE
10 IF ICO
15 TEMP(1,J)=D1
  TEMP(2,J)=D2
  IF(I .GT. 99) WRITE(6,16) J,I
16 FORMAT(10X,'J=',I3,3X,I3,'ITERATIONS')
20 CONTINUE
  GAMA=TEMP(1,1)
  BETA=TEMP(2,1)
  C1=-GAMA/ALPHA
  C2=-BETA/ALPHA
  D1=DCOSH(GAMA*DT)*DCOS(BETA*DT)
  D2=DSINH(GAMA*DT)*DSIN(BETA*DT)
  WRITE(6,17)
1  FORMAT(10X,'** DISCRETE CASE **' DATA FOR LEAST STABLE MODE')
  WRITE(6,2) D1,D2
  WRITE(6,3) C1,C2
  WRITE(6,4) GAMA,BETA,ALPHA
2  FORMAT(10X,'OMEGA= ',F13.8,3X,'OMEGT= ',F13.8,3X,'ZETA= ',F13.8)
3  FORMAT(10X,'D1= ',F13.8,3X,'D2= ',F13.8)
4  FORMAT(10X,'C1= ',F13.8,3X,'C2= ',F13.8)
5  FORMAT(10X,'GAMA= ',F13.8,3X,'BETA= ',F13.8,3X,'ALPHA= ',F13.8//)
100 IF(NUMVEC .GE. C) CALL OUTPUT(NUMVEC)
  RETURN
END

```

```

SUBROUTINE SETMAT
COMMON / FIELDS /
COMMON / SPACES /
COMMON / ARRAYS /
COMMON / PARAMS /
1 COMMON / FACTOR /
2
  W,VAL,Y,U
  P,BI,TEMP,VECT
  IORD(101),INUM(101)
  NM1,NM2,NM3,NM4,NM5,NH,NHM1,NHM2,NHM3,NHM4,
  XN,XNM1,XNH,XNHM1,XDX,CY,DXSOR,DYSQR,RATIO,
  RATIOOP,DT,DTT,FRACFL,XLANDA,ALPHA,H,REYNLD,
  ZETA,OMEGA,OMEGT,C1,C2,D1,D2,GAMA,BETA,DETRM,

```



```

3 COMMON / EXTRA /
DOUBLE PRECISION
DOUBLE PRECISION
DOUBLE PRECISION
1
2
3 FAC,PUNT,CRIT,P1,P2,P3,P4
NUMVEC
W(2,100,100),VAL(2,100),Y(201),U(201)
B(100,100),RI(100,100),TEMP(2,100),VECT(2,100)
XN,XNM1,XNH,XNHM1,DX,DY,DXSOR,DYSQR,PRATIO,
PATIOP,DT,DTT,FRA,CEL,XLAMDA,ALPHA,HETA,DETRM,
ZETA,OMEGA,OMEST,C1,C2,D1,D2,GAMMA,P2,P4
FAC,PUNT,CRIT,P1,P2,P3,P4

```

CCC

```

ZERO ARAYS

```

```

DO 10 I=1,NHM1
VAL(1,I)=0.00
VAL(2,I)=0.00
TEMP(1,I)=0.00
TEMP(2,I)=0.00
DO 10 J=1,NHM1
W(1,I,J)=0.00
W(2,I,J)=0.00
B(1,J)=0.00
CONTINUE
10

```

CCC

```

SET UP AND INVERT MATRIX B

```

```

DO 20 I=1,NHM2
B(1,I)=OMEGA
B(1,I+1)=1.00
B(1+1,I)=1.00
CONTINUE
20 R(NHM1,NHM1)=OMEGA
WRITE(6,22)
FORMAT(1H0,10X,'ENTER MINV:')
CALL MINV(8,NHM1,DETRM,IORD,INUM)
WRITE(6,23)
FORMAT(1H0,10X,'EXIT MINV')
23 IF(DETRM.LT.0.10-06) WRITE(6,21) DETRM
21 FORMAT(1H0,10X,'B ALMOST SINGULAR. DETRM= ',E10.4//)

```

CCC

```

SET UP MATRIX W

```

```

DETRM=-3.00*ZETA*DYSQR
DO 30 I=1,NHM2
W(2,I,I)=ZETA*U(I+1)*OMEGA-DETRM
W(2,I+1,I)=ZETA*U(I+2)
W(2,I,I+1)=ZETA*U(I+1)
CONTINUE
30 W(2,NHM1,NHM2)=2.00*ZETA*U(NH)

```



```

W(2,NHM1,NHM1)=ZETA*U(NH)*OMEGA
DO 40 I=1,NHM1
DO 40 J=1,NHM1
DO 40 K=1,NHM1
W(1,I,J)=W(1,I,J)+B(I,K)*W(2,K,J)
CONTINUE
40 DO 50 I=1,NHM1
DO 50 J=1,NHM1
W(2,I,J)=W(1,I,J)
W(1,I,J)=0,DO
CONTINUE
50 DETRM=1,DO/(REYNLD*DYSOR)
DO 60 I=1,NHM2
W(1,I,I)=DETRM*OMEGT
W(1,I+1,I)=DETRM
W(1,I,I+1)=DETRM
CONTINUE
60 W(1,NHM1,NHM1)=DETRM*OMEGT
W(1,NHM1,NHM2)=2,DO*DETRM
DO 70 I=1,NHM1
W(1,I,1)=W(1,I,1)*P1*DETRM
W(1,I,2)=W(1,I,2)+B(I,1)*P2*DETRM
W(1,I,3)=W(1,I,3)+B(I,1)*P3*DETRM
W(1,I,4)=W(1,I,4)+B(I,1)*P4*DETRM
CONTINUE
70 NORMALIZE MATRIX W
FAC=DSORT(W(1,NHM1,NHM1))*2*W(2,NHM1,NHM1)**2)
FAC=1,DO/FAC
DO 75 I=1,NHM1
DO 75 J=1,NHM1
W(1,I,J)=W(1,I,J)*FAC
W(2,I,J)=W(2,I,J)*FAC
CONTINUE
75 OBTAIN THE EIGENVALUES AND EIGENVECTORS OF W
WRITE(6,72)
FORMAT(10X,'ENTER DAlMAT')
CALL DAlMAT(W,VAL,NHM1,NCAL)
WRITE(6,71) NCAL
71 FORMAT(1H0,10X,'*** ',I3,' EIGENVALUES AND EIGENVECTORS CALCULATE
1D'//)
OBTAIN THE NORMALIZING FACTOR FROM THE COMPUTED EIGENVALUES
DO 80 I=1,NCAL

```



```

      VAL(1,I)=VAL(1,I)/FAC
      VAL(2,I)=VAL(2,I)/FAC
      VAL(2,I)=-VAL(2,I)
      CONTINUE
80
      FIND THE STABILITY ORDER OF THE EIGENVALUES --- MAX REAL PART
      ARRAY IORD(I)=STORAGE LOCATION OF EIGENVALUE OR EIGENVECTOR
      WITH STABILITY NUMBER=I
      ARRAY INUM(I)=STABILITY NUMBER OF EIGENVALUE OR EIGENVECTOR
      WITH STORAGE NUMBER=I
      DO 100 IC=1,NCAL
      PUNT=-1D35
      DO 90 I=1,NCAL
      IF (VAL(1,I) .GT. PUNT) I=I
      PUNT=OMAX1(PUNT,VAL(1,I))
      CONTINUE
90
      IORD(IC)=I
      INUM(I)=IC
      PUT EIGENVALUES IN ARRAY TEMP IN STABILITY ORDER
      TEMP(1,IC)=VAL(1,I)
      TEMP(2,IC)=VAL(2,I)
      VAL(1,I)=-1D35
      CONTINUE
100
      DO 110 I=1,NCAL
      II=INUM(I)
      VAL(1,I)=TEMP(1,II)
      CONTINUE
110
      NORMALIZE THE EIGENVECTORS
      IF (NUMVEC .LE. 0) GO TO 130
      DO 126 K=1,NUMVEC
      JJ=ICRD(K)
      PUNT=-W(2,NHM1,JJ)/W(1,NHM1,JJ)
      DO 120 I=1,NHM1
      VECT(1,I)=W(1,II,JJ)-PUNT*W(2,I,JJ)
      VECT(2,I)=W(2,I,II,JJ)+PUNT*W(1,I,JJ)
      CONTINUE
120
      PUNT=0.0
      PUNT=VECT(1,NHM1)
      PUNT=1.0/PUNT
      DO 125 I=1,NHM1
      W(1,I,JJ)=PUNT*VECT(1,I)
      W(2,I,JJ)=PUNT*VECT(2,I)
      CONTINUE
126

```


130 RETURN
END

```

SUBROUTINE OUTPUT(NUMVEC)
COMMON / FIELDS / W,VAL,V,U
COMMON / SPACES / B,BI,TEMP,VECT
COMMON / ARRAYS / IORD(101),INUM(101),NM2,NM3,NM4,
COMMON / PARAMS / M,N,NM1,NM2,MODE,NCAL,NM5,NH,NHM1,NHM2,NHM3,NHM4,
COMMON / FACTOR / XN,XNM1,XNH,XNHM1,DX,DY,DXSOR,DYSOR,RATIO,
RATIOCP,DI,DT,DTT,FRACFL,XLANDA,ALPHA,H,REYNLD,
ZETA,OMEGA,CIT,B1,P2,P3,P4
COMMON / FACTOR / ZETA,OMEGA,CIT,B1,P2,P3,P4
COMMON / FACTOR / FAC,PUNT,CIT,VAL(2,100),Y(201),U(201)
COMMON / FACTOR / W(2,100,100),BI(100),TEMP(2,100),VECT(2,100)
COMMON / FACTOR / XN,XNM1,XN4,XNHM1,DX,DY,DXSOR,DYSOR,RATIO,
RATIOCP,DI,DT,DTT,FRACFL,XLANDA,ALPHA,H,REYNLD,
ZETA,OMEGA,CIT,B1,P2,P3,P4
COMMON / FACTOR / FAC,PUNT,CIT,PI,P2,P2,P4

```

DOUBLE PRECISION
DOUBLE PRECISION
DOUBLE PRECISION

123
123

PRINT THE EIGENVALUES

```

11 WRITE(6,11) STORNUM, STABNUM, IOX, EIGENVALUE, 23X, STORNUM, STABNUM
12 FORMAT(5X, EIGENVALUE)
13 DO 10 I=1,NCAL
14 WRITE(6,12) INUM(I), VAL(1,I), VAL(2,I), IORD(I), I, TEMP(1,I),
15 TEMP(2,I)
16 FOPMAT(7X, I2, 3X, E13.7, ' + ', E13.7, ' * I',
17 E13.7, ' + ', E13.7, ' * I',
18 CONTINUE

```

PRINT EIGENVECTORS

```

15 IF(NUMVEC.GT. NCAL) NUMVEC=NCAL
16 IF(NUMVEC.LT. 1) GO TO 30
17 NSTART=1
18 NN=4
19 NNN=MIN0(NUMVEC,NN)
20 WRITE(6,13) (I,I=NSTART,NNN)
21 FORMAT(11X, 3( ' STABNUM = ', I3, 17X), ' STABNUM = ', I3)
22 WRITE(6,14)
23 FORVAT(4( 9X, 'REAL', 8X, 'IMAGINARY'))
24 DO 20 I=1,NNM1
25 WRITE(6,16) (W(1,I,IORD(J)), W(2,I,IORD(J)), J=NSTART,NNN)
26 CONTINUE
27 WRITE(6, 99)

```


MINV 650
MINV 660
MINV 670
MINV 680
MINV 690
MINV 700
MINV 710
MINV 720
MINV 730
MINV 740
MINV 750
MINV 760
MINV 770
MINV 780
MINV 790
MINV 800
MINV 810
MINV 820
MINV 830
MINV 840
MINV 850
MINV 860
MINV 870
MINV 880
MINV 890
MINV 900
MINV 910
MINV 920
MINV 930
MINV 940
MINV 950
MINV 960
MINV 970
MINV 980
MINV 990
MINV 1000
MINV 1010
MINV 1020
MINV 1030
MINV 1040
MINV 1050
MINV 1060
MINV 1070
MINV 1080
MINV 1090
MINV 1100
MINV 1110
MINV 1120

```

17=N*(J-1)
DO 20 I=K,N
  IJ=I+J
  IF(DABS(BIGA)-DABS(A(IJ))) 15,20,20
10 BIGA=A(IJ)
15 L(K)=I
20 M(K)=J
  CONTINUE

```

CCC

INTERCHANGE ROWS

```

J=L(K)
IF(J-K) 35,35,25
25 KI=K-N
DO 30 I=1,N
  KI=KI+N
  HOLD=-A(KI)
  JI=KI-K+J
  A(KI)=A(JI)
30 A(JI)=HOLD

```

CCC

INTERCHANGE COLUMNS

```

35 I=M(K)
IF(I-K) 45,45,38
38 IP=N-(I-1)
DO 40 J=1,N
  JK=NK+J
  JI=JP+J
  HOLD=-A(JK)
  A(JK)=A(JI)
40 A(JI)=HOLD

```

CCCC

DIVIDE COLUMN BY MINUS PIVOT (VALUE OF PIVOT ELEMENT IS
CONTAINED IN BIGA)

```

45 IF(BIGA) 48,46,48
46 D=0.0
  RETURN
48 DO 55 I=1,N
  IF(I-K) 50,55,50
50 IK=NK+I
55 A(IK)=A(IK)/(-BIGA)
  CONTINUE

```

CCC

REDUCE MATRIX

```

DO 65 I=1,N

```


MINV11130
MINV11140
MINV11150
MINV11160
MINV11170
MINV11180
MINV11190
MINV11200
MINV11210
MINV11220
MINV11230
MINV11240
MINV11250
MINV11260
MINV11270
MINV11280
MINV11290
MINV11300
MINV11310
MINV11320
MINV11330
MINV11340
MINV11350
MINV11360
MINV11370
MINV11380
MINV11390
MINV11400
MINV11410
MINV11420
MINV11430
MINV11440
MINV11450
MINV11460
MINV11470
MINV11480
MINV11490
MINV11500
MINV11510
MINV11520
MINV11530
MINV11540
MINV11550
MINV11560
MINV11570
MINV11580
MINV11590
MINV11600

```

IK=NK+I
HOLD=A(IK)
IJ=I-N
DO 65 J=1,N
  IJ=IJ+N
  IF(I-K) 60,65,60
  IF(J-K) 62,65,62
60  KJ=IJ-I+K
62  A(IJ)=HOLD+A(KJ)+A(IJ)
65  CONTINUE

      DIVIDE ROW BY PIVOT
      KJ=K-N
      DO 75 J=1,N
        KJ=KJ+N
        IF(J-K) 70,75,70
70  A(KJ)=A(KJ)/BIGA
75  CONTINUE

      PRODUCT OF PIVOTS
      D=D*BIGA

      REPLACE PIVOT BY RECIPROCAL
      A(KK)=1.0/BIGA
80  CONTINUE

      FINAL ROW AND COLUMN INTERCHANGE

100  K=N
      KE=(K-1)
      IF(K) 150,150,105
105  I=L(K)
      IF(I-K) 120,120,108
108  JQ=N*(K-1)
      JR=N*(I-1)
      DO 110 J=1,N
        JK=JQ+J
        HOLD=A(JK)
        JI=JR+J
        A(JK)=-A(JI)
110  A(JI)=HOLD
120  J=M(K)
      IF(J-K) 100,100,125
125  KI=K-N
      DO 130 I=1,N

```


MINV1610
MINV1620
MINV1630
MINV1640
MINV1650
MINV1660
MINV1670
MINV1680

DALMA044
DALMA052

DALMA053
DALMA054

DALMA045
DALMA047
DALMA048
DALMA049
DALMA050
DALMA051
DALMA056
DALMA057
DALMA058
DALMA059
DALMA060
DALMA061
DALMA062
DALMA063
DALMA064
DALMA065
DALMA066
DALMA067
DALMA068
DALMA069
DALMA070
DALMA071
DALMA072
DALMA073
DALMA074
DALMA075
DALMA076
DALMA077
DALMA078
DALMA079
DALMA080
DALMA081
DALMA082
DALMA083
DALMA084
DALMA085
DALMA086
DALMA087
DALMA088
DALMA089
DALMA090
DALMA091
DALMA092
DALMA093
DALMA094
DALMA095
DALMA096
DALMA097
DALMA098
DALMA099
DALMA100
DALMA101
DALMA102
DALMA103
DALMA104
DALMA105
DALMA106
DALMA107
DALMA108
DALMA109
DALMA110
DALMA111
DALMA112
DALMA113
DALMA114
DALMA115
DALMA116
DALMA117
DALMA118
DALMA119
DALMA120
DALMA121
DALMA122
DALMA123
DALMA124
DALMA125
DALMA126
DALMA127

130 KI=KI+N
HOLD=A(KI)
JI=KI-K+J
A(KI)=-A(JI)
A(JI)=HOLD
GO TO 100
150 RETURN
END

```

SUBROUTINE DALMAT(A,LAMBDA,M,IA,NCAL)
  IMPLICIT REAL*8 (A-H), REAL*8 (G-Z)
  COMMON / SPACES / HL,MULT,VECT
  COMMON / EXTRA / NU*VEC
  COMPLEX*16 CSORG, CCNUQ
  REAL*8 REAO,ALMAO,CBO,SORG,FLOAO,ABO
  COMPLEX*16 HL(100),H(100,100),MULT(100),VECT(100)
  COMPLEX*16 A(IA,1),LAMBDA(1),SHIFT(3),TEMP,SIN,COS,TEMP1,TEMP2
  LOGICAL INT(100),TWICE
  INTEGER INT(100),R,RPI,RP2

```

PROG. AUTHORS JOHN RINZEL, R. E. FUNDERLIC, UNION CARBIDE CORP.,
NUCLEAR DIVISION, CENTRAL DATA PROCESSING FACILITY,
OAK RIDGE, TENNESSEE

PURPOSE DALMAT CALCULATES IN DOUBLE-PRECISION THE EIGENVALUES AND EIGEN-
VECTORS OF AN ARBITRARY COMPLEX MATRIX BY USE OF THE QR ALGOR-
ITHM AND THE WIELANDT INVERSE POWER METHOD FOR VECTORS.

USAGE CALL DALMAT (A,VAL,M,IA,NCAL)

DESCRIPTION OF PARAMETERS.
A : INPUT MATRIX, DOUBLY-DIMENSIONED, COMPLEX, IN TYPE, EIGEN-
VECTORS OF THE INPUT MATRIX, DALMAT WILL CONTAIN THE COMPLEX EIGEN-
SINGLY-DIMENSIONED COMPLEX*16 ARRAY IN WHICH DALMAT
RETURNS THE EIGENVALUES OF THE INPUT MATRIX, VAL(I)
CORRESPONDS WITH MATRIX, EIGENVECTOR*4,
ORDER OF INPUT MATRIX, INTRINSIC OF A IN THE CALLING PROGRAM
IS THE ROW INDICATOR; UPON RETURN FROM DALMAT IT CONTAINS
INTEGRAL INDICATOR; UPON RETURN FROM DALMAT IT CONTAINS
THE NUMBER OF EIGENVALUES WITH CORRESPONDING EIGEN-
VECTORS WHICH HAVE BEEN CALCULATED.

REMARKS

CC

DALMAL01
DALMAL02
DALMAL03
DALMAL04
DALMAL05
DALMAL06
DALMAL07
DALMAL08
DALMAL09
DALMAL10
DALMAL11
DALMAL12
DALMAL13
DALMAL14
DALMAL15
DALMAL16
DALMAL17
DALMAL18
DALMAL19
DALMAL20
DALMAL21
DALMAL22
DALMAL23
DALMAL24
DALMAL25
DALMAL26
DALMAL27
DALMAL28
DALMAL29
DALMAL30
DALMAL31
DALMAL32
DALMAL33
DALMAL34
DALMAL35
DALMAL36
DALMAL37
DALMAL38
DALMAL39
DALMAL40
DALMAL41
DALMAL42
DALMAL43
DALMAL44
DALMAL45
DALMAL46
DALMAL47

```

6 A(INTER,I)=TEMP
DO I=1,N
  TEMP=A(I,RPI)
  A(I,INTER)=TEMP
7 A(I,INTER)=TEMP
8 DO I=1,N
  I=RP2,N
  A(I,R)=A(I,R)/A(RPI,R)
9 MULT(I)=MULT(I)
  A(I,R)=MULT(I)
  TEMP=0
DO I=1,N
  J=RP2,N
  TEMP=TEMP+A(I,J)*MULT(J)
10 A(I,RP1)=A(I,RP1)+TEMP
11 DO I=1,N
  I=RP2,N
  TEMP=0
DO I=1,N
  J=RP2,N
  TEMP=TEMP+A(I,J)*MULT(J)
12 A(I,RP1)=A(I,RP1)+TEMP-MULT(I)*A(RPI,RP1)
13 DO I=1,N
  I=RP2,N
  TEMP=0
DO I=1,N
  J=RP2,N
  A(I,J)=A(I,J)-MULT(I)*A(RPI,J)
14 A(I,J)=A(I,J)-MULT(I)*A(RPI,J)
15 CONTINUE
  CALCULATE EPSILON
EPS=0
DO I=1,N
  I=1,N
  EPS=EPS+CABG(A(1,I))
DO I=1,N
  I=2,N
  SUM=0
  I=1,N
  J=1,N
  SUM=SUM+CABG(A(I,J))
17 IF(SUM>GT2)EPS=SUM
18 IF(SUM>GT2)EPS=SUM
  EPS=EPS*1.0-12
  IF(EPS>GT2)EPS=1.0-12
DO I=1,N
  I=1,N
  J=1,N
  H(I,J)=A(I,J)
19 IF(N,N)=A(I,J)
20 IF(N,N)=A(I,J)
  LAMRDA(M)=A(1,1)+SHIFT(1)
  GO TO 37
21 IF(N,N)=A(1,1)
22 IF(N,N)=A(1,1)
  NE=0
  OR=AIMAQ(A(N,N))-NE*0
  IF(REAQ(A(N,N))-1)/A(N,N))+ABQ(AIMAQ(A(N,N))-1)/A(N,N))-1.0-9
  IF(ABQ(REAQ(A(N,N))-1))+ABQ(AIMAQ(A(N,N))-1))+GE*EPS
  GO TO 25
23 IF(ABQ(REAQ(A(N,N))-1))+ABQ(AIMAQ(A(N,N))-1))+GE*EPS
  GO TO 25

```

CCC


```

24 LAMBDA(MN1)=A(N,N)+SHIFT(1)
   ICOUNT=0
   N=N-1
   GO TO 21

```

CCC

```

   DETERMINE SHIFT

```

```

25 SHIFT(2)=(A(N-1,N-1)+A(N,N)+CSQRQ((A(N-1,N-1)+A(N,N))*2
   -4*(A(N,N)*A(N-1,N-1)-A(N,N-1)*A(N-1,N)))/2
   IF(RFAQ(SHIFT(2))%NE%0%OR%AIMAQ(SHIFT(2))%NE%0%)GO TO 26
   SHIFT(3)=A(N-1,N-1)+A(N,N)
   GO TO 27
26 SHIFT(3)=(A(N,N)+A(N-1,N-1)-A(N,N-1)*A(N-1,N))/SHIFT(2)
27 IF(CABQ(SHIFT(2)-A(N,N))%LT%CARQ(SHIFT(3)-A(N,N)))GO TO 28
   INDEX=3
   GO TO 29
28 INDEX=2
29 IF(CABQ(A(N-1,N-2))%GE%EPS)GO TO 30
   LAMBDA(MN1)=SHIFT(2)+SHIFT(1)
   LAMBDA(MN1+1)=SHIFT(3)+SHIFT(1)
   ICOUNT=0
   N=N-2
   GO TO 20

```

```

30 SHIFT(1) = SHIFT (1) + SHIFT(INDEX)
   DO 31 I=1,N
31 A(I,I)=A(I,I)-SHIFT(INDEX)

```

CCC

```

   PERFORM GIVEN ROTATIONS, QR ITERATES
   IF(ICOUNT%LE%10)GO TO 32
   INCAL=M-N
   GO TO 37

```

```

32 NM1=N-1
   TEMP1=A(1,1)
   TEMP2=A(2,1)
   DO 36 P=1,NM1
   RPI=RP+1
   RHO=SQRQ(REALQ(TEMP1)**2+AIMAQ(TEMP1)**2+
1 REALQ(TEMP2)**2+AIMAQ(TEMP2)**2)
   IF(CHO%CO%0%)GO TO 36
   COS=TEMPPI/RHO
   SIN=TEMPPI/RHO
   INDEX=X=VAXQ(R-1,1)
   DO 33 I=INDEX,N
   TEMP3=CONJQ(COS)*A(R,I)+CONJQ(SIN)*A(RPI,I)
   A(RPI,I)=TEMP
33 A(R,I)=A(RPI,RPI)
   TEMP1=A(RPI,RPI)

```

DALMAI 48
DALMAI 49
DALMAI 50
DALMAI 51
DALMAI 52
DALMAI 53
DALMAI 54
DALMAI 55
DALMAI 56
DALMAI 57
DALMAI 58
DALMAI 59
DALMAI 60
DALMAI 61
DALMAI 62
DALMAI 63
DALMAI 64
DALMAI 65
DALMAI 66
DALMAI 67
DALMAI 68
DALMAI 69
DALMAI 70
DALMAI 71
DALMAI 72
DALMAI 73
DALMAI 74
DALMAI 75
DALMAI 76
DALMAI 77
DALMAI 78
DALMAI 79
DALMAI 80
DALMAI 81
DALMAI 82
DALMAI 83
DALMAI 84
DALMAI 85
DALMAI 86
DALMAI 87
DALMAI 88
DALMAI 89
DALMAI 90
DALMAI 91
DALMAI 92
DALMAI 93
DALMAI 94
DALMAI 95

DALMA196
DALMA197
DALMA198
DALMA199
DALMA200
DALMA201
DALMA202
DALMA203
DALMA204
DALMA205
DALMA206
DALMA207
DALMA208
DALMA209
DALMA210
DALMA211
DALMA212
DALMA213
DALMA214
DALMA215
DALMA216
DALMA217
DALMA218
DALMA219
DALMA220
DALMA221
DALMA222
DALMA223
DALMA224
DALMA225
DALMA226
DALMA227
DALMA228
DALMA229
DALMA230
DALMA231
DALMA232
DALMA233
DALMA234
DALMA235
DALMA236
DALMA237
DALMA238
DALMA239
DALMA240
DALMA241
DALMA242
DALMA243

```

TEMP2=A(R+2,R+1)
DO 34 I=1,R
  TEMP=COS*A(I,R)+SIN*A(I,RP1)
  A(I,RP1)=-CONJQ(SIN)*A(I,R)+CONJQ(COS)*A(I,RP1)
34  A(I,R)=TEMP
  INDEX=MINO(R+2,N)
  DO 35 I=RP1,INDEX
    A(I,RP1)=SIN*A(I,RP1)
35  A(I,RP1)=CONJQ(COS)*A(I,RP1)
36  CONTINUE
  ICOUNT=ICOUNT+1
  GO TO 22

  CALCULATE VECTORS

37  IF (NCAL.EQ.0) GO TO 57
  NM1=NM-1
  IF (NM.NE.2) GO TO 38
  IPS=DMAX*0.0
  IF (CABQ(LAMBDA(1)),CABQ(LAMBDA(2))) #1.0-9
  H(1,1)=A(1,1)
  H(1,2)=A(2,1)
  H(2,1)=A(2,2)
  H(2,2)=A(1,2)
  DO 39 I=1,NCAL
    DO 40 J=1,N
      HL(I,J)=HL(I,J)-LAMBDA(L)
39  HL(I,J)=HL(I,J)
40  DO 41 I=1,NM1
    MULT(I)=0
    IF (I.NE.1) MULT(I)=0
    IF (CABQ(HL(I+1,I)).LE.CABQ(HL(I,I))) GO TO 42
    INTH(I)=0
    DO 41 J=1,N
      TEMP=HL(I+1,J)
      HL(I+1,J)=HL(I,J)
      HL(I,J)=TEMP
41  HL(I,J)=TEMP
42  IF (R.EQ.0) AND (AIMAQ(HL(I,I)).EQ.0) GO TO 44
    MULT(I)=IP1
    DO 43 J=1,N
      HL(I+1,J)=HL(I,J)+MULT(I)*HL(I,J)
43  HL(I+1,J)=HL(I,J)
44  CONTINUE
    NM1=NM-1
    DO 45 I=1,N
      VECT(I)=1
45  TWICE=0
  IF (TWICE.EQ.0)

```

CCC


```

46 IF (REALQ(HL(N,N)) $\neq$ 0.0) AND (AIMAQ(HL(N,N)),EQ $\neq$ 0.0) HL(N,N)=EPS
   VECT(N)=VECT(N)/HL(N,N)
DO 49 I=1,NM1
  K=N-I
DO 47 J=K,NM1
  VECT(K)=VECT(K)-HL(K,J+1)*VECT(J+1)
47 IF (REALQ(HL(K,K)) $\neq$ 0.0) AND (AIMAQ(HL(K,K)),EQ $\neq$ 0.0) HL(K,K)=EPS
48 VECT(K)=VECT(K)/HL(K,K)
  BIG=0.
DO 49 I=1,N
  SUM=ABQ(REALQ(VECT(I)))+ABQ(AIMAQ(VECT(I)))
49 IF (SUM,GT,BIG) BIG=SUM
  DO 50 I=1,N
    I=VECT(I)/BIG
50 VECT(I)=VECT(I)*BIG
  IF (TWICE) GO TO 52
DO 51 I=1,NM1
  IF (.NOT. INT(I)) GO TO 51
  TEMP=VECT(I)
  VECT(I)=VECT(I+1)
  VECT(I+1)=TEMP
51 VECT(I+1)=VECT(I)+MULT(I)*VECT(I)
  TWICE=.TRUE.
  GO TO 45
52 IF (N,EQ,2) GO TO 55
  NM2=N-2
DO 54 I=1,NM2
  NI=N-I-1
  NI1=N-I-1
  DO 53 J=NI1,N
    VECT(J)=H(J,NI1)*VECT(NI1+1)+VECT(J)
53 INDEX=INT(NI1)
  TEMP=VECT(NI1+1)
  VECT(NI1+1)=VECT(INDEX)
  VECT(INDEX)=TEMP
54 DO 56 I=1,N
55 A(I,L)=VECT(I)
56 RETURN
END
REAL FUNCTION CABQ*8 (Z)
COMPLEX*16 Z
CABQ=COABS(Z)
RETURN
END
REAL FUNCTION SQRO*8 (X)
REAL*8 X
SQRO=DSQRT(X)
RETURN
END

```

DALMA244
 DALMA245
 DALMA246
 DALMA247
 DALMA248
 DALMA249
 DALMA250
 DALMA251
 DALMA252
 DALMA253
 DALMA254
 DALMA255
 DALMA256
 DALMA257
 DALMA258
 DALMA259
 DALMA260
 DALMA261
 DALMA262
 DALMA263
 DALMA264
 DALMA265
 DALMA266
 DALMA267
 DALMA268
 DALMA269
 DALMA270
 DALMA271
 DALMA272
 DALMA273
 DALMA274
 DALMA275
 DALMA276
 DALMA277
 DALMA278
 DALMA279
 DALMA280
 DALMA281
 DALMA282
 DALMA283
 DALMA284
 DALMA285
 DALMA286
 DALMA287
 DALMA288
 DALMA289
 DALMA290
 DALMA291


```

REAL FUNCTION FLOAQ**8(I)
FLOAQ = DFLOAT(I)
RETURN
END
REAL FUNCTION ABQ*8(X)
ABQ = DABS(X)
RETURN
END
COMPLEX FUNCTION CSQRQ*16 (Z)
COMPLEX*16 Z
CSQRQ = CDSQRT(Z)
RETURN
END
COMPLEX FUNCTION CONJQ*16 (Z)
COMPLEX*16 Z
CONJQ = DCONJG (Z)
RETURN
END
REAL FUNCTION REAQ*8 (Z)
COMPLEX*16 Z
REALQ = Z
RETURN
END
REAL FUNCTION AIMAQ*8 (Z)
COMPLEX*16 Z
AIMAQ = Z*(0.00,-1.00)
RETURN
END

```

```

DALMA292
DALMA293
DALMA294
DALMA295
DALMA296
DALMA297
DALMA298
DALMA299
DALMA300
DALMA301
DALMA302
DALMA303
DALMA304
DALMA305
DALMA306
DALMA307
DALMA308
DALMA309
DALMA310
DALMA311
DALMA312
DALMA313
DALMA314
DALMA315
DALMA316
DALMA317
DALMA318
DALMA319
DALMA320

```


BIBLIOGRAPHY

- Arakawa, A., "Computational Design for Long-Term Numerical Integration of the Equations of Fluid Motion: Two-Dimensional Incompressible Flow. Part 1.," Jour. Comp. Physics, 1, 1, pp. 119-143, (1966).
- Aziz, K. and Hellums, J. D., "Numerical Solution of the Three-Dimensional Equations of Motion for Natural Convection," Phys. Fluids, 10, 7, pp. 314-324, (1967).
- Cooley, J. W. and Tukey, J. W., "An Algorithm for the Machine Calculation of Complex Fourier Series," Math. Comp., 19, 90, pp. 297-301, (1965).
- Davey, A. and Drazin, P. G., "The Stability of Poiseuille Flow in a Pipe," Jour. Fluid Mech., 36, 2, pp. 209-218, (1969).
- Deardorff, J. W., "A Numerical Study of Three-dimensional Turbulent Channel Flow at Large Reynolds Numbers," Jour. Fluid Mech., 41, 2, pp. 453-480, (1970).
- Dixon, T. N., "A Study on Stability and Incipient Turbulence in Poiseuille and Plane Poiseuille Flow by Finite Difference Simulation," Ph.D. Dissertation, Rice University, (1966).
- Douglas, J. and Rachford, N. H., "On the Numerical Solution of Heat Conduction Problems in Two and Three Space Variables," Trans. American Math. Soc., 82, pp. 421-439, (1956).
- Du Fort, E. C. and Frankel, S. P., "Stability Conditions in the Numerical Treatment of Parabolic Differential Equations," Math. Tables and Other Aids to Computation, 7, pp. 135-152, (1953).
- Francis, J. G. F., "The Q R Transformation, Parts I and II," Computer Jour., 4, pp. 265-271, 332-345, (1962).
- Fromm, J. E., A Method for Computing Non-Steady, Incompressible, Viscous Fluid Flows, Los Alamos Scientific Laboratory Report No. LA-2910, (1963).
- Fischer, G., "A Survey of Finite-Difference Approximations to the Primitive Equations," Monthly Weather Rev., 93, 1, pp. 1-9, (1965).
- Galloway, F. M., "On a Finite-Difference Approach to Turbulence Problems," Ph.D. Dissertation, Case Western Reserve Univ., (1968).
- Gawain, T. H., Pritchett, J. W., "A Unified Heuristic Model of Fluid Turbulence," to be published Jour. Comp. Phys., (1970).
- Grosch, C. E., and Salwen, H., "The Stability of Steady and Time-dependent Plane Poiseuille Flow," Jour. Fluid Mech., 34, 1, pp. 177-205, (1968).

- Hamming, R. W., Numerical Methods for Scientists and Engineers, McGraw-Hill, (1962).
- Harlow, F. H. and Welch, J. E., "Numerical Calculation of Time Dependent Viscous Incompressible Flow of Fluid with Free Surface," Phys. Fluids, 8, 12, pp. 2182-2189, (1964).
- Harlow, F. H. and Welch, J. E., The MAC Method, Los Alamos Scientific Laboratory Report No. LA-3425, (1965).
- Heisenberg, W., "Über Stabilität und Turbulenz von Flüssigkeitsströmen," Ann. Phys., 4, 74, pp. 577-627, (1924).
- Kraichnan, R. H., "Inertial Ranges in Two-Dimensional Turbulence," Phys. Fluids, pp. 10, 7, (1967).
- Kurihara, Y., "On the use of Implicit and Iterative Methods for the Time Integration of the Wave Equation," Monthly Weather Rev., 93, 1, pp. 33-46 (1965).
- Lilly, D. K., "On the Computational Stability of Numerical Solutions of Time-Dependent Non-linear Geophysical Fluid Dynamics Problems," Monthly Weather Rev., 93, 1, pp. 11-26, (1965).
- Lilly, D. K., Numerical Solution of Field Problems in Continuum Physics, VII SIAM-AMS Proceedings, American Mathematical Society, pp. 41-53, (1970).
- Lin, C. C., "On the Stability of Two-dimensional Parallel Flows," Parts I, II, III, Quarterly Applied Math., 3, pp. 117-142, pp. 218-234, pp. 277-301, (1945).
- Lin, C. C., Theory of Hydrodynamic Stability, Cambridge Univ. Press, (1955).
- Meksyn, D. and Stuart, J. T., "Stability of Viscous Motion between Parallel Planes for Finite Disturbances," Proc. Royal Soc., A 208, pp. 517-526, (1951).
- Nachtshein, P. R., An Initial Value Method for the Numerical Treatment of the Orr-Sommerfeld Equation for the Case of Plane Poiseuille Flow, NASA TN D-2414, (1964).
- O'Brien, G. G., Hyman, M. A. and Kaplan, S., "A Study of the Numerical Solutions of Partial Differential Equations," Jour. Math. and Phys., 29, 4, pp. 223-251, (1951).
- Pai, S. I., Viscous Flow Theory II, Turbulent Flow, D. Van Nostrand Co., (1957).
- Parlett, B. N., Mathematical Methods for Digital Computers, Vol. II, Ed. A. Ralston and H. Wilf, Wiley & Sons Inc., (1967).

- Peaceman, D. W. and Rachford, H. H., "The Numerical Solution of Parabolic and Elliptic Differential Equations," Jour. S. I. A. M., 3, pp. 28-35, (1955).
- Pearson, C. E., "A Computational Method for Viscous Flow Problems," Jour. Fluid Mech., 21, 4, pp. 611-622, (1965).
- Pekeris, C. L. and Shkoller, "Stability of Plane Poiseuille Flow to Periodic Disturbances of Finite Amplitude," Jour. Fluid Mech., 39, 3, pp. 611-627, (1969).
- Pekeris, C. L. and Shkoller, "The Neutral Curves for Periodic Perturbations of Finite Amplitude of Plane Poiseuille Flow," Jour. Fluid Mech., 39, 3, pp. 629-639, (1969).
- Pekeris, C. L. and Shkoller, "Stability of Plane Poiseuille Flow to Periodic Disturbances of Finite Amplitude in the Vicinity of the Neutral Curve," Jour. Fluid Mech., 29, 1, pp. 31-38, (1967).
- Potter, M. C., "Stability of Plane Couette-Poiseuille Flow," Jour. Fluid Mech., 24, 3, pp. 609-619, (1966).
- Phillips, N. A., The Atmosphere and the Sea in Motion, pp. 501-504, Rockefeller Inst. Press, (1959).
- Prandtl, L., "Über die Ausgebildete Turbulenz," Z. angew Math. u Mech., 5, 136, (1925).
- Reynolds, O., "An Experimental Investigation of the Circumstances which Determine whether the Motion of Water shall be Direct or Sinous, and the Law of Resistance in Parallel Channels," Phil. Trans. Royal Soc., 174, pp. 935-982, (1883).
- Reynolds, W. C., and Potter, M. C., "Finite Amplitude Instability of Parallel Shear Flows," Jour. Fluid Mech., 27, 3, pp. 465-492, (1967).
- Richtmyer, R. D., and Morton, K. W., Difference Methods for Initial-Value Problems, 2nd Ed., Interscience, (1967).
- Schensted, I. V., "Contributions to the Theory of Hydrodynamic Stability," Ph.D. Dissertation, Univ. Michigan, (1960).
- Smith, G. D., Numerical Solution of Partial Differential Equations, Oxford Univ. Press, (1965).
- Stuart, J. T., "On the Non-linear Mechanics of Hydrodynamic Stability," Jour. Fluid Mech., 4, 1, pp. 1-21, (1958).
- Stuart, J. T., "On the Non-linear Mechanics of Wave Disturbances in Stable and Unstable Parallel Flows," Part 1. "The basic Behavior in Plane Poiseuille Flow," Jour. Fluid Mech., 9, 2, pp. 353-370, (1960).

- Thomas, L. H., "The Stability of Plane Poiseuille Flow," Phys. Rev., 91, 4, pp. 780, (1953).
- Varga, R. S., Matrix Iterative Analysis, Prentice-Hall, (1962).
- Watson, J., "On the Non-linear Mechanics of Wave Disturbances in Stable and Unstable parallel Flows, Part 2. The Development of a Solution for Plane Poiseuille Flow and for Plane Couette Flow," Jour. Fluid Mech., 9, 2, pp. 371-389, (1960).
- Wilkinson, J. A., The Algebraic Eigenvalue Problem, pp. 485-569, Clarendon Press, (1965).
- Williams, G. P., "Numerical Integration of the Three-dimensional Navier-Stokes Equations for Incompressible Flow," Jour. Fluid Mech., 37, 4, pp. 727-750, (1969).

INITIAL DISTRIBUTION LIST

| | No. Copies |
|--|------------|
| 1. Defense Documentation Center Cameron Station Alexandria, Virginia 22314 | 2 |
| 2. Library, Code 0212 Naval Postgraduate School Monterey, California 93940 | 2 |
| 3. Chairman, Department of Aeronautics Naval Postgraduate School Monterey, California 93940 | 1 |
| 4. Professor T. H. Gawain, Code 57Gn Department of Aeronautics Naval Postgraduate School Monterey, California 93940 | 5 |
| 5. Professor D. J. Collins, Code 57Co Department of Aeronautics Naval Postgraduate School Monterey, California 93940 | 1 |
| 6. Professor F. D. Faulkner, Code 53Fa Department of Mathematics Naval Postgraduate School Monterey, California 93940 | 1 |
| 7. Associate Professor J. A. Miller, Code 57Mo Department of Aeronautics Naval Postgraduate School Monterey, California 93940 | 1 |
| 8. Associate Professor J. V. Sanders, Code 61Sd Department of Physics Naval Postgraduate School Monterey, California 93940 | 1 |
| 9. Associate Professor R. T. Williams, Code 51Wu Department of Meteorology Naval Postgraduate School Monterey, California 93940 | 1 |
| 10. Lieutenant Commander George D. O'Brien, USN 4817 Bayard Boulevard Washington, D. C. 20016 | 3 |

11. Deputy Director 1
Advanced Research Projects Agency
Attn: Dr. S. Lukasik

12. Mr. Ronald Bailey 1
Theoretical Branch
NASA Ames Research Center
Moffett Field, California 94035

13. Prof. W. H. Clark 1
Department of Aeronautics
Naval Postgraduate School
Monterey, California 93940

14. Dr. F. M. Galloway 1
Case Western Reserve University
Cleveland, Ohio 44106

15. Information Research Associates 2
2140 Shattuck Avenue
Berkeley, California 94720

16. Los Alamos Scientific Laboratory 1
Los Alamos, New Mexico 87544
Attn: Dr. F. Harlow

17. Commander 2
Naval Air Systems Command
Attn: Dr. E. S. Lamar - 1
Dr. H. J. Mueller - 1
Navy Department
Washington, D. C. 20360

18. Commanding Officer 2
Naval Ship Research and Development Center
Carderoc, Maryland
Attn: Dr. F. Frenkiel - 1
Dr. J. Schott - 1

19. Office of Naval Research 4
Navy Department
Washington, D. C. 20360
Attn: Physical Sciences Div., E. H. Weinberg, Code 420 - 1
Mathematical & Information Sciences Div., R. J. Lindegard,
Code 430 - 1
Morton Cooper, Code 438 - 1
Ralph Cooper - 1

20. Dr. W. C. Reynolds 1
Dept. of Mechanical Engineering
Standord University
Stanford, California 94034

DOCUMENT CONTROL DATA - R & D

(Security classification of title, body of abstract and indexing annotation must be entered when the overall report is classified)

| | | | |
|--|--|---|-----------------------|
| 1. ORIGINATING ACTIVITY (Corporate author) Naval Postgraduate School Monterey, California 93940 | | 2a. REPORT SECURITY CLASSIFICATION Unclassified | |
| | | 2b. GROUP | |
| 3. REPORT TITLE A Numerical Investigation of Finite-Amplitude Disturbances in a Plane Poiseuille Flow | | | |
| 4. DESCRIPTIVE NOTES (Type of report and inclusive dates) Doctoral Dissertation, June 1970 | | | |
| 5. AUTHOR(S) (First name, middle initial, last name) George Donoghue O'Brien | | | |
| 6. REPORT DATE June 1970 | | 7a. TOTAL NO. OF PAGES 204 | 7b. NO. OF REFS 49 |
| 8a. CONTRACT OR GRANT NO. | | 9a. ORIGINATOR'S REPORT NUMBER(S) | |
| b. PROJECT NO. | | | |
| c. | | 9b. OTHER REPORT NO(S) (Any other numbers that may be assigned this report) | |
| d. | | | |
| 10. DISTRIBUTION STATEMENT This document has been approved for public release and sale; its distribution is unlimited. | | | |
| 11. SUPPLEMENTARY NOTES | | 12. SPONSORING MILITARY ACTIVITY Naval Postgraduate School Monterey, California 93940 | |
| 13. ABSTRACT <p>A consistent and stable finite-difference approximation of the vorticity transport equations has been applied to a plane Poiseuille flow with spatially periodic disturbances of finite amplitude.</p> <p>By application of the discrete Fourier transform to the solution of a Poisson equation significant improvements in the speed and accuracy of the calculations have been obtained. Numerical tests indicate that the usual iterative schemes are inadequate if a large number of mesh points are employed.</p> <p>The effect of mesh size has been determined by extensive calculations based on a consistent second-order representation of the linear eigenvalue problem. The results indicate that a fine mesh is required to accurately represent the behavior of even the large-scale unstable motions. The stability and accuracy of the present formulation was demonstrated, in the linear range, by comparison with the established results of the linear theory.</p> <p>Calculations in the non-linear range, at a moderate value of the Reynolds number, indicate the existence of an equilibrium state. The calculated values of the mean spectral density of kinetic energy are consistent with the exponential law predicted by Kraichnan for two-dimensional turbulence. The program, developed in this investigation, provides a means, of demonstrated accuracy, for the extensive investigation of two dimensional turbulence in a shear flow.</p> | | | |

KEY WORDS

Hydrodynamic stability
 Finite-differences
 Turbulence
 Plane Poiseuille flow

LINK A

LINK B

LINK C

ROLE

WT

ROLE

WT

ROLE

WT

1266171 19435

Thesis 124643
019 O'Brien
c.1 A numerical investiga-
tion of finite-ampli-
tude disturbances in
a plane Poiseuille flow.

1266171 19435

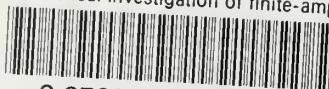
ga-

124643

Thesis
019 O'Brien
c.1 A numerical investiga-
tion of finite-ampli-
tude disturbances in
a plane Poiseuille flow.

thes019

A numerical investigation of finite-ampl



3 2768 001 97610 3

DUDLEY KNOX LIBRARY